AFRL-SR-BL-TR-98-

0231

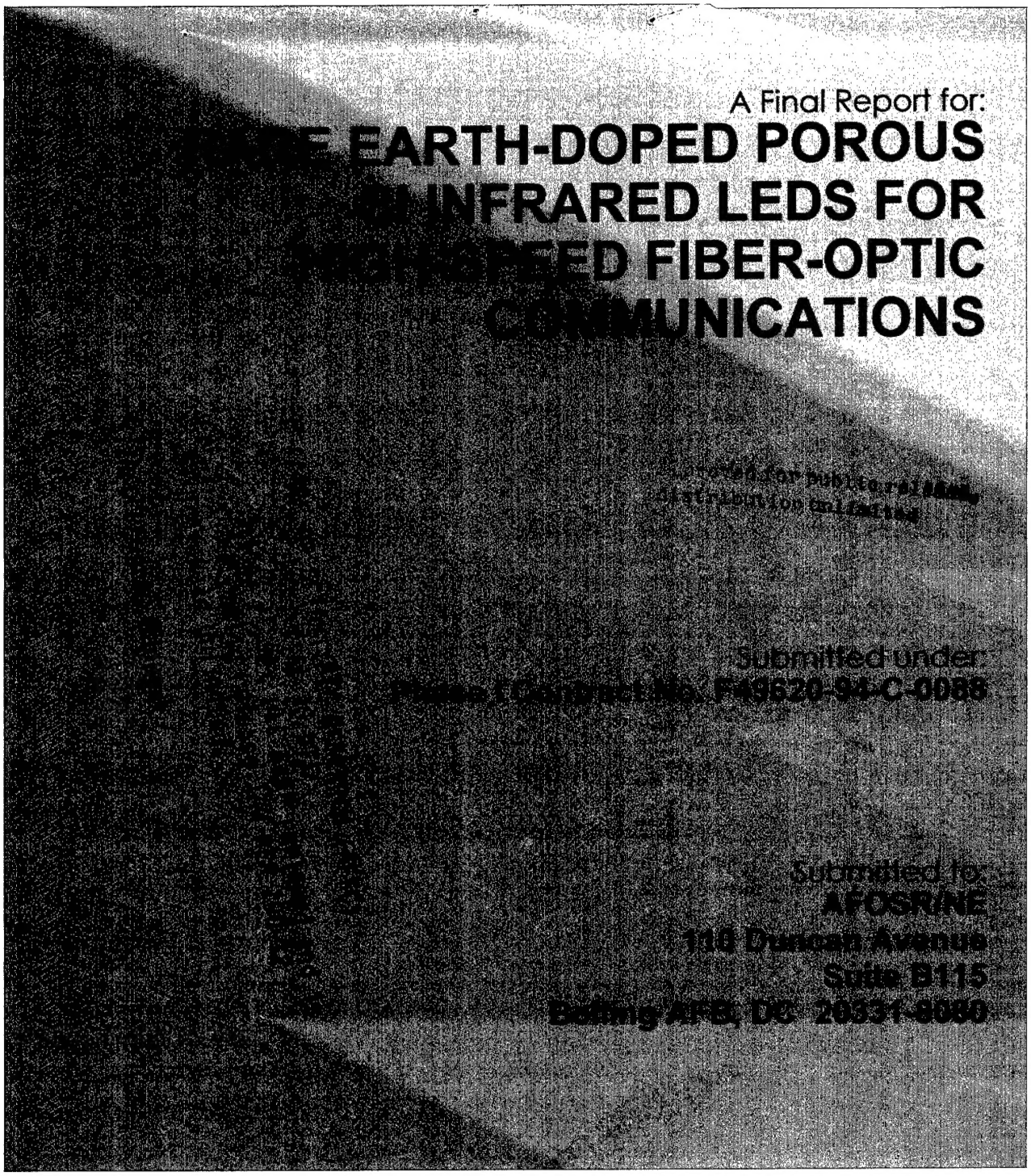

spire

FR-10161

A Final Report for:

RARE-EARTH-DOPED POROUS Si INFRARED LEDs FOR HIGH-SPEED FIBER-OPTIC COMMUNICATIONS

Reporting period:

1 October 1994 through 30 September 1997

Submitted under:

Contract No. F49620-94-C-0088

Submitted to:

AFOSR/NE

110 Duncan Avenue

Suite B115

Bolling AFB, DC 20331-8080

Prepared by:

Fereydoon Namavar, Sc.D.

Submitted by:

Spire Corporation

One Patriots Park

Bedford, MA 01730-2396

REPORT DOCUMENTATION PAGE

Form Approved OMB No. 0704-0188

1. AGENCY USE ONLY *(Leave blank)*	2. REPORT DATE	3. REPORT TYPE AND DATES COVERED
	2/24/98	Final 10/1/94 through 9/30/97

4. TITLE AND SUBTITLE
Rare Earth-doped Porous Si Infrared LEDs for High-speed Fiber-optic Communications

5. FUNDING NUMBERS
F49620-94-C-0088

6. AUTHOR(S)
Fereydoon Namavar, Sc.D.

7. PERFORMING ORGANIZATION NAME(S) AND ADDRESS(ES)
Spire Corporation
One Patriots Park
Bedford, MA 01730-2396

8. PERFORMING ORGANIZATION REPORT NUMBER
10161

9. SPONSORING/MONITORING AGENCY NAME(S) AND ADDRESS(ES)
AFOSR/NE
110 Duncan Avenue
Suite B115
Bolling AFB, DC 20331-8080

10. SPONSORING/MONITORING AGENCY REPORT NUMBER

11. SUPPLEMENTARY NOTES

12a. DISTRIBUTION/AVAILABILITY STATEMENT
Unlimited

12b. DISTRIBUTION CODE

13. ABSTRACT *(Maximum 200 words)*

This program has demonstrated intense 1.54 μm PL emission from Er-implanted porous silicon (Er:p-Si) up to temperatures as high as 475K. Intensity of Er emission was about 8% of the PL intensity of a highly doped $In_{0.53}Ga_{0.47}As$ grown on InP. The full width at half maximum of the 1.54 μm PL peak is 40 cm^{-1}. Er was implanted using a commercial implanter operating at 200 keV. The emission characteristics of Er:p-Si samples has been extensively studied including temperature dependence, time decay, excitation power dependence, excitation wavelength dependence and correlation between visible and IR emission.

There is a strong correlation between the visible PL emission from p-Si host and the 1.54 μm PL emission from Er^{3+} in p-Si. P-Si samples that exhibited a visible PL spectrum with peak near 750 nm before or after Er implantation resulted in the strongest 1.54 μm PL emission. Nearly identical PLE spectra measured for the Er-related 1.54 μm emission and the p-Si related visible emission provide the first experimental evidence that Er^{3+} ions are confined in Si nanocrystallites of p-Si. A reduction in 1.54 μm PL intensity of less than a factor of two was observed over 9 to 300K temperature range. Our results indicate that p-Si is an excellent host for 1.54 μm emission. However, in order to make practical devices, one must first develop a process to fabricate porous layer reproducibly and uniformly.

14. SUBJECT TERMS
Porous Si, nanostructures, Er, Pr implantation, infrared emission, LEDs, fiberoptics

15. NUMBER OF PAGES
94

16. PRICE CODE

17. SECURITY CLASSIFICATION OF REPORT	18. SECURITY CLASSIFICATION OF THIS PAGE	19. SECURITY CLASSIFICATION OF ABSTRACT	20. LIMITATION OF ABSTRACT
Unclassified	Unclassified	Unclassified	Unlimited

ABSTRACT

This program has demonstrated intense 1.54 μm PL emission from Er-implanted porous silicon up to temperatures as high as 475K. Intensity of Er emission was about 8% of the PL intensity of a highly doped, lattice-matched, device-quality $In_{0.53}Ga_{0.47}As$ grown on InP. Samples were produced by implantation of Er at 190 to 400 keV using a commercial implanter operating at 200 keV. A reduction in 1.54 μm PL intensity of less than a factor of two from Er:porous Si over 9 to 300K temperature range was observed which is consistent with Er in wide bandgap materials. The full width at half maximum of the 1.54 μm PL peak is 34 cm^{-1} at 15K. The observed large broadening of the 1.54 μm PL emission in Er:porous Si, compared with that reported for crystalline Si, 8 cm^{-1}, indicates that the Er^{3+} ions occupy a range of sites in porous Si, and that the emission spectrum is inhomogeneously broadened. This result is consistent with the possible differences in the local environment (crystal field) of Er^{3+} ions due to different crystallite sizes in the porous layer.

There is a strong correlation between the visible PL emission from porous Si host and the 1.54 μm PL emission from Er^{3+} in porous Si. Porous Si samples that exhibited a visible PL spectrum with peak near 750 nm before or after Er implantation resulted in the strongest 1.54 μm PL emission. Photoluminescence excitation (PLE) studies on the near infrared and visible PL peaks show nearly identical PLE spectra. These results provide the first direct experimental evidence that the near IR PL emission in Er:porous Si and the visible PL emission have the same origin of excitation suggesting that Er^{3+} ions are confined in Si nanocrystallites of porous Si. Measurements of 1.54 μm PL peak intensity as a function of excitation laser power density show a square root relationship, consistent with the results reported in the literature for other Er-doped host materials. Temperature-dependent PL decay measurements of Er-implanted porous Si samples show a non-exponential PL decay at temperatures ranging from 10 to 375K. This non-exponential PL decay is a result of superposition of a fast and a slow decay components. At 10K, the slow decay component is 1.37 ms and the fast component is 145 μs.

PL data presented in this work clearly indicates that porous Si is an excellent host for strong 1.54 μm emission from Er^{3+}. To determine feasibility of porous Si as a substrate for Si-based IR emitting devices we have fabricated impact excited and injection luminescence devices. However, despite of our enormous experimental effort, the fabrication of efficient 1.54 μm Er:porous Si LED was hampered by lack of reproducibility and uniformity of porous Si substrates. The absence of reproducibility and nonuniformity of porous Si originates from the randomness of the porous Si etching process. In order to make porous Si device-worthy, one must first develop a process to fabricate porous Si reproducibly and uniformly. It should be noted that physical confinement or isolation of nanocrystalline Si in porous Si, which facilitates strong IR PL emission results in a weak EL emission, because of poor electrical conductivity of porous Si and difficulty to make good electrical contacts.

TABLE OF CONTENTS

Page

TABLE OF CONTENTS (Concluded)

LIST OF FIGURES

LIST OF FIGURES (Continued)

Page

LIST OF FIGURES (Concluded)

LIST OF TABLES

1 INTRODUCTION

In recent years attention has been focused on the development of new materials which would improve the speed and efficiency of optical information transfer in computer and communication systems. Through the rapid progress of integrated circuit technology, silicon is widely recognized as a leading semiconductor material. Unfortunately, its indirect bandgap has prevented its use for photonics. Extensive efforts are in progress to incorporate compound semiconductor light-emitting diodes (LEDs) and laser diode technologies into silicon very large scale integration (VLSI) processes by heteroepitaxial growth. However, the most promising III-V light-emitting compounds are not easily processed on Si substrates due to lattice and thermal expansion mismatches. Incompatibility problems generally degrade the performance of III-V compound LEDs grown on silicon. An alternate approach involves mounting III-V-based devices onto Si wafers, but this is costly, time-consuming, and labor-intensive. If a process could be developed to allow efficient light emission directly from silicon, Si-based optoelectronic devices could be used as an essential component in optical interconnects for the next generation of high-speed computers and low-cost information transfer/display systems.

1.1 Porous Silicon Visible LEDs

During the past several years, strong room-temperature[1] visible light emission from anodically-etched porous silicon has been demonstrated. Electroluminescence (EL) from porous Si devices based on p-n junction or Schottky contacts has also been shown by a number of groups.[2-4] However, the quantum efficiency of present devices has been compromised because the contacting areas between wide-bandgap materials (p-n devices) or metal contacts (Schottky) and porous Si are only a very small portion[5] of the total porous Si surface (Figures 1 and 2a). Sputtering or e-beam evaporation techniques, used for LED fabrication, provide contact only to the tip of the pores (see Figures 1 and 2); therefore, most of the surface of the light-emitting porous Si region is inactive in EL. Use of transparent conducting polymers, in principle, may result in an enhancement in EL efficiency. However, at the present time, these devices suffer from a lack of stability. A process which could result in conformal coverage (Figure 2b) of a transparent, conductive wide bandgap material[6] into porous Si might enhance the quantum efficiency to the impressive efficiency levels observed from porous Si with a liquid junction.[7] For example, atomic layer epitaxy (ALE) growth of GaN (side-wall epitaxy),[8] or electroplating of a transparent conducting oxide could increase the contact area, resulting in an enhancement of EL efficiency.

Another phenomenon which influences the external quantum efficiency of light-emitting devices (including porous Si) is self-absorption, which is not well understood in porous silicon. Since Si is transparent to wavelengths longer than 1.1 μm, the self-absorption or reduction of external quantum efficiency will not be a problem if porous Si is used as a medium for rare-earth elements or as a light source for infrared (IR) emission at wavelengths longer than 1.1 μm. In that case, restrictions on the thickness and optical properties of the contact material to the porous region would be relaxed, and IR could exit from either side of the wafer. In particular, if the visible light from porous Si is used to pump embedded erbium, the absorption would not be a problem.

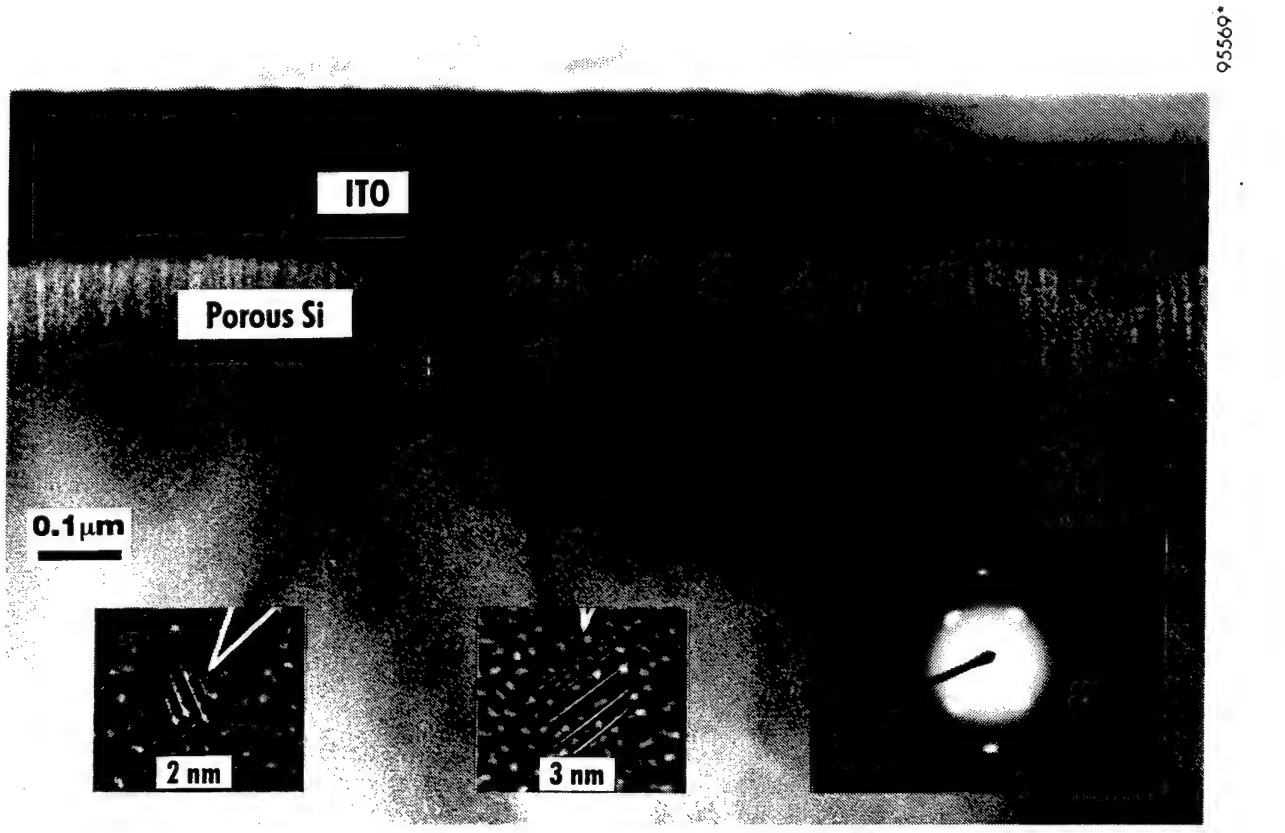

Figure 1 *A cross-sectional transmission electron microscopic image of a working np-heterojunction porous Si LED fabricated by sputtering indium-tin-oxide (n-type), which contacts only the tip of the pores. Note the lattice image of the Si nanoparticles. The lack of <200> spots in the electron diffraction pattern also confirms the presence of nanoparticles.*[5]

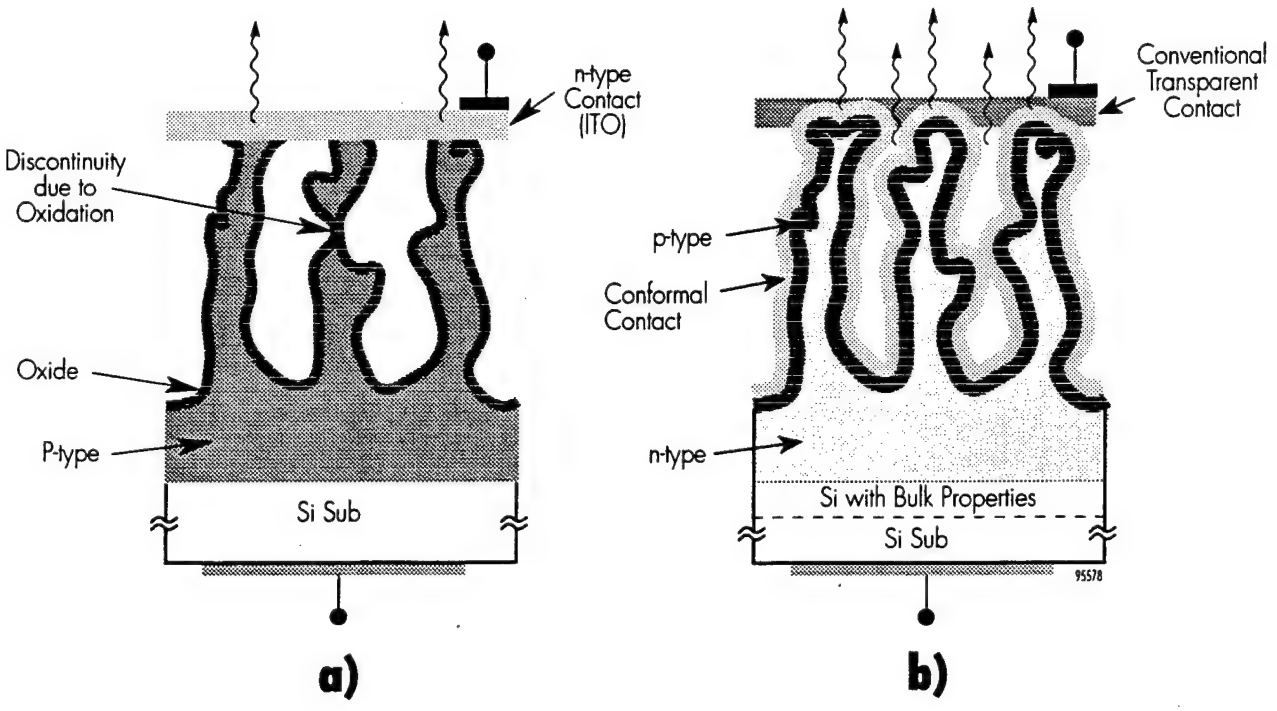

Figure 2 *Comparison of (a) a contact layer produced by sputtering or evaporation, and (b) an idealized structure with a conformal contact covering the entire porous Si surface.*

1.2 Erbium in Bulk Si

During the past decade, extensive effort has been focused on the doping of rare-earth elements into III-V compound semiconductors.[9-11] Erbium has attracted the most interest because it exhibits sharp-line luminescence at 1.54 μm, the result of an intra-4f-shell transition ($^4I_{13/2} \rightarrow_{15/2}$) of Er^{3+}. The 1.54 μm emission is important since the absorption loss is minimal at this wavelength in silica-based optical fibers. A similar transition has been observed in Er-doped glass,[12] which has become the most common method of amplification in optical fiber communications. Since the 5s- and 5p-shells shield the 4f-shell orbitals of Er^{3+}, the intra-4f-shell transitions are insensitive to the first-order host lattice effects. The luminescence peak from erbium is extremely narrow and possesses excellent temperature stability (see Figure 3).

Room-temperature infrared LEDs have been demonstrated by MeV implantation of Er into single-crystal Si. However, the luminescent efficiency needs to be improved.[13] Earlier work has suggested that the solubility of Er in silicon is 1.3 x $10^{18}/cm^3$ at 900°C. Precipitates take the form of platelets of erbium silicide 100 to 300Å in diameter and 10Å thick. The photo-luminescence (PL) saturates at an Er concentration of 5 x $10^{17}/cm^3$, below the apparent solubility limit.[14] At a Materials Research Society meeting, Kimerling *et al.*[15] reported that the solubility of Er in Si is even lower than that previously reported. It has been suggested that erbium concentrations approaching $10^{20}/cm^3$ are required to obtain high LED intensities at room temperature.[16]

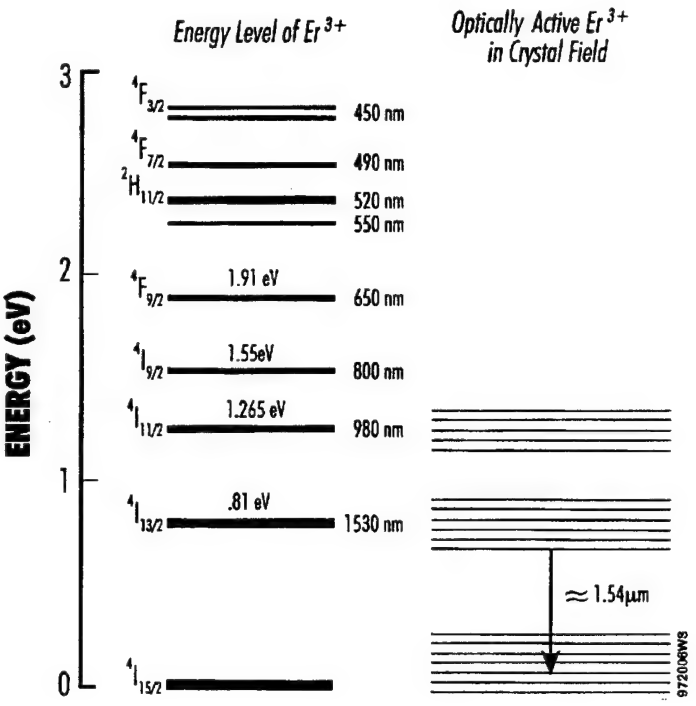

Figure 3 *Transitions between energy levels of isolated Er^{3+} ions (left) are forbidden by parity selection rules. Splitting of these levels in a crystal field (right) provides the necessary conditions for optical transitions. Note that the split sublevel energies are not drawn to scale.*

Researchers have applied a variety of methods to increase the solubility or the number of optically active Er centers in Si. Several papers[17-20] have indicated that, after introducing oxygen or other elements, the light emission of Er-implanted silicon is enhanced. Indeed, recently, the results of Er-implanted silicon measured with extended X-ray absorption fine-structure (EXAFS) show Er-implanted, Czochralski-grown Si involves a sixfold bonding of the Er to oxygen impurity atoms and forms an optically-active species.[20] In contrast, Er-implanted, float-zone Si, which contains far less oxygen, results in a twelvefold bonding of erbium to silicon, forming an optically-inactive species.[20]

1.3 Porous Si: A Suitable Host for Er^{3+} Luminescence

Our progress in this program indicates that porous silicon is a suitable host for luminescent Er because:

- Porous Si has a higher bandgap (1.8 to 2.0 eV) than bulk Si (1.1 eV). Based on the work of Favennec *et al.*[17] (see Figure 4), stronger IR emission and weaker temperature dependence are expected.

- In contrast to Er in bulk Si, Er in porous Si does not precipitate because porous Si consists of free-standing, Si nanostructures with distinct physical boundaries that limit diffusion to a few nanometers (see Figures 1 and 2).

- The importance of an erbium-oxygen complex for efficient light emission of Er in bulk Si has been demonstrated.[17-20] Without coimplantation of oxygen, Er in porous Si can easily acquire oxygen and form an Er-O complex, because (1) the surface area of the nanostructures is enormous, and (2) the average distance between the erbium and surface oxygen is on the order of only a few nanometers.

- The recovery of damage from implantation into Si nanostructures may occur at much lower annealing temperatures than in bulk Si. Defects such as vacancies or interstitials created by Er implantation need only travel a relatively small distance to reach the free surface (sink) compared to those produced by MeV implantation into bulk Si in which defects must travel rather long distances (several hundred/thousand angstroms) to reach the sink. Annealing at 900°C or higher is used to recrystallize the bulk Si; however, this high temperature could result in formation of silicides rather than in erbium with oxygen coordination.

Porous Si (visible) LEDs rely on minority-carrier injection (injection luminescence), which requires a good junction.[21,22] On the other hand, for Er in porous Si one can provide pumping by impact excitation (hot electrons), which simplifies device fabrication. Indeed, a metal contact to a porous silicon LED is equivalent to the metal-insulator-semiconductor contact that is required for tunneling injection in a hot-electron LED.[23] The cross-section for exciting Er by hot electrons is more than four orders of magnitude larger than the optical pumping cross-sections of erbium.[24] Recent work in bulk Si junction LEDs has shown much higher luminescence efficiency for Er through impact excitation under reverse bias (5.3 V),[25] compared to minority-carrier injection under forward bias. Although it appears to be speculative, in principle the visible (red) emission in porous Si may be used to self-pump ($^4I_{15/2} \rightarrow {}^4F_{9/2}$) Er within porous Si.

2 OBJECTIVE

The overall goal of this program was to fabricate room-temperature, Si-based IR light-emitting devices (LEDs). To achieve these objectives a systematic study was carried out in order to understand the mechanism involved in light emission from Er- and Pr-implanted porous Si and to optimize the processes for enhanced emission efficiency. Two types of electroluminescent (EL) devices have been fabricated: those operating based on injection-induced luminescence (LEDs), and those operating based on impact-excited luminescence.

3 EXPERIMENTAL PROCEDURE

Our experimental work involves two facets: an understanding of the basics of porous Si to help us fabricate high efficiency devices, and device fabrication.

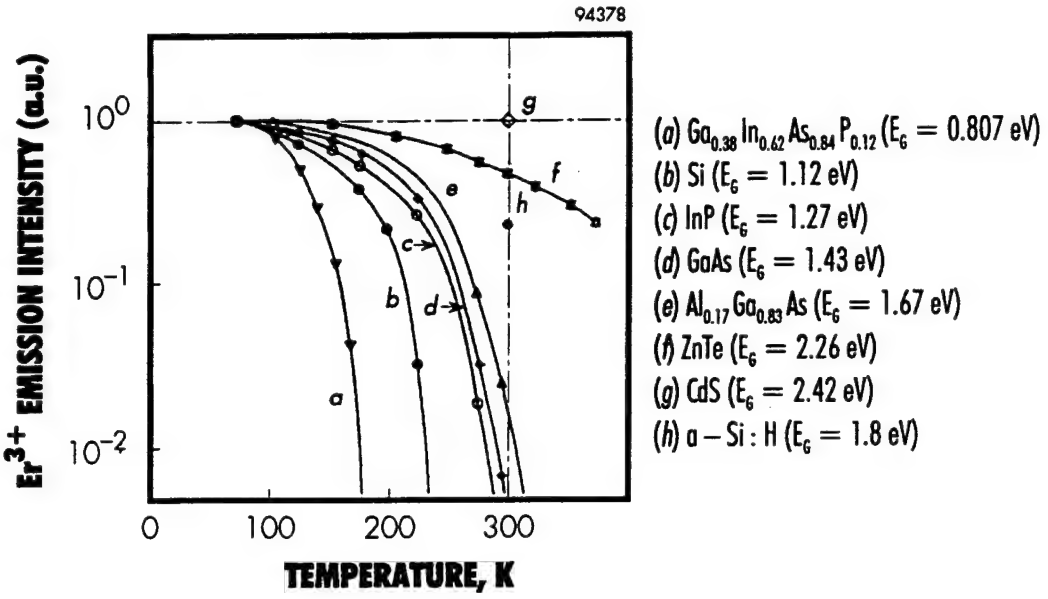

Figure 4 *Temperature dependence of Er^{3+} emission from various semiconductor hosts.*[1]

3.1 Preparation of Si Wafers

The strength of IR emission in Er:PSi is critically dependent on two factors: (1) substrate conditions, and (2) processing conditions. Many substrate conditions, from resistivity to wafer quality, influence emission from Er-implanted porous Si. Therefore, to carry out the program with maximum efficiency, we obtained various lots of prime quality wafers with resistivity ranging from 0.1 to 1.2 Ω-cm. Although the task of purchasing suitable wafers was time consuming (since most industries use 6" or 8" wafers and few U.S. manufacturers supply 3" and 4" wafers), we have been able to procure ample wafers to the required specifications.

3.1.1 Aluminum Back Contact

To fabricate uniform porous Si (p-type), a good ohmic contact to the back of the wafer is necessary. In the past, we typically deposited 2000Å of aluminum on the back of the wafer. In this process the wafer surfaces were first cleaned in a buffered HF dip before e-beam evaporating an ohmic contact. At the beginning of the program we deposited aluminum on three batches of eight wafers. In these runs, a contact was made either to the back (unpolished) side of the wafers, or the front (polished) side. An aluminum thickness ranging from 2015Å to 2070Å was measured using Dektak measurements. As an alternative to evaporating aluminum as a back contact (which is necessary during anodic etching of porous Si), we also sputtered approximately 600Å of gold on a few Si wafers using a desktop sputtering system. We experimented with this technique because it is quicker and more economical; however, we found that samples with Al evaporated on the back produced a much more uniform porous region as compared to samples which had Au sputtered on the back.

One of our initial batches of Er-implanted wafers showed no IR emission. From RBS analysis, we determined that the Al etch used to remove the aluminum back contact not only removed the aluminum, but also removed some, if not all, of the implanted erbium. Therefore, it became necessary to remove the Al back contact before Er implantation. Another method of contact deposition, discussed below, was investigated and used for some of the wafers.

3.1.2 Ion Implantation of Layers for Ohmic Contact

To avoid using aluminum as a back contact and still provide ohmic contact, we implanted the back side of bulk (p-type) Si wafers with boron to create a p^+ layer. The back side of bulk Si wafers was implanted with a dose of 5 x 10^{15} boron/cm^2 at 20 keV. Several wafers were implanted with an additional dose of 5 x 10^{15} boron/cm^2 at 60 keV. Wafers were annealed at 900°C for 30 minutes in N_2 to form the p^+ back contact. In addition, a highly doped (low-resistivity) Si wafer was placed directly behind the Si wafer to be etched in the etching apparatus. The Si contact wafer was not exposed to the HF solution. The additional Si wafer aids in distributing current uniformly throughout the wafer being anodically etched.

3.2 Fabrication of Porous Si

Wafers were anodically etched in a 1:1 HF:ethanol solution using conditions to achieve red-emitting porous Si. The system used relies on a current source with the sample connected as the anode (+) and a platinum foil as the cathode (-) (see Figure 5). The HF:ethanol solution is contained in a teflon vessel. The silicon wafers are held in a specially-prepared jig which exposes only the front surface to the solution, isolating the electrical contact on the back from any liquid. The silicon samples were carefully etched in the HF solution using currents ranging from 10 mA to 100 mA for periods of 30 to 150 minutes. Many of the samples fabricated yielded red-emitting porous Si, which according to initial results provided the strongest IR emission (discussed later).

3.3 Implantation of Rare Earth Elements

Porous Si wafers are mounted on a square steel plate. The ion beam scans a region about 20% larger than the wafer. Once the porous Si wafer has been mounted, the remaining space around the wafer is used to implant into other substrates. In addition, we often mask a part of the porous Si wafer (with a piece of Si) in order to compare unimplanted versus implanted regions; therefore, other samples are also mounted on the Si mask. This optimization of space allows us to perform additional Er implantation into other substrates (such as GaN) at no cost to the program. Figure 6 shows one of Spire's ion implanters similar to that used in this work.

Rare-earth elements are generally difficult to implant. One method to produce an Er beam is the use of Cl_2 carrier gas. (Note that sputtering of Er is the most reliable way to produce an Er beam. However, sputtering is a very slow and expensive process, and to do so would require major modification of our ion source.) For example, Er, when combined with chlorine, forms erbium chloride ($ErCl_3$) which is generally hydroscopic. As a result, residual compounds collect around the pumps and the source region, and the pumping system can degrade, resulting in a contaminated beam. In addition, elements which have low work functions, including many of the rare-earth elements, are classified as electron emitters. Therefore, as the plasma begins

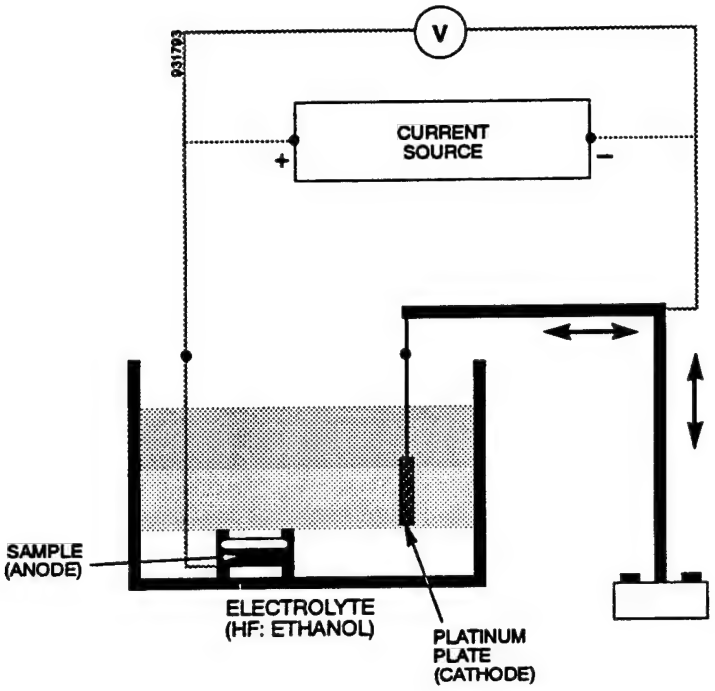

Figure 5 *Schematic diagram of the anodic etching apparatus used at Spire for fabricating porous silicon wafers.*

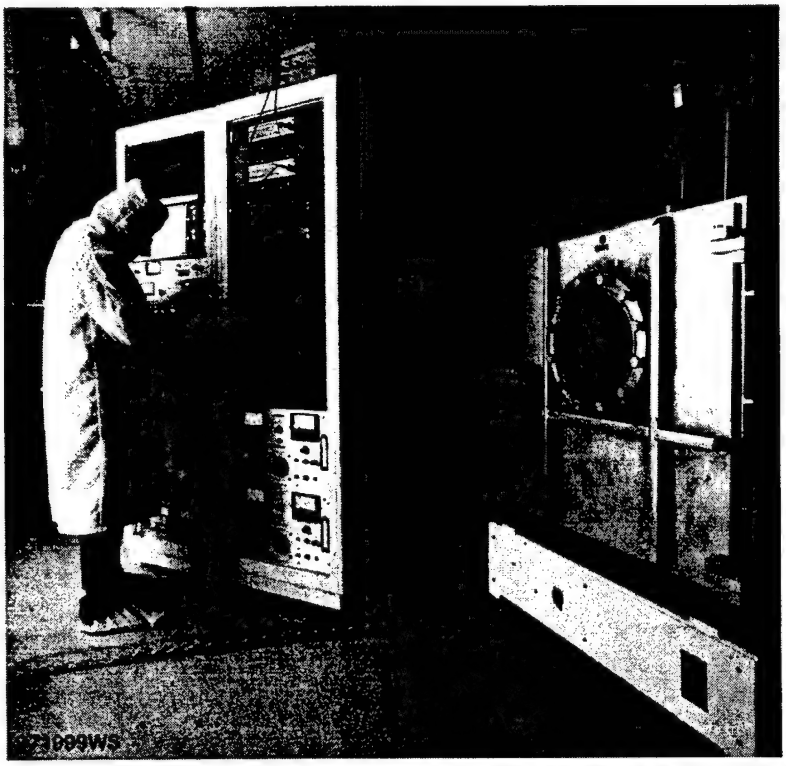

Figure 6 *Spire ion implanter similar to the one used for this research project.*

generating ions, additional electrons are emitted from the $ErCl_3$ coated chamber. The additional generation of electrons interferes with the plasma in the arc chamber resulting in the absence of a beam or one with very low current. To increase the current, the source must be changed and the chamber cleaned.

Special attention to the implanter facility was needed to obtain an uncontaminated beam and a beam with high current density. Therefore, we cleaned the implanter system prior to each Er and Pr implantation. This extra process enables us to achieve a beam with the least probability of contaminants and a higher total current beam.

3.3.1 Erbium

Er was implanted with a dose of $1x10^{15}$ Er/cm^2 at 190 keV and 380 keV into porous Si and Si. Table 1 lists conditions of Er-implanted samples which were metallized with Au and Al. Table 2 lists Er-implanted samples which were contacted using our new method of boron implantation and a Si wafer contact. Annealing of all Er-implanted samples was performed in a conventional furnace in N_2 for 30 to 60 minutes at temperatures ranging from 530-650°C.

3.3.2 Praseodymium

Praseodymium was implanted with a dose of 10^{15} Pr/cm^2 at 380 keV into porous Si, Si, quartz and sapphire. Table 3 lists conditions of Pr-implanted samples. Some of the samples were annealed in a nitrogen ambient at temperatures ranging from 500°C to 650°C for periods of 30 to 60 minutes.

3.3.3 Co-implantation of Er, O and F

It is reported in the literature that co-doping of fluorine with erbium increases the number of optically active erbium centers in a host material. Therefore, we have co-implanted erbium with fluorine in some samples. To determine the optimum conditions, we produced a matrix with various doses of erbium and fluorine. Four doses of erbium ranging from $1x10^{14}$ to $2x10^{15}$ Er^+/cm^2 were implanted. Four doses of fluorine were also implanted ranging from $1x10^{15}$ to $5x10^{16}$ F^+/cm^2. Figure 7 shows the matrix grid with 16 different combination doses. This wafer was annealed in a nitrogen ambient at 600°C for four hours. Samples with each of the different doses were sent to Dr. Jacques Pankove and Dr. Robert Feuerstein's group at the University of Colorado for photoluminescence (PL) and cathodoluminescence (CL) measurements. According to Dr. Feuerstein, PL measurements show room-temperature IR emission from erbium co-implanted with fluorine. PL data on Er- and F-doped bulk Si is presented in a paper submitted for publication through a collaboration with Kewell *et al.* at the University of Surrey (see Appendix A).

Table 1 *Fabrication conditions and visible PL properties of Er-implanted wafers (first batch).*

Sample ID	Metallization	Etch Conditions	Visible PL Intensity	Implant Conditions
SW32-PS1	Back-Au	100 mA 60 min	red-orange	
SW32-PS2	Front-Au	100 mA 60 min	orange	
SW32-PS3	Front-Au	100 mA 60 min	orange	
A1	Front	100 mA 60 min	orange	380 keV Er 1E15
A2	Front	100 mA 60 min	red-orange	380 keV Er 1E15
A3	Back	10 mA 60 min	orange-yellow	380 keV Er 1E15
A4	Front	100 mA 30 min	red	380 keV Er 1E15
A5	Front	100 mA 30 min	red	380 keV Er 1E15
A6	Front	100 mA 45 min	red	380 keV Er 1E15
A7	Back	100 mA 45 min	red	380 keV Er 1E15
A8	Front	10 mA 60 min Additional: 100 mA 30 min	orange-yellow orange-yellow	380 keV Er 1E15
NMK Er4	Back	100 mA 32 min	red	190 keV Er 1E15
NMK Er5	Back	100 mA 32 min	red	190 keV Er 1E15
SS2	p-type Si <100> 0.8 to 1.2 Ω-cm			190 keV Er 1E15
6554-SiA	p-type Si <100> 0.1 to 0.2 Ω-cm			380 keV Er 1E15

Table 2 *Fabrication and annealing conditions of Er-implanted porous Si wafers (second batch).*

Sample ID	Boron Implant for Back Contact	p^+ Wafer used as a Back Contact	Anodic Etching	Er Implantation	Anneal 530°C	Anneal 650°C
RT-1	5E15 20 keV	+	100 mA, 60 min	1E15, 380 keV		+
UN-3	5E15 20 keV	+	100 mA, 60 min	1E15, 380 keV	+	+
RT-7	5E15 20 keV 5E15 60 keV	+	100 mA, 60 min	1E15, 380 keV		+
UN-8	5E15 20 keV 5E15 60 keV	+	50 mA, 30 min 100 mA, 30 min	1E15, 380 keV	+	+
UN-A	–	+	100 mA, 150 min	1E15, 380 keV	+	+

Table 3 *Fabrication and visible PL properties of Pr-implanted wafers.*

Sample ID	Metallization	Etch Conditions	Visible PL Intensity	Implant Conditions
ER1	back	100 mA 90 min	orange-yellow	380 keV Pr 1E15
ER2	back	100 mA 32 min	red	380 keV Pr 1E15
ER3	back	100 mA 32 min	red	380 keV Pr 1E15
6554 (4" Si) p-type, <100> 0.1-0.2 Ω-cm				380 keV Pr 1E15
SS1 (Si) p-type, <100> 0.8-1.2 Ω-cm				380 keV Pr 1E15
Sapphire				380 keV Pr 1E15
Quartz				380 keV Pr 1E15

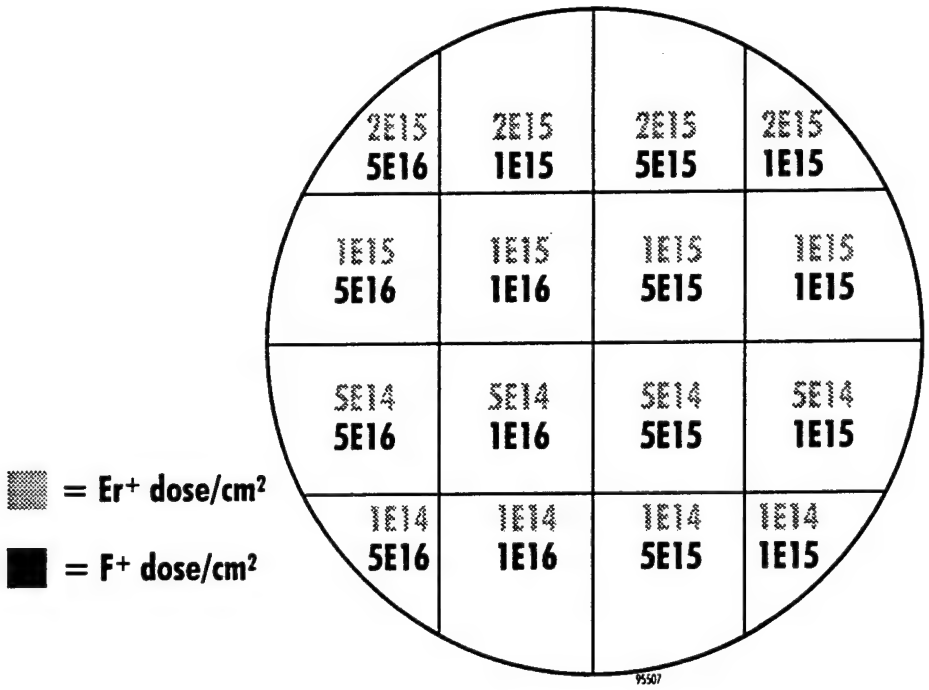

Figure 7 *Schematic of a Si wafer implanted with various doses of erbium and fluorine.*

3.4 Photoluminescence

Visible PL was measured at room temperature using an argon laser with an excitation wavelength at 488 nm and a laser power between 25 and 100 mW. The IR PL was excited with a Coherent Innova 70 Ar^+ laser with either the 457.9, 476.5, 488, 496.5, or 514.5 nm line of the argon beam. The 580 nm output of a dye laser (pumped by the argon laser) was additionally used to excite IR emission. IR PL was carried out for laser powers between 10 and 450 mW. An interference band-pass filter was placed in front of the samples to eliminate plasma lines from the laser beam. The samples were illuminated from the porous side and IR PL was collected at a near-backscattering geometry. An SPEX 1401, 0.75 m double monochromator equipped with a pair of 600 line/mm gratings was utilized for the IR PL studies. The PL signal was detected by a liquid nitrogen cooled Northcoast Ge detector. A thin GaAs wafer polished on both sides or a 850 nm long pass filter (Schott RG 850) was placed in front of the collecting lens of the detector to filter lines from the second- and third-order grating scattering. Both entrance and exit slits of the monochromator were set at 1000 μm, resulting in a spectral resolution of ~ 1 nm, which was much smaller than the Er peak widths (≥ 7 nm) observed from the samples. The PL signal was processed using standard lock-in amplifier technique. For the excitation wavelength dependence study, the laser power was set constant to 15 mW. In the power-temperature dependence study, the sample was irradiated with a focused excitation beam having a spot size diameter of 1 mm and the power was varied between 20 and 300 mW. The spectral resolution in the IR PL measurements was 1.6 nm.

In all experiments cooling was achieved by mounting the sample onto the cold finger of a closed cycle helium refrigerator. The refrigerator allowed us to perform studies in the temperature range from 15 to 300K. The PL spectra were not corrected for the spectral response of the system.

For photoluminescence excitation (PLE) measurements, an optical parametric oscillator (Surelite OPO, Continuum) pumped by a Q-switched Nd:YAG laser (Surelite II, Continuum) was used as the excitation source. The PL signal was recorded as the ratio between PL intensity and excitation power, and included the system response. The signal was processed by a boxcar averager (SR250 Stanford Research Systems). The sample was cooled on the cold finger of a two-stage closed-cycle refrigerator capable of reaching a temperature of 12K.

For time resolved PL measurements, a 400 mW, 488 nm Ar^+ laser beam was mechanically chopped at 50 Hz. A digital storage oscilloscope or a boxcar averager was used to acquire the decay transients.

3.5 Device Fabrication

We have fabricated impact-excited and injection-induced IR-emitting devices from Er-implanted porous Si. Since the lateral conduction of current is impeded by the presence of voids in porous Si, the design of ohmic contacts to porous Si plays an important role in optimization of the current conduction and the light collection efficiencies. Ti/Pd/Au ohmic contacts were deposited using various shadow masks on the porous surface and substrate sides of the wafers. Details of contact deposition and shadow masks are discussed later.

4 EXPERIMENTAL RESULTS

Although the focus of this work is to fabricate Er-doped porous Si LEDs, extensive work was required to understand the mechanism involved in Er emission in porous Si. In order to fabricate working devices, we needed to increase the efficiency of Er luminescence in porous Si. To do this, one must understand the interactions between Er and porous Si. We also analyzed the many parameters which influence Er luminescence. First, we determined what type of porous Si was suitable as a substrate for Er implantation, and also what processing conditions would yield the best porous Si.

In the following we present data from wafers which were produced for device fabrication, and data from measurements which were carried out to determine the dependence of luminescence on porous Si material and optical characteristics.

4.1 Photoluminescence of Er^{3+}:Porous Si

4.1.1 Dependence of IR Emission on Annealing Temperature

It is well known that post-implantation anneal conditions play an important role in optimizing the near-IR PL emission intensity in Er-implanted materials. Thus we have carried out a systematic annealing study in order to optimize the room-temperature near-IR emission from Er:porous Si. We have annealed our samples in N_2 atmosphere for 30 minutes at various temperatures. Figure 8 shows the room-temperature near-IR PL spectra of as-implanted and annealed (500, 530, 650, and 850°C) Er:porous Si. From these results, it is clear that annealing Er:porous Si at 650°C for 30 minutes in N_2 yields the strongest near-IR PL emission at room temperature.

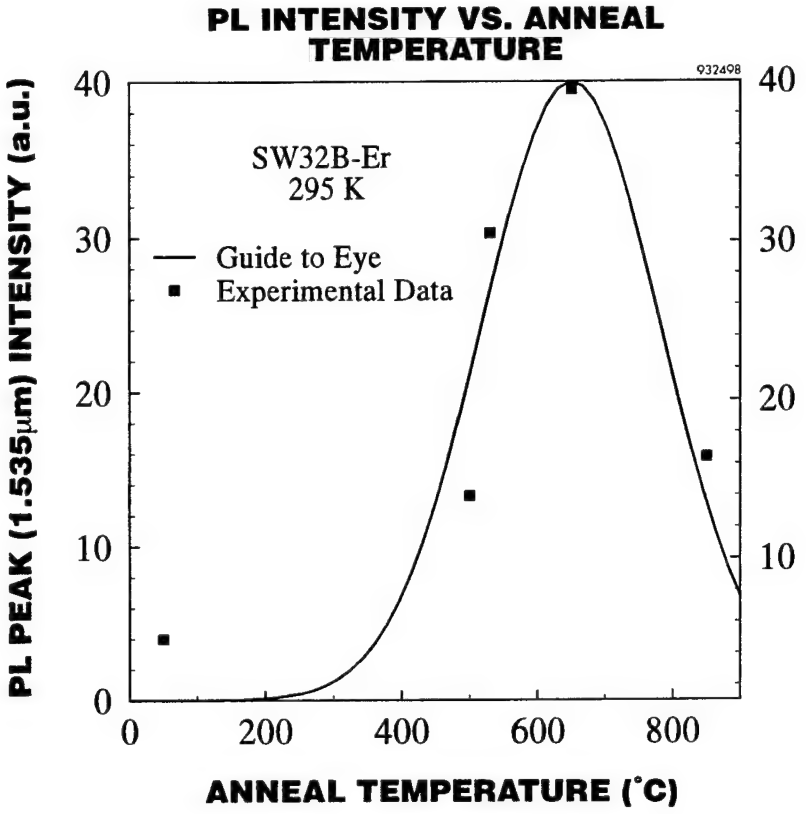

Figure 8 *Room-temperature PL spectra of as-implanted and annealed Er:porous Si samples. Erbium was implanted with a fluence of $10^{15}/cm^2$ at 190 keV and annealed at different temperatures.*

Figure 9 compares the visible and near-IR PL intensities of Er:porous Si as a function of annealing temperature. There is an inverse relationship between the near-IR and the visible PL emission from Er:porous Si for all annealing temperatures. Note that the Er:porous Si samples annealed at 650°C show maximum near-IR intensity and minimum visible emission intensity. However, it should be noted that the visible emission intensity in porous Si samples without implantation *also* exhibits identical annealing temperature dependence.

4.1.2 Origin of Strong 1.54 μm Emission in Er-implanted Porous Si

Erbium-implanted porous Si emits strongly at 1.54 μm at room temperature. Figure 10 compares room-temperature IR PL spectra of a typical Er-implanted ($10^{15}/cm^2$, 190 keV) porous Si sample with a device-quality, 2-μm $In_{0.53}Ga_{0.47}As$ film grown on InP substrate. $In_{0.53}Ga_{0.47}As$ is a direct-bandgap material which is used for room-temperature, commercial IR LEDs. Note that the intensity of IR emission from Er:porous Si is approximately 8% of that of $In_{0.53}Ga_{0.47}As$.

Erbium, when implanted into porous Si, can be incorporated in the oxidized surface regions of porous Si (SiO_2), the unetched bulk Si, or the columns of porous Si. Thus, in an attempt to investigate the origin of the strong 1.54 μm PL emission from Er:porous Si, we have compared its IR PL spectra to Er:crystalline Si and Er:quartz (crystalline SiO_2).

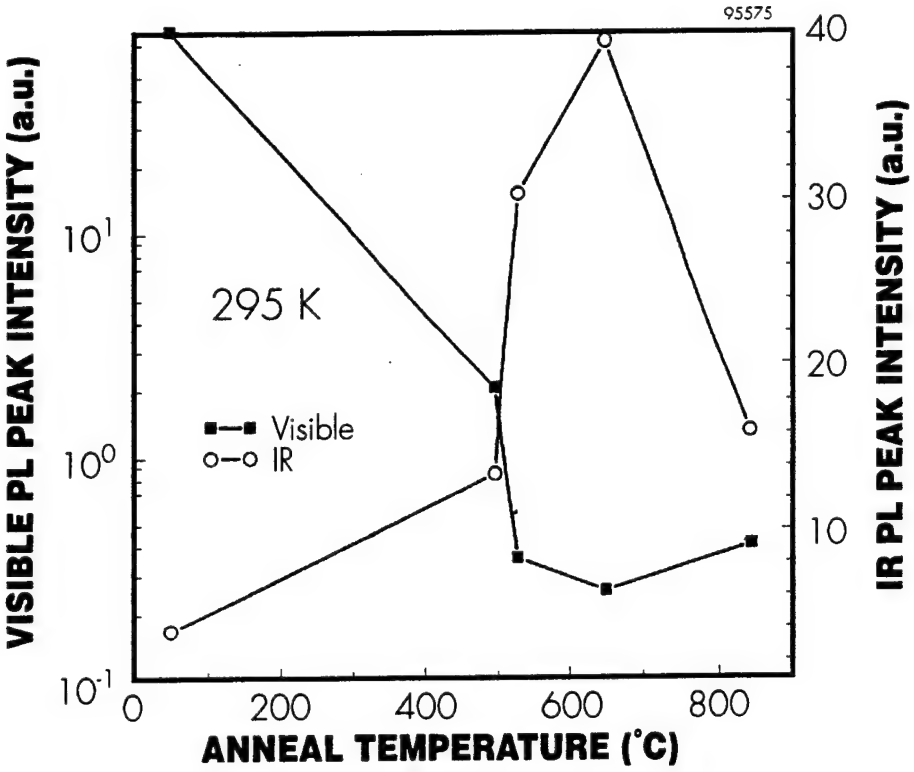

Figure 9 *Comparison of visible PL emission and near-IR PL emission from Er:porous Si as a function of post-implantation anneal temperature. Erbium was implanted with a fluence of 10^{15} Er^{+}/cm^{2} at 190 keV.*

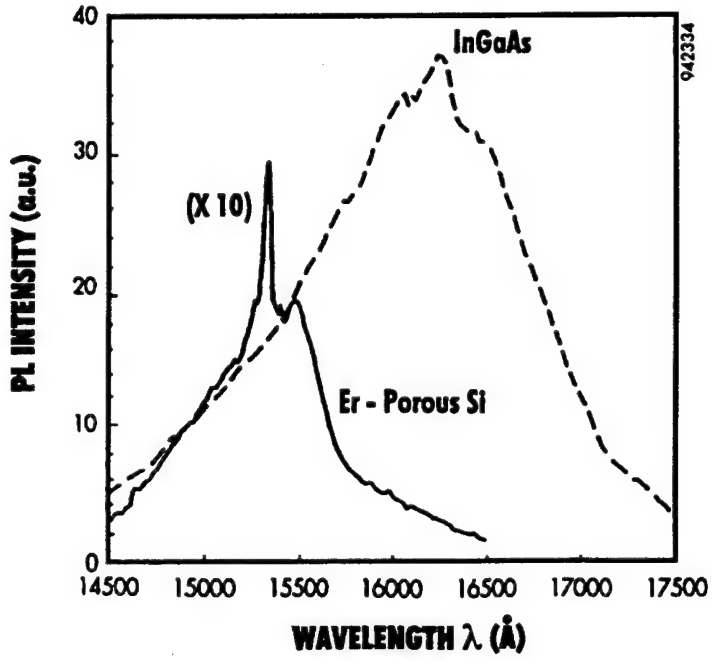

Figure 10 *Room temperature IR PL spectra from Er-implanted ($10^{15}/cm^{2}$, 190 keV) porous Si and a 2-μm thick device-quality, highly doped ($10^{17}/cm^{3}$), lattice-matched $In_{0.53}Ga_{0.47}As$ film grown on InP.*

Erbium was implanted into porous Si, bulk Si, and quartz with a dose of 1 x 10^{15}/cm^2 at 190 keV and annealed for 30 minutes in N_2 at temperatures ranging from 500°C to 900°C under identical conditions. No RT infrared (IR) emission was observed from Er-implanted quartz and silicon after annealing at 650°C (although after annealing at 900°C very weak emission was observed from quartz at 9K). The highest RT emission intensity at 1.54 μm was from Er:PSi with a peak concentration of 1.5 x 10^{20}/cm^3 and annealed at 650°C. The Er depth profile and concentration were determined from Rutherford backscattering data (see Figure 11). The luminescence intensity from Er:PSi annealed at 500°C was about 26 times higher than that observed from quartz implanted with Er at 400 keV and annealed at 900°C (see Figure 12). We observed a reduction in photoluminescence (PL) intensity of only about a factor of two from Er:PSi over the 9 to 300K temperature range.

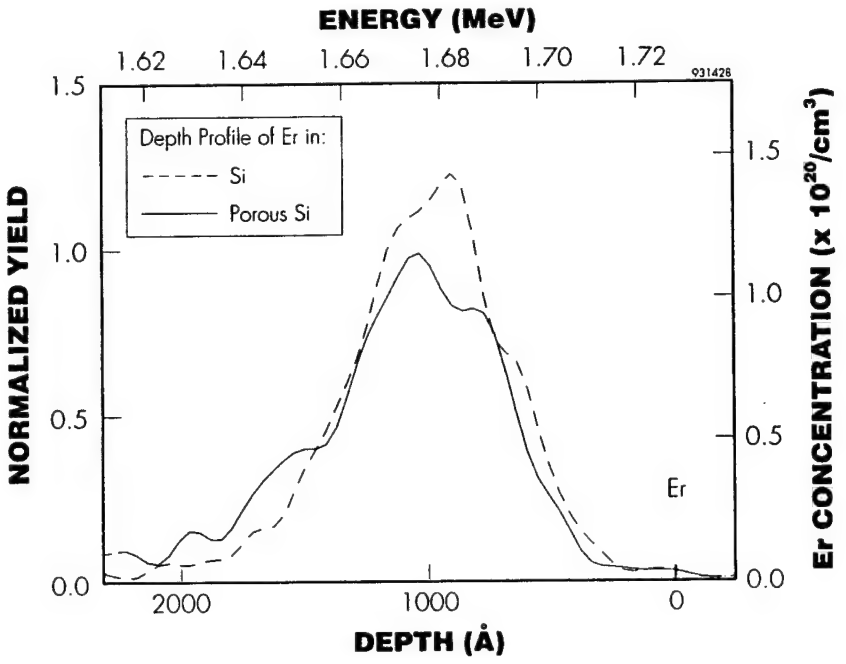

Figure 11 *Comparison of concentration depth profiles of Er-implanted at 190 keV into porous Si and bulk Si.*

The strong IR (1.54 μm) emission from Er:porous Si, compared with that from Er:Si and Er:quartz, suggests that Er is not in SiO_2 or Si with bulk properties, but may be confined in Si with quantum-confined properties. Preliminary data indicate that porous Si is a good substrate for rare-earth elements because a high concentration of optically active Er^{3+} can be obtained by using a commercial ion implanter which operates below 200 keV.

Self-absorption of visible light emission in porous Si imposes a restriction on the fabrication of visible light-emitting devices (LEDs). However, since porous Si and Si are transparent to 1.54 μm wavelengths, fabrication of IR LEDs is simplified. Furthermore, we anticipate that it may be possible to use visible light emission from porous Si to pump Er^{3+}.

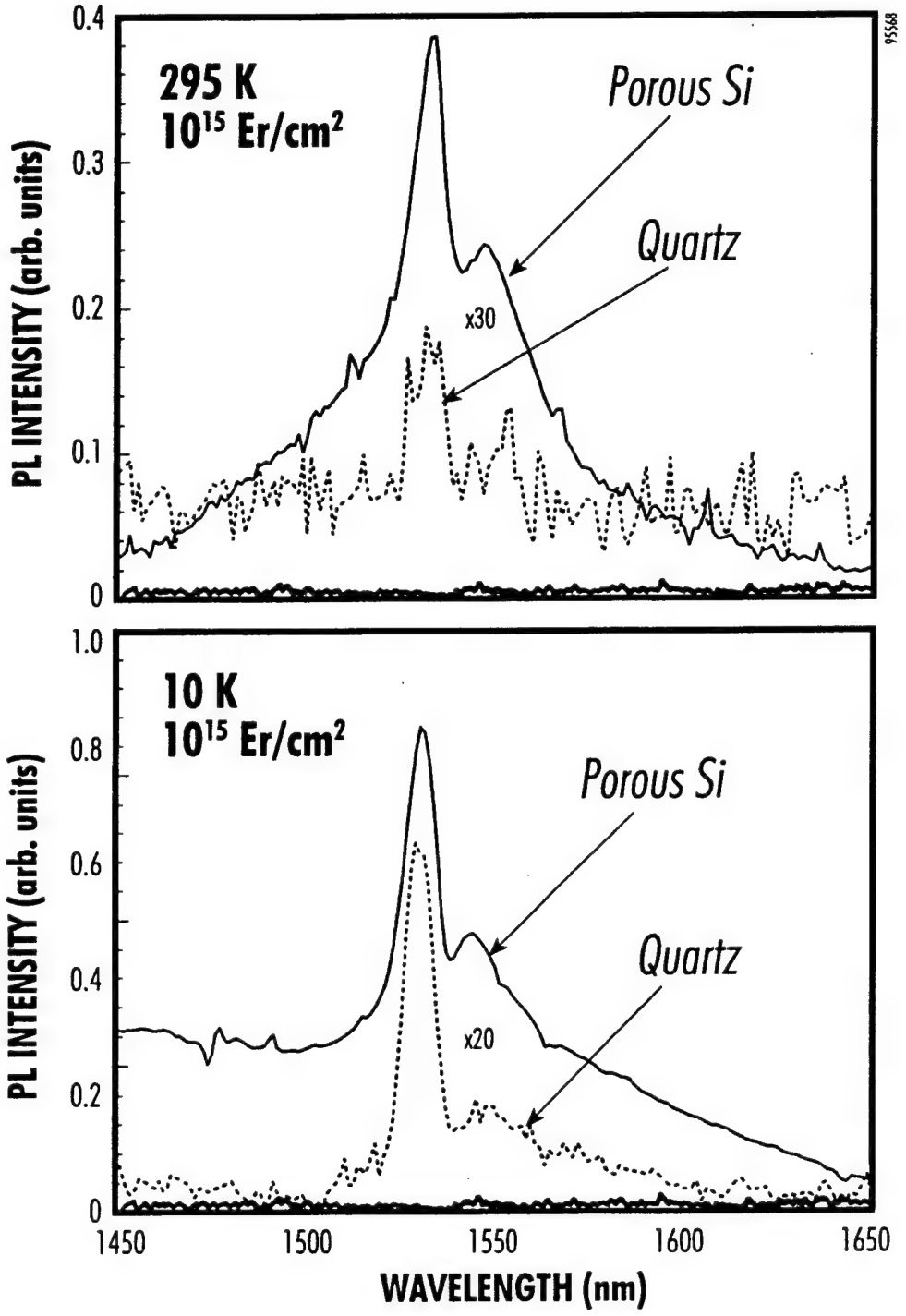

Figure 12 *IR PL spectra of Er-implanted bulk Si, quartz and porous Si measured at 300K and 10K. Erbium was implanted with a dose of 10^{15} Er^{+}/cm^{2}. As shown, strong IR emission was observed for Er implanted at 190 keV into porous Si and annealed at 650°C. In contrast, no IR emission was observed for bulk Si or quartz under identical conditions. The spectra shown is from Er implanted at 400 keV into quartz and annealed at 900°C.*

4.1.3 Temperature Dependence

Realization of optoelectronic devices based on erbium-doped porous silicon depends on the intensity and temperature stability of the Er^{3+} emission at and above room temperature. One of the problems facing the development of rare-earth-doped materials and devices is the strong thermal quenching of Er^{3+} emission in many host materials near room temperature. The temperature-dependent measurements of PL intensity and its time decay behavior have been shown to be valuable in understanding the excitation and de-excitation mechanisms of Er^{3+}.[26,27] We have investigated the temperature dependence of 1.54 μm PL emission intensity and its decay lifetime in Er-implanted porous silicon. From this study, we propose a mechanism for the excitation and relaxation of Er^{3+} ions in porous silicon.

We have studied temperature dependence of Er^{3+} emission in porous Si from liquid helium to room temperature, and we have determined that this dependence is partially due to the porosity of the sample. In actual applications of Er^{3+}: porous Si devices, one would expect the operating temperature to rise above room temperature; therefore, we have carried out sets of measurements by heating our samples to about 475K.

Figure 13 shows 1.54 μm PL spectra of Er^{3+}:porous Si measured from (a) 10 to 295K, and (b) from 300 to 455K. The full width at half maximum (FWHM) of the main 1.54 μm PL peak is about 8 nm. This relatively large line width, compared to the reported value of ~ 1.9 nm (1 meV) for Er^{3+}:Si, suggests that the Er^{3+} ions occupy a range of sites, and that the emission spectrum is mainly inhomogeneously broadened. Figure 14 shows the temperature dependence of the integrated PL intensity. Note that the integrated intensity at room temperature is about 60% of that at 15K. The temperature dependence of 1.54 μm emission from Er:porous Si is comparable to the result reported for Er:3C-SiC[28]. Figure 15 shows a comparison of temperature dependence of 1.54 μm PL emission in Er:porous Si and Er:3C-SiC. The solid triangular symbol represents the data for Er^{3+}:3C SiC, and the open square symbol represents that for Er^{3+}:porous Si. The dashed line through the Er^{3+}:porous Si data points is drawn to guide the eye. We compare our results with Er^{3+}:3C SiC because of the closeness of the bandgap (bandgaps of porous Si and 3C SiC are ~ 1.9 eV and 2.3 eV, respectively). These results indicate that porous Si is an excellent host material for Er^{3+} emission at 1.54 μm.

4.1.4 Excitation Power Dependence

If Er^{3+} ions are not directly excited, then they are most likely excited through the recombination of an electron-hole pair bound to the Er center. Assuming that the recombination energy of this electron-hole pair is nonradiatively transferred either (1) to a conduction electron (Auger process) or to (2) the Er^{3+} ion, Benyattou *et al.*[29] have shown that the 1.54 μm PL intensity (number of excited Er^{3+} ions) is proportional to the square root of the excitation power. In this two-channel nonradiative recombination scheme, the rate of increase of excited Er^{3+} ions (n^*) can be written in the form:

$$\frac{dn^*}{dt} = AI\frac{Pe}{Pe + C\sqrt{I}} - \frac{n^*}{\tau} \qquad (1)$$

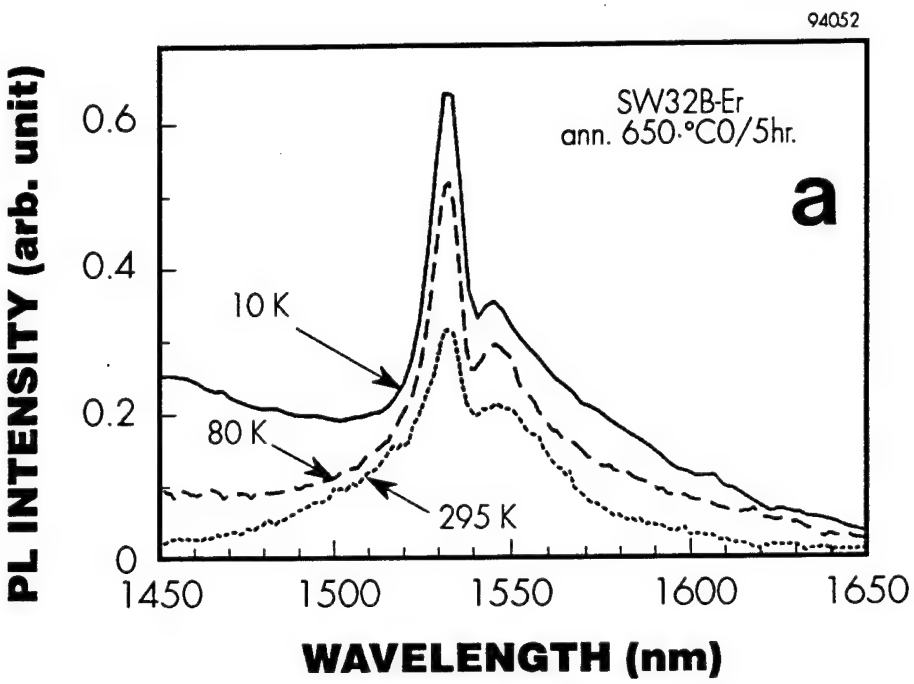

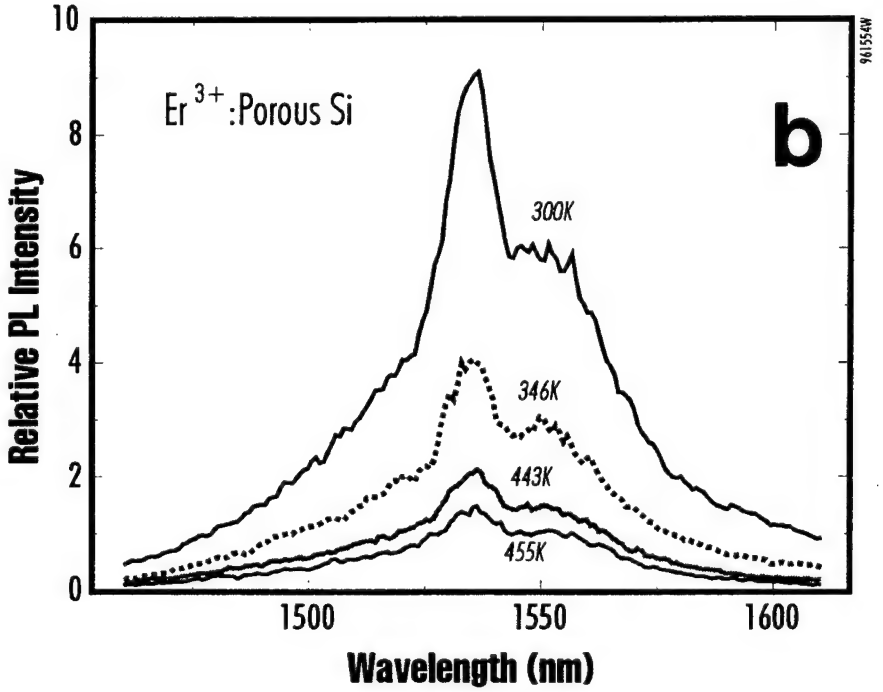

Figure 13 *1.54 μm PL spectra of Er^{3+}:porous Si measured from (a) 10 to 295K, and (b) from 300 to 455K.*

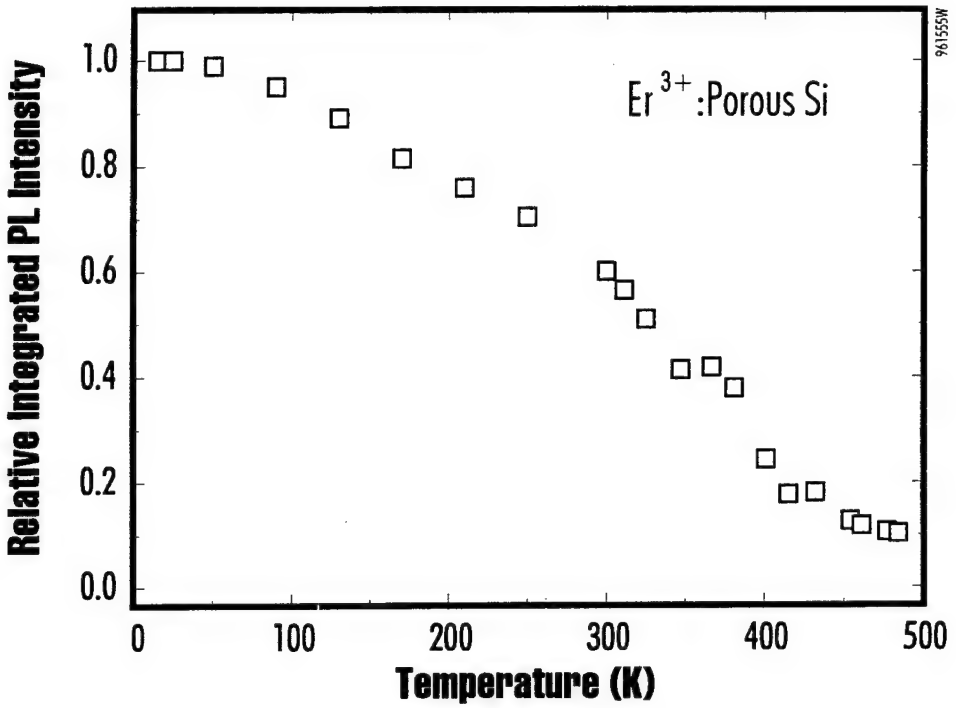

Figure 14 *Normalized 1.54 μm integrated PL intensity of Er^{3+}:porous Si measured from 15K to 475K.*

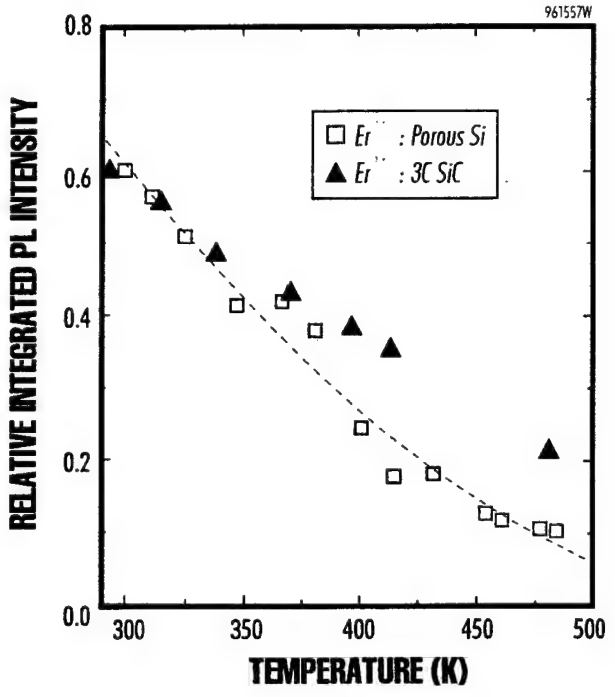

Figure 15 *Comparison of temperature dependence of 1.54 μm PL emission in Er:porous Si and Er:3C-SiC.*[28]

where A is the number of created bound electron-hole pairs, P_e is the probability of energy transfer to the Er^{3+} ion, I is the excitation intensity and τ is the fluorescence decay time constant of the first excited state $^4I_{13/2}$ of Er^{3+}. $C\sqrt{I}$ is the Auger recombination probability, assuming a bimolecular recombination of the photogenerated carriers. At pump powers for which the Auger process is dominating, *i.e.*, $C\sqrt{I} >> P_e$, the steady state situation can be written as follows:

$$n^* = \frac{\tau A P_e}{C}\sqrt{I} \qquad (2)$$

The 1.54 μm PL intensity is proportional to the number density of excited erbium ions (n^*). Therefore, the 1.54 μm PL intensity is proportional to the square root of the excitation power. In order to investigate the dependence of 1.54 μm luminescence on pumping power, we have carried out a systematic PL study at different temperatures. The samples were excited using the 514.5 nm line of an Ar ion laser. Figures 16 and 17 show the 1.54 μm PL intensity measured from 15K to 300K as a function of excitation power (mW) and square root of excitation power ($mW^{1/2}$), respectively. PL intensity is proportional to the square root of the excitation power below 150 mW at all measured temperatures above 75K. From these results, it is clear that a model similar to that described by Benyattou *et al.*[29] can describe the Er^{3+} excitation process in Er:porous Si.

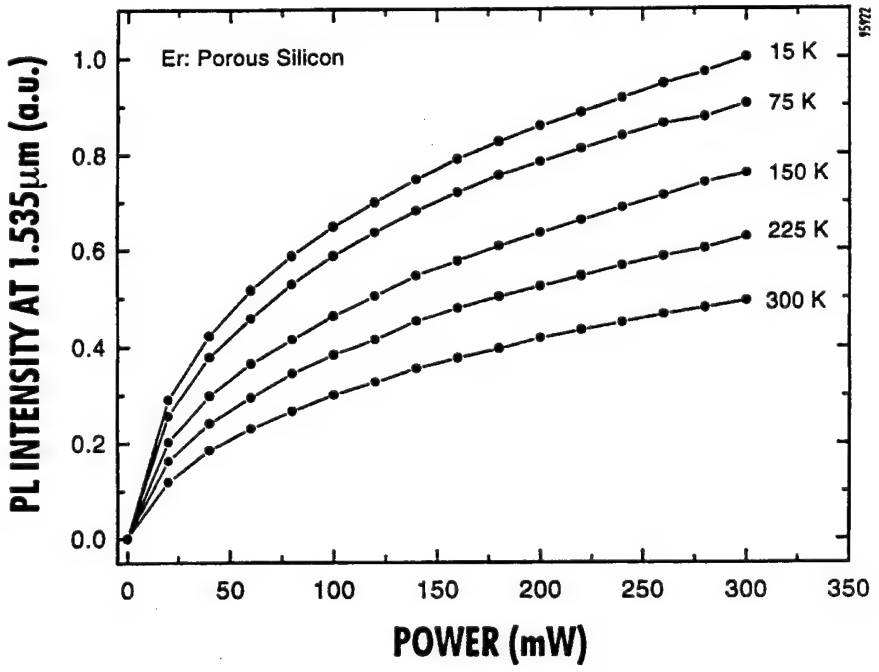

Figure 16 *PL intensity as a function of linear excitation power for Er:porous Si.*

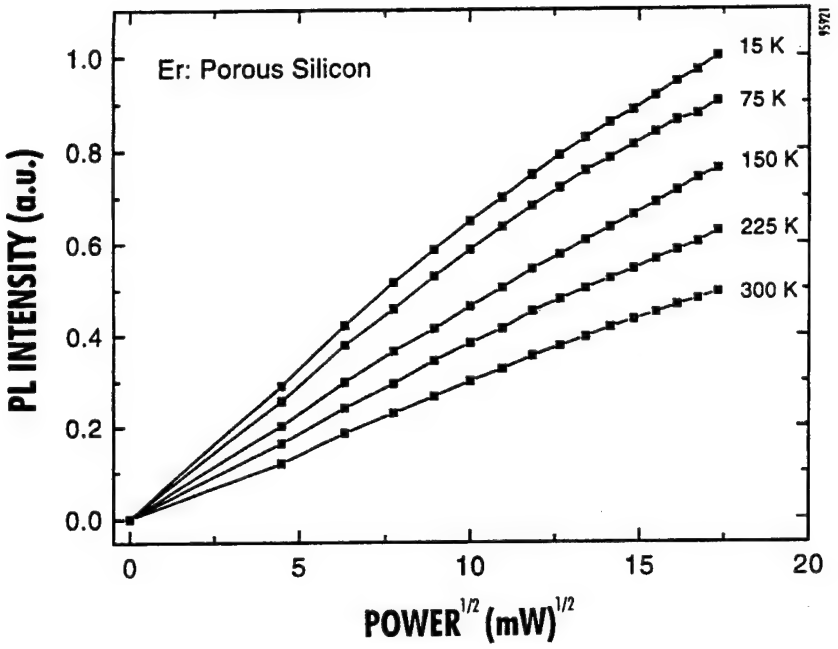

Figure 17 *PL intensity as a function of square root of excitation power for an Er-implanted porous Si sample.*

The 1.54 μm PL intensity in Er:porous Si increased rapidly with pump powers up to 150 mW at all temperatures and saturated at higher powers. The sublinear power dependence of the Er PL intensity above 150 mW indicates the onset of PL saturation;[32] however, complete saturation (which means that all optically active Er^{3+} ions are excited) was not obtained. It should be noted that the shapes of the curves after correction for thermal quenching effects were similar (less than 5% deviation); hence, the pump power at which complete saturation occurs will be temperature independent. We believe that the concentration of optically active Er^{3+} ions in Er:PSi must be high. Similar to Er- and O-doping in bulk Si, additional oxygen co-doping in Er:PSi may increase the Er^{3+} concentration further.

4.1.5 Excitation Wavelength Dependence

4.1.5.1 PLE Measurements on Er-implanted Porous Si

Photoluminescence excitation spectroscopy (PLE) is a valuable experimental tool to probe the different groups of crystal field split energy levels of Er^{3+} and thereby investigate the different types of Er^{3+} centers in Er doped semiconductors, if direct excitation of Er^{3+} is possible. In this technique, the intensity of the luminescence wavelength of interest (1.54 μm) is recorded as a function of excitation wavelength. Corrections should be made for the spectral responses of the detector and the monochromator and spectral line shapes in this range of excitation wavelengths. Thus, the low temperature PLE measurements could provide information on different types of Er^{3+} centers and their site symmetries in Er doped semiconductors. By studying the thermal quenching properties of these individual Er^{3+} centers and correlating these centers to certain impurities or defects, it may be possible to optimize performance of 1.54 μm Er^{3+} emission in Er-doped semiconductors.

Furthermore, the possibility of direct excitation of Er^{3+} ions in Er doped semiconductors will be advantageous since commercially available diode laser sources (980 nm for example) can be used to excite 1.54 μm Er^{3+} luminescence without being influenced by the host material properties. For example, commercially available laser sources operating at 650, 800 and 980 nm can be used to excite the Er^{3+} ions from the ground state $^4I_{15/2}$ to the excited states $^4F_{9/2}$, $^4I_{9/2}$ and $^4I_{11/2}$, respectively. However, due to the complex nature of the Er^{3+} centers, it has not always been possible to excite the Er^{3+} ions directly.

We have carried out photoluminescence experiments on Er^{3+}:porous Si samples in an attempt to understand the excitation mechanism of Er^{3+} ions in Er^{3+}:porous Si. Several discrete excitation wavelengths including 488, 514.5, 800 and 980 nm have been used. There are relatively narrow absorption bands of Er^{3+} around 488, 514.5, 800 and 980 nm which correspond to transitions[1] of $^4I_{15/2} \rightarrow {}^4F_{7/2}$, $^4I_{15/2} \rightarrow {}^2H_{11/2}$, $^4I_{15/2} \rightarrow {}^4I_{9/2}$ and $^4I_{15/2} \rightarrow {}^4I_{11/2}$. If the Er^{3+} ions are directly excited then we should observe a significant increase in Er^{3+} related PL intensity for the above excitation wavelengths.

Figure 18 shows room-temperature 1.54 μm PL spectra of Er:porous Si excited with excitation wavelengths 457.9, 476.5, 488, 496.5 and 514.5 nm. The insert shows a schematic energy level diagram of Er^{3+} determined for Er-doped glasses.

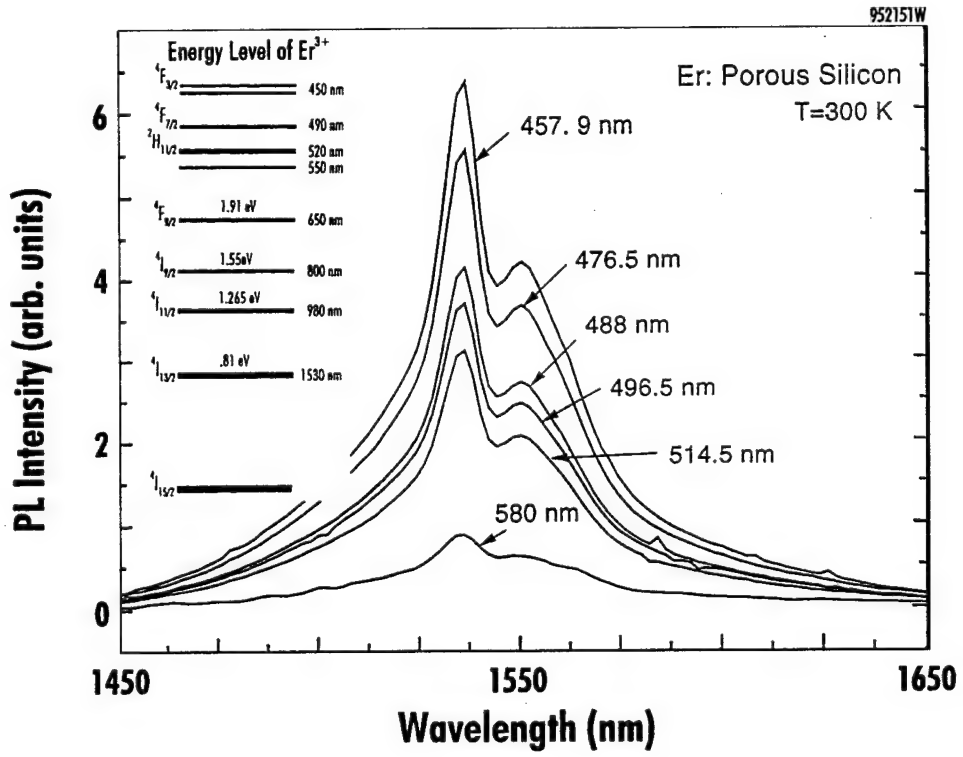

Figure 18 *Room temperature 1.5 μm photoluminescence spectra of Er:porous Si excited with different excitation wavelengths. The insert shows the energy level of Er^{3+} determined for Er in glasses.*

There is no observable change in spectral line shape for these different excitation wavelengths. However, the intensities decrease with increasing wavelength. No IR emission from Er was observed when samples were excited at 980 nm with 100 mW power. The IR emission was observed only for excitations above the bandgap of porous Si (>1.9 eV). These results indicate that there is no direct excitation of Er^{3+} ions in Er:porous Si, and the excitation energy transfer is mediated by photogenerated carriers. The decreasing PL intensities for increasing excitation wavelengths could be explained by the wavelength dependent absorption and will be discussed in Section 4.1.5.2. A decrease in absorption within porous Si leads to a decrease in the number of photogenerated carriers near the surface where Er atoms reside, resulting in a decrease in the 1.54 μm PL intensity. Note that our RBS studies show that the penetration depth of implanted Er at 380 keV is approximately 2500Å.

We have also studied the visible PL spectra of the sample shown in Figure 18, using different excitation wavelengths in order to investigate the visible spectral line shapes for these excitation wavelengths as well as its relation to IR PLE. The changes in spectral line shapes for these excitation wavelengths are negligibly small. Thus, the error in PLE measurements resulting from changes in luminescence spectral line shapes for different excitation wavelengths will be neglected.

Figure 19 shows photoluminescence spectra of Er:PSi samples with two different porosities. Sample A's visible emission peaked at 750 nm and sample B's visible emission peaked at 650 nm. In the second year of the program we had the opportunity to measure PLE spectra using continuous excitation wavelengths. In the new experimental setup, we have been able to measure PLE spectra of both the substrate (visible light emission from porous Si) and Er:porous Si (1.54 μm).

Figure 20 shows photoluminescence excitation spectra (PLE) in the visible and near infrared from the same Er:porous Si sample. The visible luminescence was monitored at 750 nm (sample A) and the IR emission was observed at 1.54 μm at 15K. The PLE spectra are essentially the same for both visible (porous Si) and IR (Er^{3+}) emission from Er:porous Si. A significant increase in the PLE signal is observed for both visible and IR emission for excitation wavelengths around 600 nm (~ 2 eV). The onset of PLE signal for the visible emission is indicative of the band gap of the porous Si material and was observed at shorter wavelengths for samples with higher porosities (see Figure 21) consistent with their higher bandgaps. This observation indicates that the excitation of Er^{3+} in Er:porous Si is a photo-carrier mediated process. Further more, the nearly identical PLE spectra for visible and IR emissions suggest that the Er^{3+} ions are located in the nanograins of porous Si.

4.1.5.2 Calculation of Photocarrier Generation rate Rs a Function of Excitation Wavelength in Er-implanted Porous Si

As a first step to understand the mechanism of optical excitation of Er^{3+}, we have calculated the number of photocarriers generated as a function of wavelength. Consider a semi-infinite slab of p-type silicon, with a photon flux, $\Phi(x)$ ($x = 2500$; the penetration depth of Er implanted in Si at 380 keV), in the material given by:

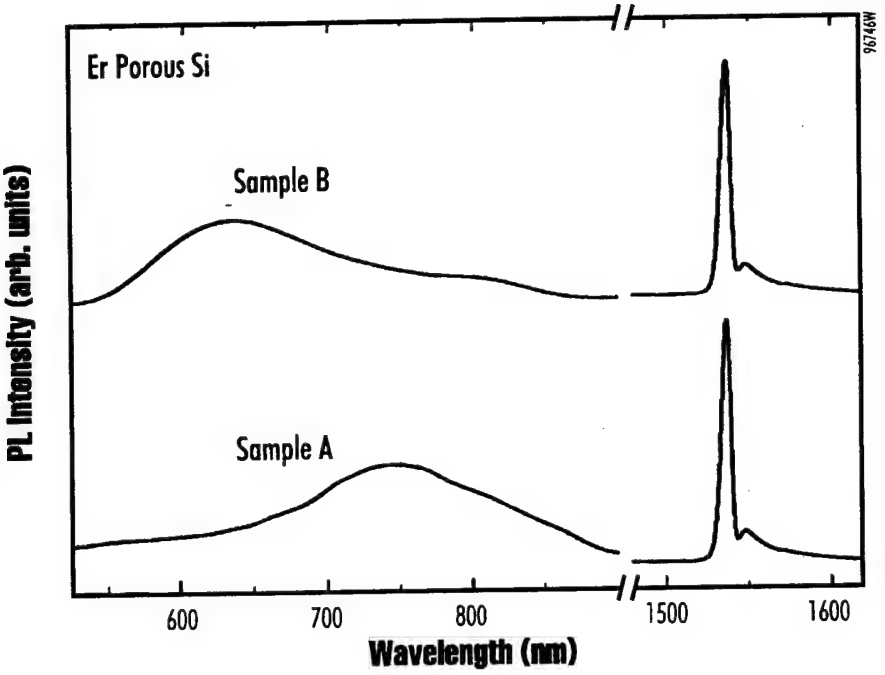

Figure 19 *Photoluminescence spectra of Er:porous Si samples with two different porosities. The porosity of sample A (visible PL peaked at 750 nm) is less than that of sample B (visible PL peaked at 650 nm).*

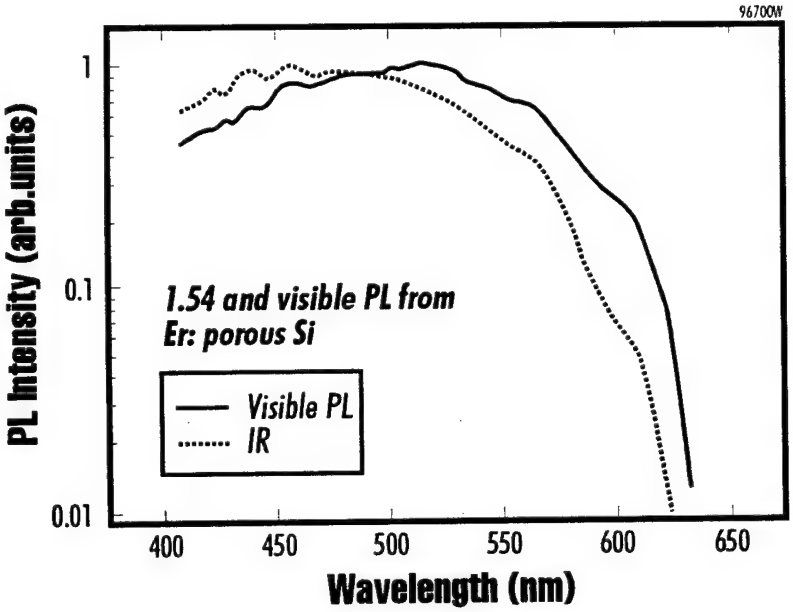

Figure 20 *Comparison of PLE of 1.54 μm and visible (PL peaked at 750 nm) emissions from Er-implanted porous Si.*

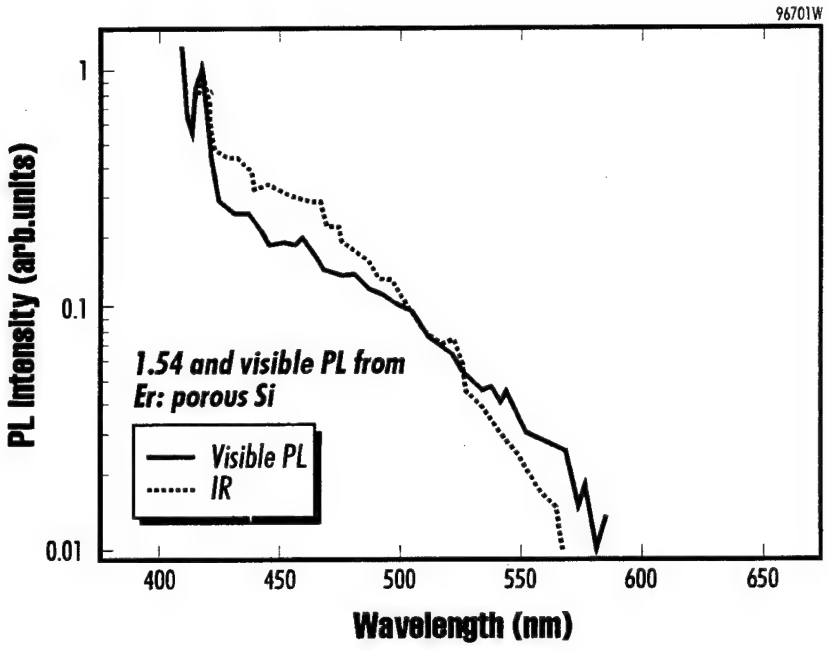

Figure 21 *PLE of 1.54 μm and visible (PL peaked at 660 nm) emissions from Er implanted porous Si with higher porosity.*

$$\Phi = \Phi_0 e^{-\alpha x} \tag{3}$$

where Φ_0 is the incident photon flux on the slab surface and $\alpha(\lambda)$ is the absorption coefficient. Then the generation rate of electron-hole pairs, $G(x)$, is[33]

$$G(x) = \alpha\, \Phi_0 e^{-\alpha x} \tag{4}$$

Under steady-state excitation, the number of minority carrier electrons created in the p-layer, n_p, is given by:[34,35]

$$D_n \frac{d^2 n_p}{d x^2} - \frac{n_p - n_{p_0}}{\tau_n} + G(x) = 0 \tag{5}$$

where D_n is the minority carrier diffusion coefficient, τ_n is the minority carrier lifetime, and n_{po} is the equilibrium electron density. The boundary conditions are equilibrium at large distances from the surface and the surface recombination boundary condition at x = 0, *i.e.*,

$$n_p = n_{p0}, \text{ at } x \to \infty \tag{6}$$

$$D_n \frac{d(n_p - n_{p_0})}{dx} = S(n_p - n_{p_0}), \text{ at } x \to \infty \quad (7)$$

The solution to equation (3) with boundary conditions (4) and (5) is:

$$n_p - n_{p_0} = C_1[e^{-\alpha x} - \frac{\alpha D_n + S}{D_n + S L_n} L_n e^{-x/L_n}] \quad (8)$$

where

$$C_1 = \frac{\Phi_0}{D_n}[\frac{\alpha L_n^2}{1 - \alpha^2 L_n^2}] \quad (9)$$

L_n is the minority carrier diffusion length (= $\sqrt{(D_n \tau_n)}$), and S is the surface recombination velocity.

The first term on the right-hand side of equation (8) is the number of electron-hole pairs created by photon absorption, per unit volume. The second term represents the loss of carriers due to both diffusion away from the absorbing region and surface recombination. For a surface layer of finite thickness t such as the Er-implanted layer, the total number of electron-hole pairs N created in that layer is given by the integral of equation (8), or:

$$N = \int_0^t n_p(x)dx \approx C_1\{\frac{-1}{\alpha}[e^{-\alpha t} - 1] + \frac{\alpha D_n + S}{D_n + S L_n} L_n^2 [e^{-t/L_n} - 1]\} \quad (10)$$

This is the total number of electron-hole pairs created by the incident flux Φ_0, per unit illuminated surface area. Using standard values from silicon for α vs. wavelength, equation (8) has been calculated and is shown in Figure 22. Here the calculated line represents N for an Er-implanted porous layer thickness t of 2500Å. Also shown in the figure is the measured dependence of both visible and infrared (1.54 μm) PL intensity vs. incident wavelength. Both the calculated and measured values have been normalized to the value obtained for the shortest measured wavelength, 457.9 nm. These results clearly show that the measured dependence of PL intensity on excitation wavelength is due to the absorption characteristics of the pump photon. That is, as the pump wavelength becomes shorter, the absorption coefficient is higher, resulting in more electron-hole pairs being created near the surface. Since the porous structure is like a sponge of interconnected 50Å grains, the carriers cannot diffuse very far before recombining. This means that more carriers stay around the implanted Er at the surface of the porous layer and for longer than would be the case in ordinary materials such as silicon. This in turn results in a proportionally higher excitation rate of Er-related emission. In silicon, the large diffusion lengths (~ 100 μm) and long minority carrier lifetimes (~ 1 ms) allow the carriers to diffuse away from the surface layer before they can recombine and excite the erbium. In Figure 23, a comparison of porous silicon and bulk silicon is shown where carrier lifetimes and diffusion lengths appropriate to each have been used in the calculation. Another way of discussing this is as follows: In bulk silicon, incident photons are absorbed near the surface by creation of electron-hole pairs. Since the diffusion coefficient is large, the excess carriers created by the

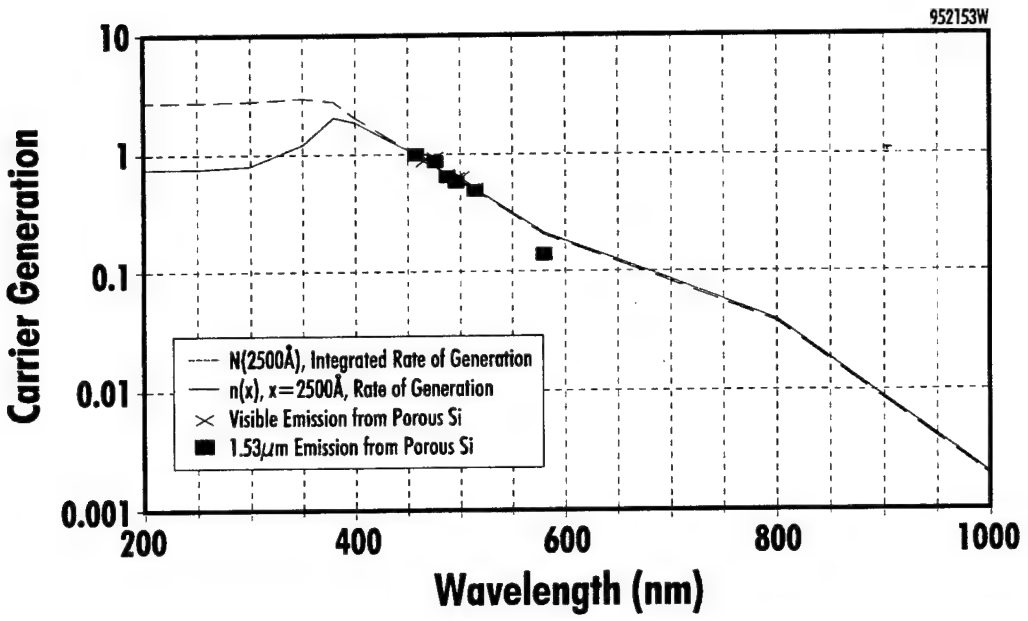

Figure 22 *The number of carriers generated at different excitation wavelengths are superimposed well on experimental PLE data for visible and IR emission from Er:porous Si.*

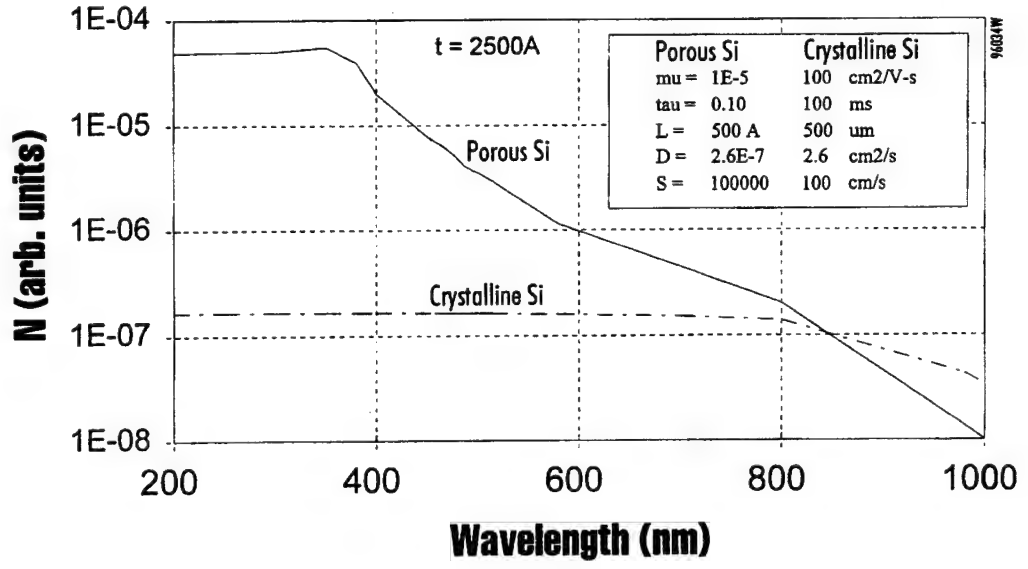

Figure 23 *Carriers generated for excitation wavelength from 200 to 1000 nm for bulk Si and porous Si with a thickness of 2500Å. For wavelengths shorter than 400 nm, carriers are influenced by surface recombination.*

light diffuse away rapidly and before they can interact with the implanted erbium. Therefore, Er emission from bulk silicon will be low. In the case of porous silicon, incident photons are also absorbed near the surface by creation of electron-hole pairs.

However, the porous nature of the film prevents the excess carriers from diffusing away from the surface. They are confined by the discrete nature of the film to stay where they are created, in the vicinity of the implanted Er, until they recombine. Based on these results, even non-quantum mechanical confinement (nanostructure confinement with dimensions > 50Å) of the electron-hole pairs would work as far as the excitation mechanism is concerned and sufficient optically active Er is present.

4.1.6 Photoluminescence Lifetime Studies

In order to enhance our understanding of the basic physics involved in the excitation and relaxation processes of Er^{3+} in Er:porous Si, we have also measured the lifetime of 1.54 μm PL emission from Er^{3+} porous Si at different temperatures. Figure 24 shows the time decay temperature dependence of 1.54 μm PL in Er^{3+}: porous Si. The decay consists of a fast component (lifetime ~ 140 μs) and a slow component (lifetime ~ 1 ms). Similar features have been reported for Er-implanted bulk Si.[36,37] The fast component is believed to be associated with the presence of impurities.[36-38] Lifetimes of the fast and slow components are obtained by fitting the measured decay curves to an expression of the form:

$$I(t) = A_{fast} \exp(-t/\tau_{fast}) + A_{slow} \exp(-t/\tau_{slow}) \quad \textbf{(11)}$$

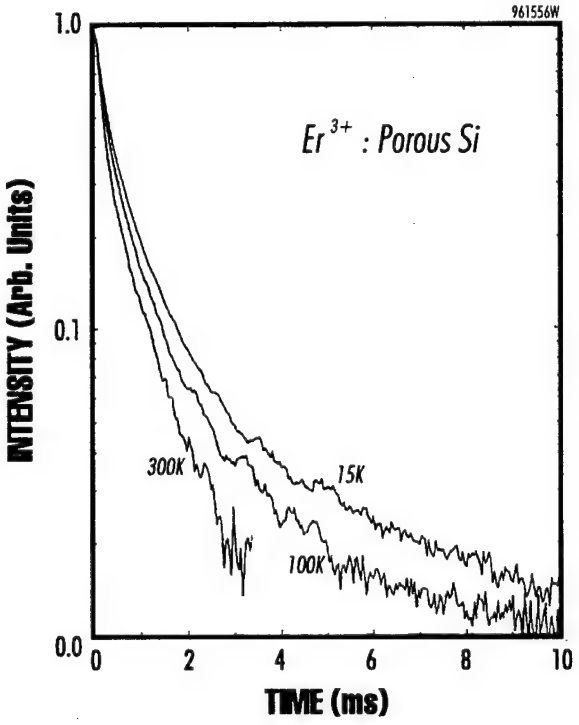

Figure 24 *1.54 μm PL decay curves of Er:porous Si measured at 15, 100 and 300K.*

Based on Equation (11), we fitted the experimental decay transients and obtained the fast and the slow lifetime components at different temperatures. Lifetime of the slow component is 1.37 ms at 15K and is reduced to 930 μs at 375K. It is also noted that the ratio of A_{fast} to A_{slow} is independent of the temperature. This observation suggests that there are two distinct classes of sites, each with a different nonradiative decay channel.

The temperature dependence of the 1.54 μm PL intensity and lifetime of the slow decay component are identical below 150K. However, above 150K, PL intensity decreases faster than the lifetime of the slow decay component. PL intensity at 375K is reduced to 45% of that observed at 15K, while the slow lifetime is only decreased to 65% of its value at 15K.

The identical temperature quenching behavior between the integrated PL intensity and the slow lifetime component in the temperature range from 15 to 150K suggests that PL quenching arises from nonradiative processes such as energy back-transfer[26,27] and multiphonon nonradiative relaxation. We assume that the main process responsible for PL quenching in this temperature range is back-transfer.

The deviation in the temperature dependence of Er^{3+} PL intensity and lifetime above 150K indicates that an intermediate level such as an Er-related donor level is involved in the Er^{3+} excitation process. In the following section, we shall present a model that explains the enhanced PL quenching above 150K.

4.1.7 Proposed Model for Erbium Excitation

In the literature, it has been reported that Er^{3+} excitation occurs via recombination of an exciton bound to an Er-related trap site.[39] Deep level transient spectroscopic (DLTS) studies in different host materials have shown the existence of Er-related levels below the conduction band.[40,41] This Er-related level was found to be a donor both by calculations[42] and by measurements.[40,41] The photogenerated carriers are first trapped at these Er-related defects and the energy of recombination of these carriers (electron-hole pairs) excites Er^{3+} ions via an Auger type process. The excited Er^{3+} ion can relax radiatively (1.54 μm emission) and nonradiatively (energy transfer to other Er^{3+} ions, or defects, and interaction with the host lattice). Figure 25 shows a schematic of the model discussed above.

At very low temperatures, nonradiative relaxation is not very significant (nonradiative transition probability is proportional to $\exp(-\Delta/KT)$: Δ = thermal activation energy). As the temperature is increased from very low temperatures, nonradiative relaxation becomes important. Thus, slight thermal quenching of 1.54 μm PL emission at low temperatures is due to nonradiative relaxation of the $^4I_{13/2}$ state of an Er^{3+} ion. As the temperature continues to increase, the electron on the Er-related level is thermalized to the conduction band. Now the trapping center becomes positively charged and the hole will be detrapped by Coulomb repulsion. As a result, the Er^{3+} excitation probability is decreased with increasing temperature. The dissociation of an exciton bound to an Er-related trap level is responsible for the observed strong thermal quenching of 1.54 μm PL emission above 150K.

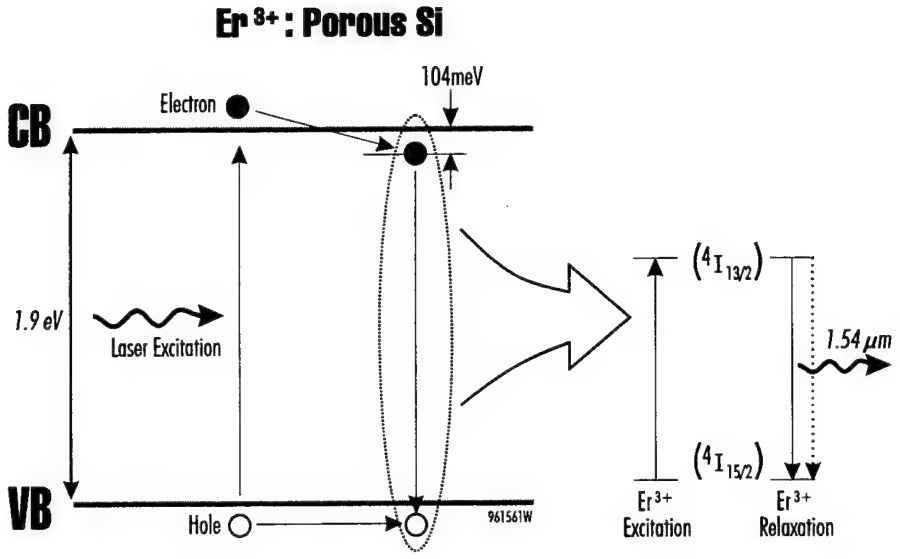

Figure 25 *A model for the excitation and relaxation of Er^{3+} in Er:porous Si.*

If we assume a similar mechanism to explain the excitation of Er^{3+} ions in porous silicon, the enhanced PL quenching above 150K can be interpreted by the following model. At steady state, the PL intensity is proportional to the concentration of excited Er^{3+} ions, *i.e.*

$$I \propto N^*/\tau_{rad} \quad \textbf{(12)}$$

where N^* is the concentration of excited Er^{3+} ions and τ_{rad} is the radiative lifetime of the $^4I_{13/2}$ state of Er^{3+}. Assuming most of the Er^{3+} ions are in the ground state ($N^* < N$; N is the total number of active Er^{3+} ions), the concentration of excited Er^{3+} ions is given by the rate equation:[7]

$$dN^*/dt = N_c/\tau_{tr} - N^*/\tau \quad \textbf{(13)}$$

with N_c is the concentration of electron-hole complexes, τ is the total lifetime of $^4I_{13/2}$ and τ_{tr} is the time required for energy transfer. At steady state ($dN^*/dt = 0$) the PL intensity is given by:

$$I \propto (N_c/\tau_{tr})(\tau/\tau_{rad}) \quad \textbf{(14)}$$

The concentration N_c can be determined by the rate equation:

$$dN_c/dt = r_C - r_D - r_E \quad \textbf{(15)}$$

where r_C is the rate at which the electron-hole complexes are formed, r_D is the dissociation rate of the complexes and r_E is the excitation rate of Er^{3+}. Assuming the excitation rate is negligible, *i.e.*, $r_E < r_C, r_D$, the concentration N_c can be approximated by:[37]

$$N_c = N\,[1 + W \exp(-E/KT)]^{-1} \quad \textbf{(16)}$$

where E is the energy difference between the conduction band and the Er-related trap level. W is defined as:

$$W = \sigma_n\, n_c/\sigma_p\, G\tau_c \quad \textbf{(17)}$$

with τ_c being the carrier lifetime, and n_c being the density of state at the bottom of the conduction band. G is the optical generation rate of electron-hole pairs, and σ_n and σ_p are capture cross-sections for electrons and holes, respectively. Combining Eqs. (14) and (16), the temperature dependence of the Er^{3+} PL intensity is given by:

$$I \propto [\tau/(\tau_{rad}\,\tau_{tr})][N/(1 + W \exp(-E/KT)] \quad \textbf{(18)}$$

where τ is described by:

$$\begin{aligned} 1/\tau &= 1/\tau_{rad} + 1/\tau_{nonrad} \\ &= 1/\tau_{rad}\,[1 + B \exp(-\Delta/KT)] \end{aligned} \quad \textbf{(19)}$$

where τ_{rad} and τ_{nonrad} are radiative and nonradiative lifetimes of $^4I_{13/2}$ state, respectively, Δ is the thermal activation energy corresponding to the energy back transfer, and *B* is a constant. The prefactor *W* in Eq. (18) is temperature-dependent. Since the dominant contribution to thermal quenching arises from the exponential factor, as a first order approximation, we treat *W* and τ_{tr} as constants. A fit of Eq. (18) to the observed PL intensity is shown as a solid line in Figure 26.

Parameters of $E = 0.104$ eV and $W = 10.6$ are used to fit our experimental data. A fit of Eq. (18) to the observed PL intensity and PL lifetime are shown as dashed lines in Figure 26. Parameters of $B = 0.84$ and $\Delta = 15.5$ meV are used to fit our experimental data. This model is in good agreement with the experimental data, indicating that the erbium ions create a new level which is 104 meV below the conduction band of porous Si. This defect related level is localized close to the Er^{3+} ion and acts as an effective channel for energy transfer between the Er site and the host. The value of *E* (0.104 eV) is comparable to that measured in Er-implanted bulk silicon by DLTS analysis.[37] The value of *W*, however, is two orders of magnitude less than that reported for Er^{3+} Si.[37] One of the possible reasons for the reduction in the value of *W* is that the photocarrier lifetime is longer in porous silicon than in bulk silicon.

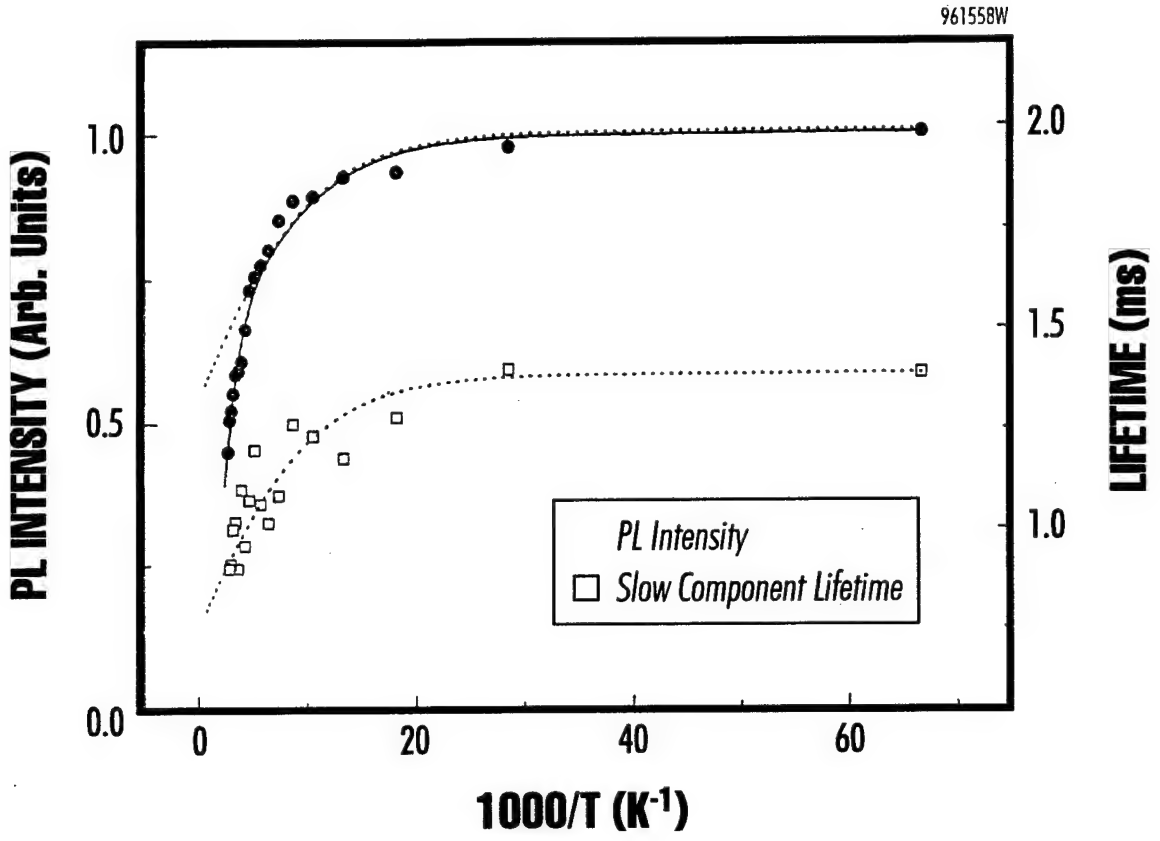

Figure 26 *Temperature dependence of PL intensity and slow lifetime component. The solid line is a fit to the expression given by Eq. (18), and the dotted line is a fit to the expression given by Eq. (19).*

In this proposed model, the thermalization of bound electrons described by Eq. (18) has a negligible effect on the Er^{3+} PL intensity below 150K. Below 150K, the temperature dependence of Er^{3+} PL intensity and lifetime (slow component) are essentially identical, and back transfer leads to weak Er PL quenching. Above 150K, however, the dissociation rate r_D (in Eq. (15)) increases significantly, which results in an enhancement of the Er^{3+} PL quenching at elevated temperatures.

4.1.7.1 Summary

In summary, we have performed temperature-dependent PL as well as PL decay measurements on Er-doped porous Si up to about 475K. From these measurements we propose a model for Er^{3+} excitation. We predict an Er-related donor level which is 104 meV below the conduction band, and that the ionization of this donor level is proposed to be responsible for the strong thermal quenching of 1.54 μm emission in porous Si:Er^{3+} above 150K. A nonradiative process with a thermal activation energy of 15.5 meV is responsible for the slight thermal quenching in the temperature range from 15K to 150K.

We propose a model for the excitation of Er^{3+} in Er:porous Si in which the excitation occurs via recombination of an exciton bound to an Er-related trap site. The photogenerated carriers are first trapped at these Er-related defects and the energy of recombination of these carriers (electron-hole pairs) excites Er^{3+} ions via an Auger type process. The excited Er^{3+} ion can relax radiatively (1.54 μm emission) and nonradiatively (energy transfer to other Er^{3+} ions, or defects, and interaction with the host lattice). The dissociation of an exciton bound to an Er-related trap level is responsible for the observed strong thermal quenching of 1.54 μm PL emission above 150K. The thermal quenching of 1.54 μm PL emission in Er^{3+} porous Si is comparable to the results reported for Er^{3+}:3C SiC.

4.2 Optical Characteristics of Ideal Host Porous Silicon Substrate

Our photoluminescence studies show that 1.54 μm PL emission in Er^{3+}:porous Si depends on the porosity of the material. The 1.54 μm PL emission is known to depend strongly on the bandgap of the host material and the bandgap of porous Si depends on its porosity (effect of quantum confinement). Note that the samples with higher porosity have a wider bandgap, and as a result, the visible PL peak shifts toward shorter wavelengths (higher energies). In other words, there is a correlation between the visible PL spectrum of porous Si and the 1.54 μm PL emission from Er^{3+}:porous Si. However, there is an optimum porosity (visible PL peak position) condition in which the strongest room temperature 1.54 μm PL emission is achieved. In the following sections we shall discuss the effects of visible luminescence properties of porous Si, Er implantation, color of the porous silicon sample and annealing conditions on the 1.54 μm PL emission from Er^{3+}:porous Si.

4.2.1 Dependence of the 1.54 μm PL Emission from Erbium on the Visible Light Emission from As-Prepared Porous Si

We observed strong room-temperature 1.54 μm PL emission from Er^{3+}:porous Si samples when the visible luminescence from porous Si peaked between 700 nm and 750 nm (~ 1.7 to 1.8 eV). When the visible emission from porous Si peaked from 650 nm to 660 nm (~ 1.88 to 1.9 eV), 1.54 μm emission was extremely weak or non-existent for room-temperature measure-

ments. In addition, it was also found that the intensity of 1.54 μm emission is directly dependent on the intensity of visible light from porous Si. Figure 27 shows room-temperature visible PL from two porous Si samples (SW32B and SW32P), fabricated under different etching conditions using identical Si wafers. The difference in visible spectral peaks indicates difference in bandgaps (porosity) of these two porous Si samples. We implanted these two samples with Er at 190 keV with a fluence of 10^{15} cm^{-2} and later annealed at 650°C for 30 minutes. The sample which showed a visible luminescence peak near 750 nm showed strong room-temperature 1.54 μm PL emission, while the second sample (visible PL peak at 650 nm) did not show any room-temperature IR emission (see Figure 28). It should be noted that the sample with relatively higher bandgap shows poorer efficiency of 1.54 μm PL emission than the sample with the lower bandgap (visible PL peak near 700 nm). The relative energy position(s) of Er-related defect level(s) in the bandgap with respect to the band edges, and phonon assisted and other non radiative relaxation (inter-impurity interactions) mechanisms may favor the porous Si host with the bandgap corresponding to the visible PL peak emission near 750 nm. A summary of data showing the correlation between the visible and the near-IR PL emission from Er:porous Si is shown in Table 4.

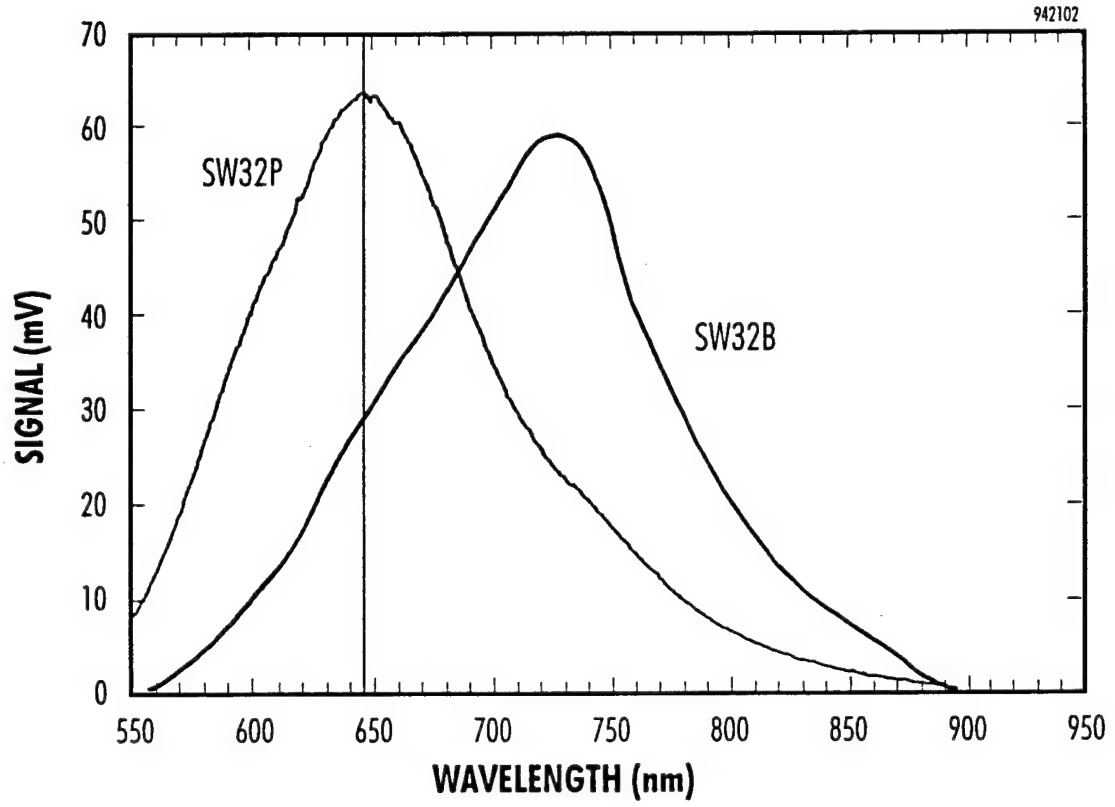

Figure 27 *Room temperature visible PL spectra from porous Si samples SW32B and SW32P fabricated under different etching conditions.*

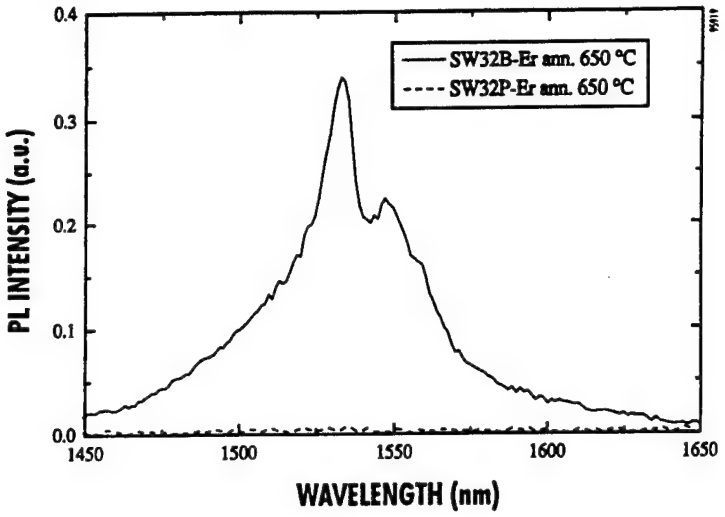

Figure 28 *Room-temperature IR PL spectra of Er implanted at 190 keV with a dose of 10^{15} Er^{+}/cm^{2} into red-emitting porous Si which peaked at 750 nm. Strong IR emission was observed for the porous Si after annealing at 650 C. In contrast, no IR emission was observed from Er implanted under similar conditions into porous Si which peaked at 650 nm.*

Table 4 *Correlation between the visible and near-IR PL emission from Er:porous Si.*

Sample ID	Visible PL (nm)	Relative Intensity (Visible)	Er-implant energy (keV)	Anneal Temp (°C)	Relative Intensity at 1.54μm
SW32B	730	strong*	190	500 530 650 850	strong**
SFPD2	730	v-good	190	500 530	strong
6554-C	735 & 850	v-good	380	650 750	v-good
6554-G	725	good	380	650	v-good
6554-I	725 & 650	good	380	650	weak
6554-F	660 & 730	good	190	650 750	weak
6554-P	650	good	380	650	weak
WA3M	640	weak	380	650	weak
6554-J	723 & 630	good	380	650	none
6554-Q	660	good	190	650	none
6554-R			190	650	none
SW32P	650	strong	190	650	v-weak
SW32Q	665	weak	190	650	none
WA3D	650	weak	50	650	none

*Relative strength compared with an $Al_{0.30}Ga_{0.70}As$ sample measured under identical PL conditions.[2]

**Relative strength compared with an $In_{0.53}Ga_{0.47}As$ on InP sample measured under identical PL conditions.[14]

In order to understand the role of visible PL emission from porous Si on the 1.54 μm PL emission, we have measured the visible PL emission before and after Er implantation, and typical results are shown in Figure 29. The integrated visible PL emission intensity after Er (190 keV) implantation is about 60% of that measured before implantation in most of the samples. From this result, it appears that there is competition between the recombination channels responsible for the visible and 1.54 μm PL in Er:porous Si.

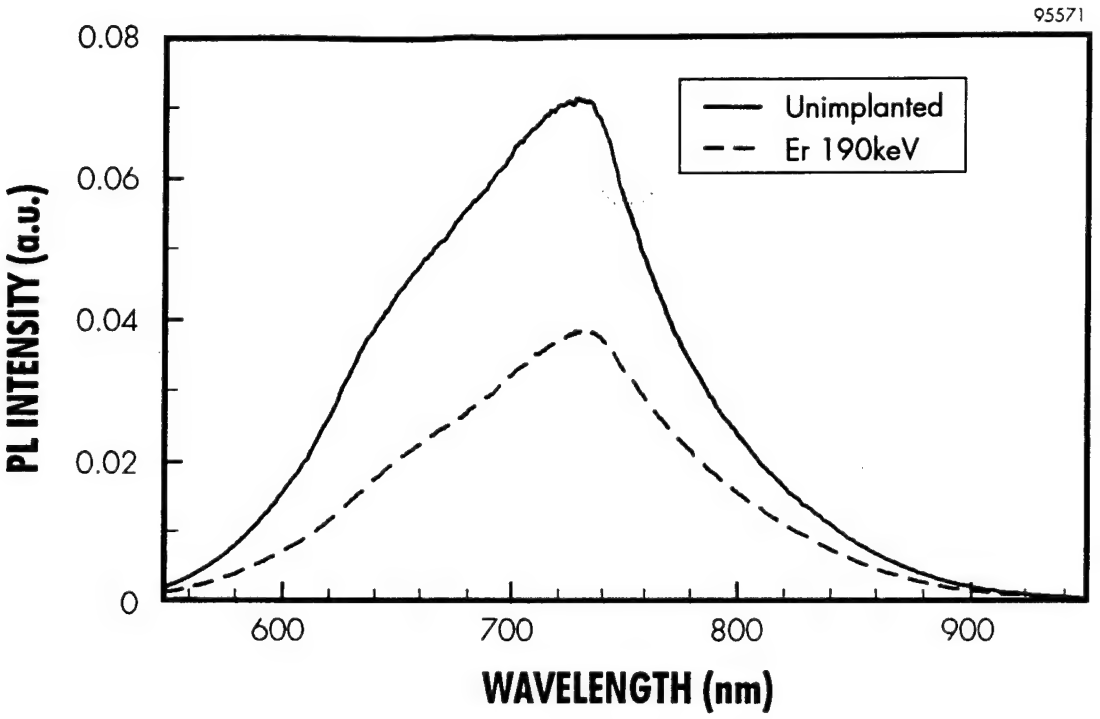

Figure 29 *Visible PL emission from porous Si before and after Er implantation.*

Figure 30 shows a comparison of IR emission from Er-implanted porous Si which peaked at 640 nm, and quartz implanted with a dose of 10^{15} Er/cm^2 at 380 keV. Both samples were annealed at 650°C. No room-temperature luminescence peak was observed from the quartz sample annealed at 650°C. However, we observed very weak room-temperature IR emission from Er in quartz annealed at 900°C, which is very similar in intensity and temperature dependence to that of Er implanted into porous Si. These results indicate that porous Si, with visible peak emission from 700 to 750 nm, is an excellent host for optically active Er^{3+} incorporation. The intensity of IR emission is proportional to that of visible light emission from the porous substrate prior to ion implantation of erbium. Implantation of Er into porous Si which showed visible PL peak near 650 nm results in extremely weak room-temperature near-IR emission, and its temperature dependence is very similar to that from Er in quartz.

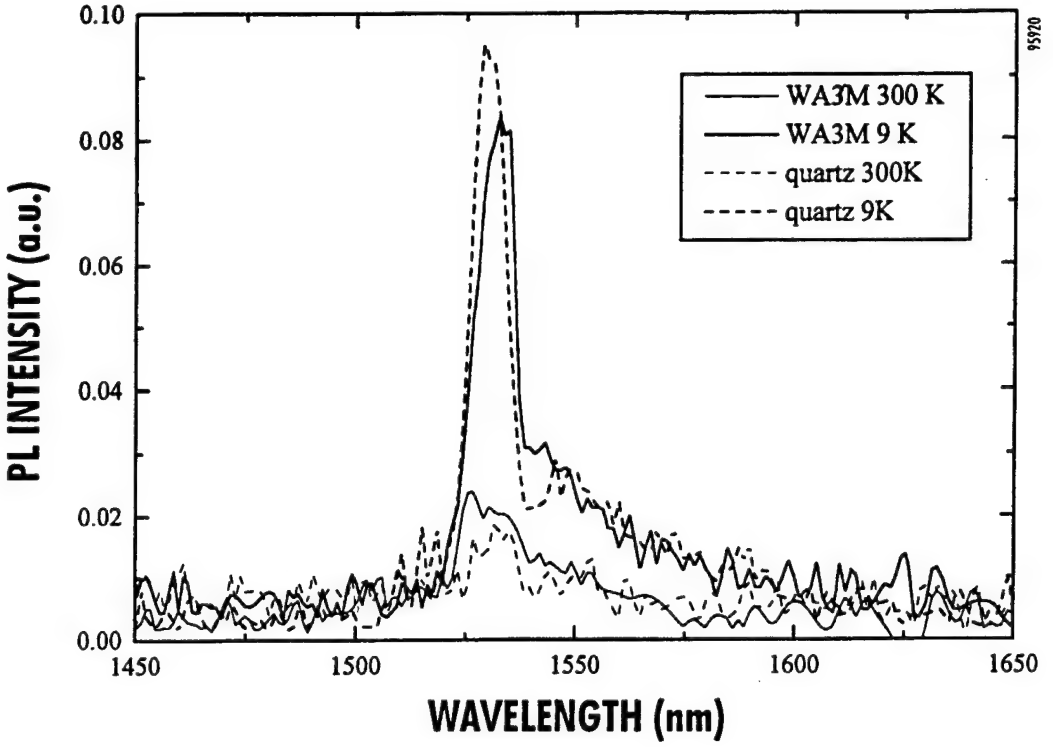

Figure 30 *Comparison of IR emission from Er-implanted (10^{15} cm^{-2}, 380 keV) porous Si and quartz. Note that the visible PL peak from porous Si was near 640 nm.*

4.2.2 Dependence of the 1.54 μm PL Emission from Erbium on the Visible Light Emission from Implanted and Annealed Porous Si

In the previous section we discussed the correlation between the 1.54 μm Er^{3+} emission and the visible emission from porous Si prior to Er implantation. This information provided us with the starting conditions to achieve strong IR emission. In this section we discuss the correlation between the 1.54 μm Er^{3+} emission and the visible emission from porous Si after Er implantation and annealing. In this study we discuss two porous Si samples (A and B) with different physical and optical properties. Sample A looked violet and sample B green-yellow in appearance. Figure 19 shows a 15K, IR PL spectra of samples A and B from 1000 to 1700 nm. Both samples exhibited Er^{3+} luminescence at 1.54 μm and a weak broad-band luminescence between 1.0 and 1.4 μm, which was probably due to porous Si.[43] The peak at 1.13 μm corresponds to the band-edge luminescence found in bulk Si.[44] The Er^{3+} PL intensity from sample A was almost four times stronger than that observed from sample B and the emission from sample A is slightly broader than that from sample B. Since both samples were prepared under identical implantation and annealing conditions, the variation in Er^{3+} emission intensity and band width for different samples (porosity) suggests that the local environment of Er^{3+} changes with the porosity of porous Si. Figure 31 shows the visible PL spectra of samples A and B measured at 15K after Er implantation and annealing. The visible luminescence from sample A is about 2 times weaker than that from sample B. This observation suggests that the nonradiative energy transfer from the host to the Er^{3+} ion is most efficient in sample A. The peak shift of the visible PL spectrum of sample B towards shorter wavelengths (~ 660 nm) indicates that sample B has a wider bandgap than sample A. If the Er^{3+} PL originates from the nanograins of the porous Si, then a weaker temperature dependence would be expected for the sample with a

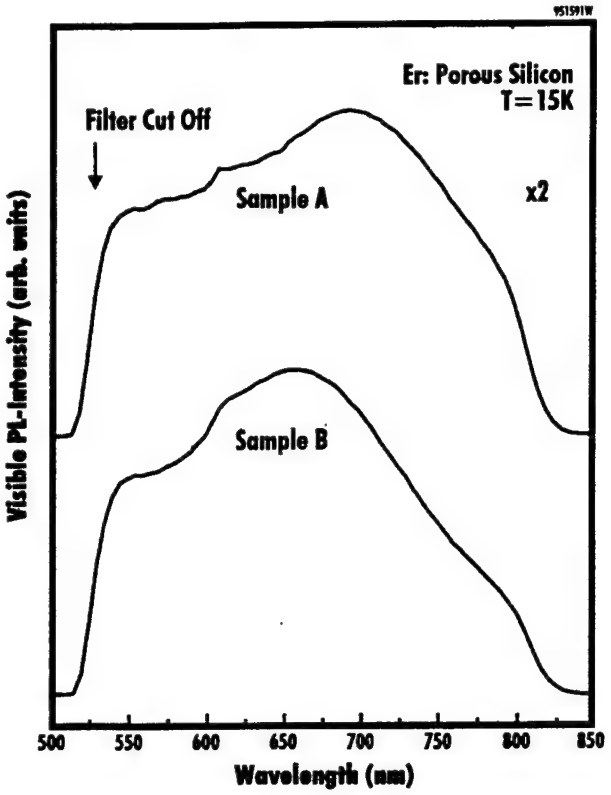

Figure 31 *Visible PL from Er-implanted and annealed porous Si samples A and B measured at 15K under identical conditions. The arrow indicates the filter cut-off wavelength.*

wider bandgap, *i.e.*, sample B. Indeed, our temperature-dependent PL study shows that sample B shows a weaker thermal quenching than sample A. The integrated PL intensity of sample A at 300K is about 60% of that at 15K, whereas it is about 70% for sample B. Figures 32a and 32b show 1.54 μm luminescence from samples A and B measured at temperatures ranging from 15 to 300K. The temperature dependence of the integrated PL intensities of samples A and B is shown in Figure 33. This difference in temperature quenching behavior is similar to that of Er in wide-bandgap III-V semiconductors.[17] This observation was explained by a reduced energy back-transfer from the excited Er^{3+} ions to the wider-bandgap host semiconductor.[17] From the above results, it is clear that by engineering the bandgap (porosity) of porous Si appropriately, one can achieve intense, temperature-stable 1.54 μm emission from Er:porous Si.

4.2.3 Summary

There is a strong correlation between the visible PL emission from porous Si and the 1.54 μm PL emission from Er-implanted and annealed porous Si. Porous Si with a visible emission peak in the wavelength range from 700 to 750 nm is an ideal host for doping of optically active Er^{3+} centers. Porous Si with visible emission peak near 650 nm results in extremely weak room-temperature emission at 1.54 μm upon Er implantation and annealing. However, this sample shows weaker thermal quenching than the former sample. This observation is consistent with thermal quenching behavior of Er-doped wide-bandgap host materials.

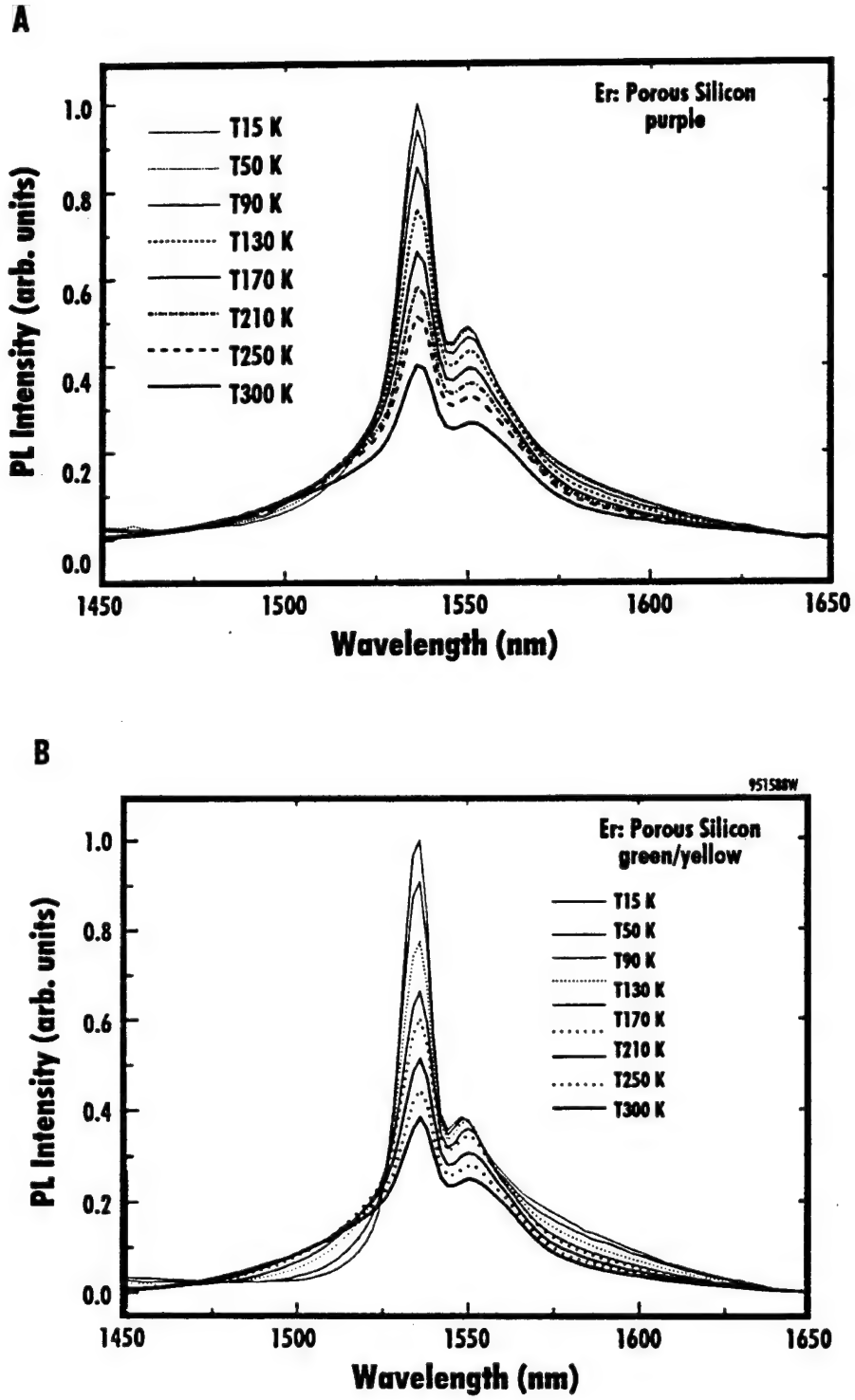

Figure 32 *PL measured from 15K to 300K from Er-implanted and annealed porous Si samples A and B.*

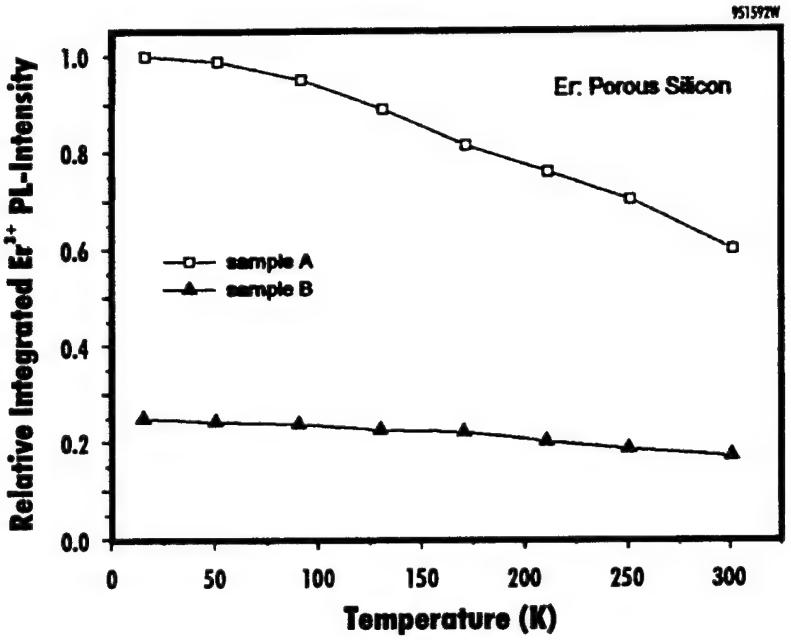

Figure 33 *PL integrated intensity as a function of temperature for samples A and B.*

We speculate that Er^{3+} centers associated with deep and shallow defect levels in the bandgaps are present in porous Si whose visible PL peaks are near 650 and 750 nm, respectively. Erbium centers associated with deep defect levels are responsible for the weak thermal quenching of 1.54 μm PL, since the energy back transfer from Er^{3+} to the host will be very low up to very high temperatures. On the other hand, erbium centers associated with shallow defect levels are responsible for the strong thermal quenching of 1.54 μm PL since the energy back transfer from Er^{3+} to the host will be very high at high temperatures. However, the intense 1.54 μm PL at room temperature in porous Si with visible PL peak near 750 nm may be due to efficient energy transfer from the host to the Er^{3+} centers or due to large number of optically active Er centers.

4.3 Photoluminescence of Pr^{3+}:Porous Si

Rutherford backscattering spectroscopy (RBS) experiments were carried out to determine the concentration of Er and Pr in Si, porous Si, and other substrates. Measurements were carried out at the University of Connecticut using a 2 MeV van de Graaff accelerator. Figure 34a shows RBS spectra of Pr-implanted Si (note that both Si and porous Si were implanted at the same time) and a simulated Si substrate. Figure 34b shows the concentration profiles of Si implanted with a dose of 1×10^{15} Pr/cm^2 at 190 keV and 380 keV; as shown, the peak concentration was about 1×10^{20}/cm^3. RBS results from other Pr-implanted samples showed that some implants had Pr, others did not. However, RBS from Er-implanted samples indicated that our Er implantation process is reproducible.

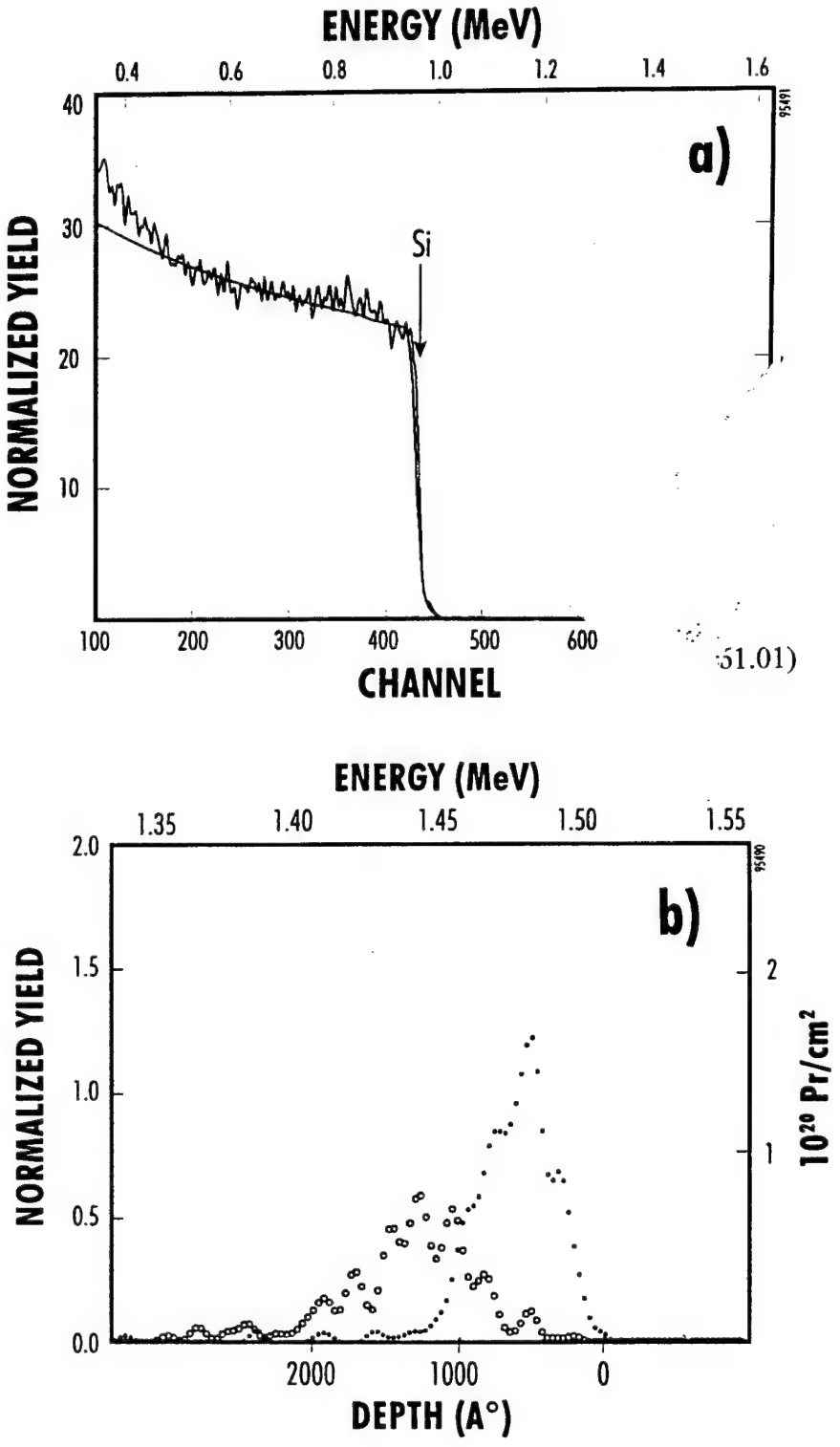

Figure 34 *RBS spectra of Pr-implanted Si; (a) compared with a simulated Si profile, and (b) showing the Pr concentration profile.*

Samples were annealed in an in-house furnace in a nitrogen ambient at temperatures ranging from 500 to 650°C for periods between 30 and 60 minutes. Er- and Pr-implanted porous Si samples were studied for visible and IR emission. Some samples were also studied by Dr. Nelson Rowell at the National Research Council of Canada (NRCC). Figures 35a and 35b show PL spectra of porous Si implanted at 190 keV with a dose of 1 x 10^{15} Pr/cm^2 (sample SSA) and annealed at 500°C for one hour. This sample was excited at the 488 nm line using an argon laser with 200 mW power. As can be seen, numerous lines exist but none of them are related to Pr^{3+}.

4.4 Processes for Er:Porous Si Device Fabrication

4.4.1 Preparation of Substrates for Devices, and Difficulties Producing Device-Quality, Uniform Porous Silicon Wafers

From our previous studies, we have discovered that 380 keV Er-implanted porous silicon wafers with porosities in the range of 50 to 60% show strong 1.54 μm Er^{3+} photoluminescence at room temperature. However, reproducing a constant porosity uniformly on porous silicon wafers has been problematic. This problem may be attributed to non-uniform electrical contact used for etching. In a new run, we have used two identical Si wafers with Al back coating. The resulting porous Si wafers looked (texture and color) uniform and emitted red under UV excitation to the naked eye. However, further PL measurement of the two wafers showed spectra with two different "red" PL peak positions, indicative of different bandgaps/porosities. In other words, the porosity of the wafers was not reproduced in wafers etched the same day under identical conditions including Al back contact to the Si wafers. The wafers were analyzed using RBS measurements in order to determine their porosities. The fabrication and wafer conditions of porous silicon and RBS results are summarized in Table 5. The Al back coating of the Si wafer generally improved the uniformity of the porous structure. Nevertheless, we observed lack of uniformity even in the best of our 3-inch and 4-inch porous Si wafers.

Figure 36 compares the RBS spectra of two porous Si samples, one with an Al contact (607302) and the other without Al contact (602282) with that of bulk silicon. The porous Si samples were anodically etched at 100 mA for sixty minutes. The porosity is determined by comparing the Si backscattering signal strength from porous Si with that of bulk Si. The estimated porosity is about 43% in the porous Si sample having the Al back contact and is about 72% in the sample without the Al back contact etching. However, this porosity has not been reproduced in other runs with identical etching conditions including Al back contact.

Figure 37 shows another example of irreproducibility of porous Si wafers. Figure 37 compares RBS spectra of porous Si samples (3-inch diameter) 609201, 609092, and 608132 with the spectrum of bulk Si. The porous Si samples were etched under identical conditions (100 mA, 60 minutes, with Al contacts during etching). The estimated porosities of samples 609201, 609092, and 608132 are 72%, 35%, and 56%, respectively. The variations in porosity for three-inch diameter wafers processed under identical conditions (100 mA, 60 minutes, with Al contacts during etching) are shown in Figure 38. This result clearly demonstrates the irreproducibility of porosity using identical etching parameters.

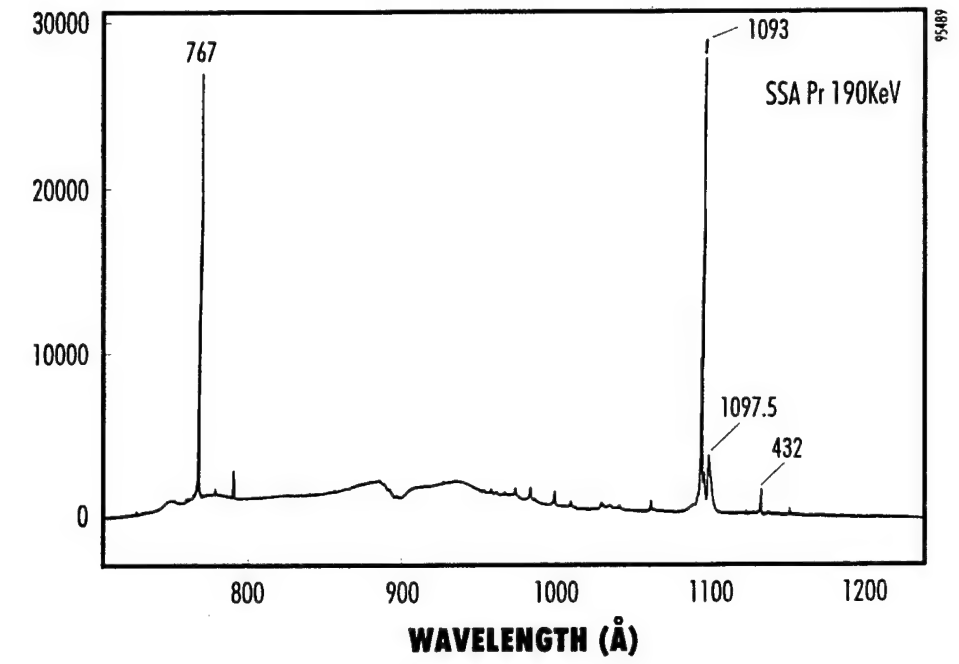

a)

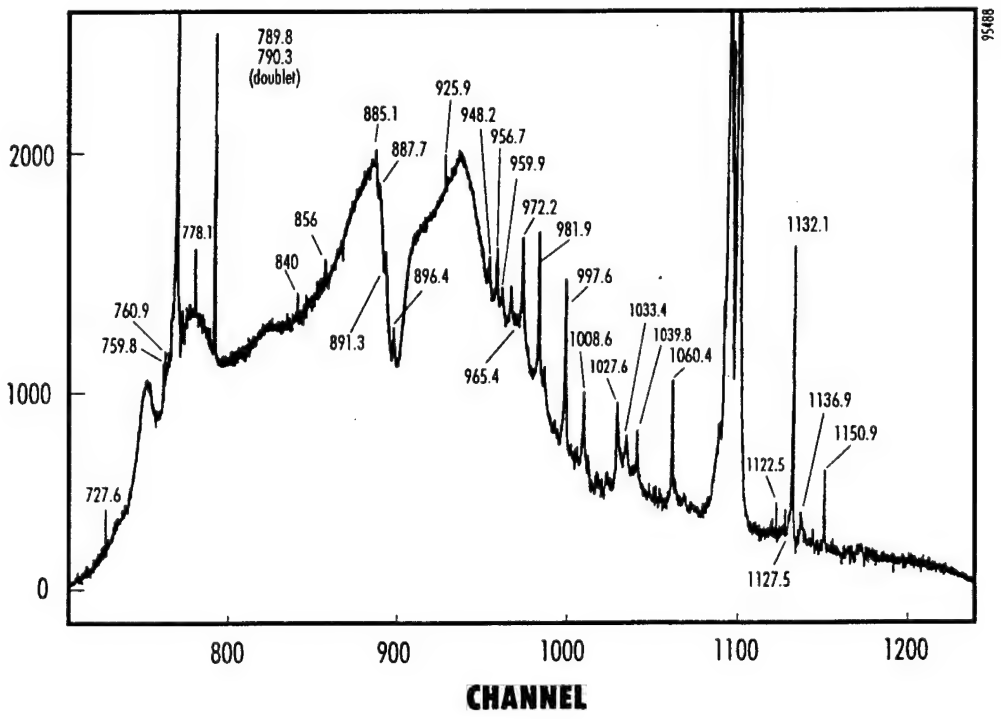

b)

Figure 35 *PL spectra of a porous Si sample implanted with Pr at 190 keV and annealed at 500°C. The observed sharp lines are well known defect-related lines in Si and not related to* Pr^{3+}.

Table 5 *Summary of porous silicon wafer processing and RBS analysis of samples discussed in this report.*

Porous Si Sample				Al back-contact	Current		Time (sec)	Current density x time Coulomb/ cm^2	Porosity (%)
Run #	Wafer Diameter (cm)	Wafer Thickness (μm)	Resistivity (Ω-cm)		Total (mA)	Density (mA/cm^2)		$\times 10^{-3}$	
602282	7.5	356-406	1-10	no	100	3	3600	10.8	72*
607302	7.5	356-406	1-10	yes	100	3	3600	10.8	43
608132	7.5	356-406	1-10	yes	100	3	3600	10.8	56
609092	7.5	356-406	1-10	yes	100	3	3600	10.8	35
609201	7.5	356-406	1-10	yes	100	3	3600	10.8	72
607301	10	475-500	1.5-3	yes	400	6	7200	43.2	59
607303	10	475-500	1.5-3	yes	300	4.7	4500	21.2	17
608131	10	475-500	1.5-3	yes	500	7.9	2700	21.3	43
608133	10	475-500	1.5-3	yes	200	3.1	3600	11.2	21
609112	10	475-500	1.5-3	yes	200 300	3.1 4.7	2700 1800	8.4 8.5	13

* Note that the wafer from run 602282 showed non-uniform red light emission, (*i.e.*, porosity) and the RBS result shown in Table 5 corresponds to the wafer region with the brightest red PL emission (high porosity).

We have carried out a number of experiments to study the effect of etching current and time on porosity using 4-inch wafers. The porosities of the 4-inch diameter wafers etched under different conditions are shown in Figure 39. Figure 40 compares RBS spectra of porous Si samples 607303 (300 mA, 75 minutes: 21.2 milliCoulomb/cm^2), and 608131 (500 mA, 45 minutes: 21.3 milliCoulomb/cm^2) with the spectrum of a Si sample. Both porous Si samples had Al back contact during etching. The estimated porosities of the samples 607303 and 608131 are 17% and 43%, respectively. This result again clearly shows the irreproducibility of porosity using identical etching conditions.

4.4.2 Difficulties Involved with Er Implantation Using High-Output Commercial Implanter

Erbium is one of the difficult elements to implant into a material. It takes a lot of experience and skills with the particular ion implanter to implant Er successfully. Since we lost an expert implantation technician in the later part of the program, we have not been able to implant Er successfully into porous Si. Most commercial ion implanters use a molybdenum arc chamber. From RBS analysis we learned that our Er-implanted samples were mostly contaminated with $MoCl_2$. This result can be expected since $MoCl_2$ and Er have about the same molecular and atomic weights, respectively. Furthermore, $MoCl_2$ is hydroscopic and can be a source of other contaminants when the system is routinely vented. The history of implantation elements in the system is also a critical factor determining the contamination.

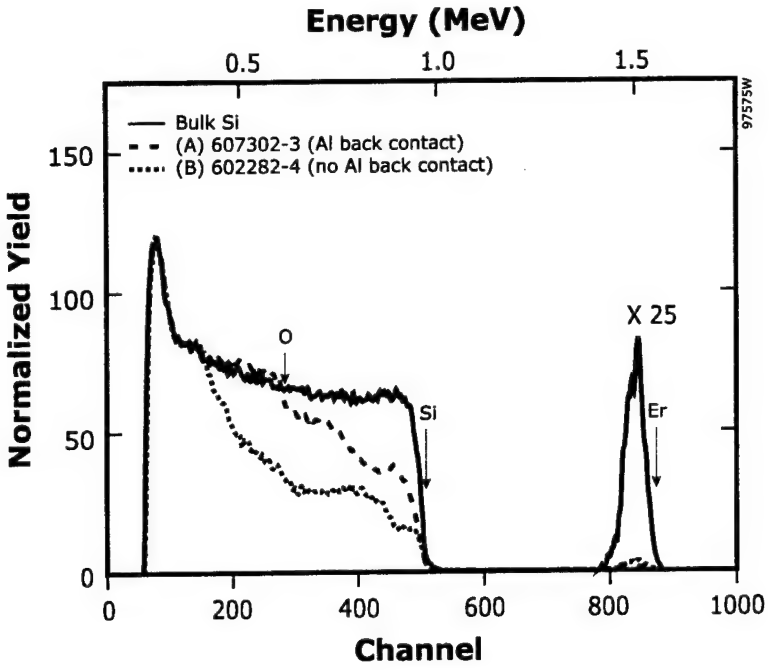

Figure 36 *Comparison of RBS spectra of two porous Si wafers, (a) with and (b) without Al back contacts etched under identical conditions (100 mA, 60 min). An RBS spectrum of Si is shown for reference.*

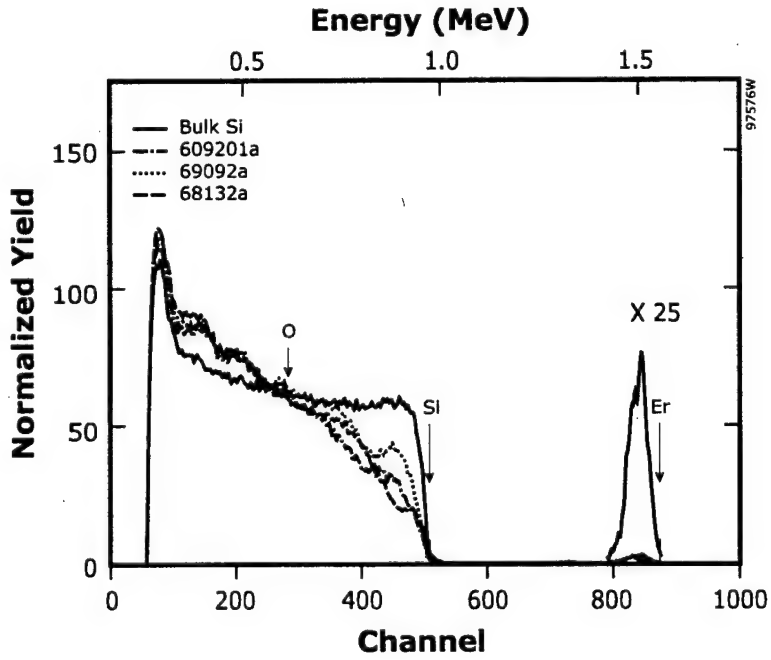

Figure 37 *Comparison of RBS spectra of three porous Si wafers etched under identical conditions (100 mA, 60 min) and Er^{3+}:Si. All three porous Si samples had Al back contacts during etching.*

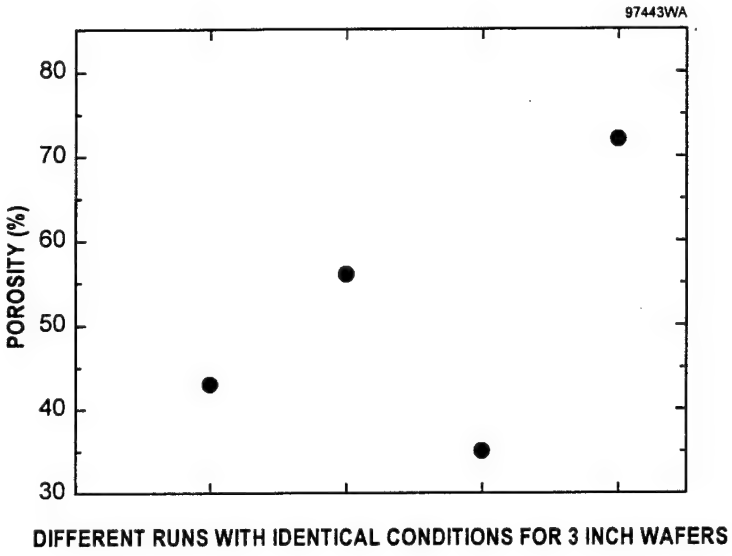

Figure 38 *Variation of porosity of 3-inch wafers processed under identical conditions (100 mA, 60 minutes, with Al contacts during etching).*

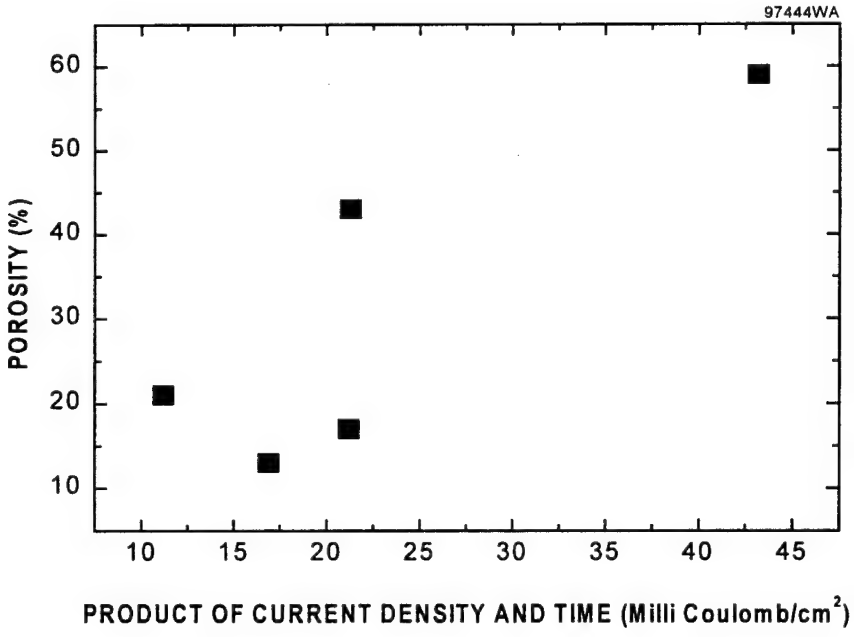

Figure 39 *Dependence of porosity on etching parameters (product of current density and time) for 4-inch wafers with Al back contacts.*

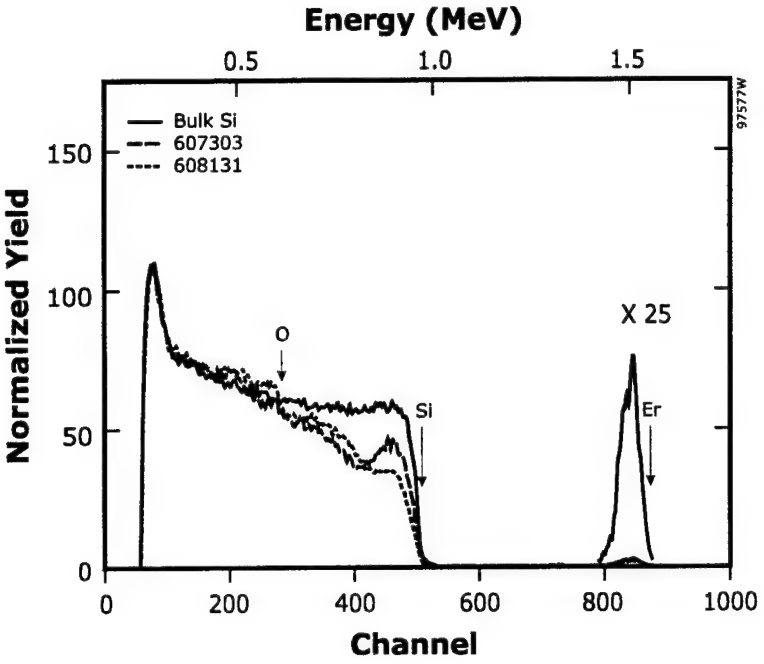

Figure 40 *Comparison of RBS spectra of porous Si wafers 607303 and 608131. Both porous Si samples had Al back contact for etching.*

In order to avoid this problem we chose to use a graphite arc chamber instead. Erbium-implanted samples using this graphite arc chamber were contaminated with carbon. An increased reaction between carbon and chlorine (CCl_4) is thought to be responsible for this result.

4.4.2.1 Contamination Control During Er Implantation

Given unlimited time and resources, a number of methods could be used to eliminate the contamination problem. We discuss these techniques in the following section.

Sputter Source of Er - The advantage in this approach is that there is no Cl_2 carrier gas involved to react with system components. On the other hand, this approach has the disadvantage of having low beam current and a difficult setup.

Different Arc Chamber Materials (Tungsten and Tantalum) - Although in principle it should work, it has yet to be proven.

Erbium Vaporizer - Erbium compounds such as $ErCl_3$ and Er_2O_3 can be thermally evaporated to create the necessary ions for implantation. In this approach again there is no chlorine carrier gas involved. Argon could be used as the carrier gas instead.

4.4.2.2 Accurate Implantation of Er and Pr for Device Fabrication

It is well-known that impurities affect the optical activation of Er^{3+} ions. For example, it has been reported[47-49] that oxygen, nitrogen, and fluorine enhance the 1.54 μm Er^{3+} luminescence in Si. It is equally likely that certain other impurities may optically deactivate the Er^{3+} ions. The recent batch of erbium-implanted, annealed porous and bulk silicon samples did not show 1.54 μm Er^{3+} luminescence. Upon investigating these samples using RBS analysis, we have observed not only the presence of erbium, but evidence of the presence of trace elements such as Cl, Ti, and Mo as well. Comparing the RBS spectra of porous Si before and after implantation suggests that these contaminants were introduced into the samples during implantation. Therefore, we attribute the absence of 1.54 μm luminescence to these impurities. It should be noted that the implantation of erbium into semiconductors is inherently difficult, since in ion implantation we select specific ions based on their mass. Since erbium is heavy and possesses many isotopes, a large number of contaminants can be found which have the same mass as erbium. A well-known example is $MoCl_2$. The atomic weight of erbium is about 167; of molybdenum, about 96; and of chlorine, about 35.5. Another example is TiCl. The atomic weight of Ti is 48, which gives TiCl a mass of 83.5 (83.5 x 2 = 167, the same mass as erbium). Because of these problems, accurate implantation of erbium becomes not only an engineering and scientific task, but also an art. In this report, we present our RBS studies to investigate the contamination problem in Er implantation. We have also implanted much higher doses in order to increase the RBS detection sensitivity.

Contaminants in Er-implanted Porous Silicon - We have been successful in the past in implanting erbium without contaminants into Si, porous silicon, and GaN wafers. These samples have shown strong emission at 1.54 μm and the results have been reported in a number of publications (see Appendix A).

A problem with the erbium implantation process was first suspected when we did not observe the characteristic 1.54 μm Er^{3+} luminescence emission from the recent batches of our Er^{3+}:porous silicon samples. At first we believed that this problem was most likely related to the porous silicon fabrication process. A number of different etching techniques were tried and have been discussed in our previous reports. Still, we were unable to achieve strong near-infrared emission. Figures 41 and 42 show RBS spectra of porous silicon samples implanted with erbium and praseodymium, respectively. The porous silicon sample in Figure 41 was etched at 500 mA for 45 minutes. Erbium was implanted at 380 keV with a fluence of 10^{15} cm^{-2}. The porous silicon sample in Figure 42 was etched at 100 mA for 60 minutes and the erbium was implanted at 380 keV with a fluence of 10^{15} cm^{-2}. From the RBS results, it is clear that the system is contaminated. In addition to erbium there appear to be other contaminants such as Ti. Thus, we began precise analysis of the entire implantation procedure to determine the source of the problem. In order to increase our sensitivity in detection of contaminants, we have implanted a bulk Si wafer with erbium at 190 keV with a fluence ranging from 10^{15} to 10^{17} cm^{-2}. High doses of erbium are not required for photo- or electroluminescence measurements. However, at very low doses detection of lighter contaminants becomes much more difficult.

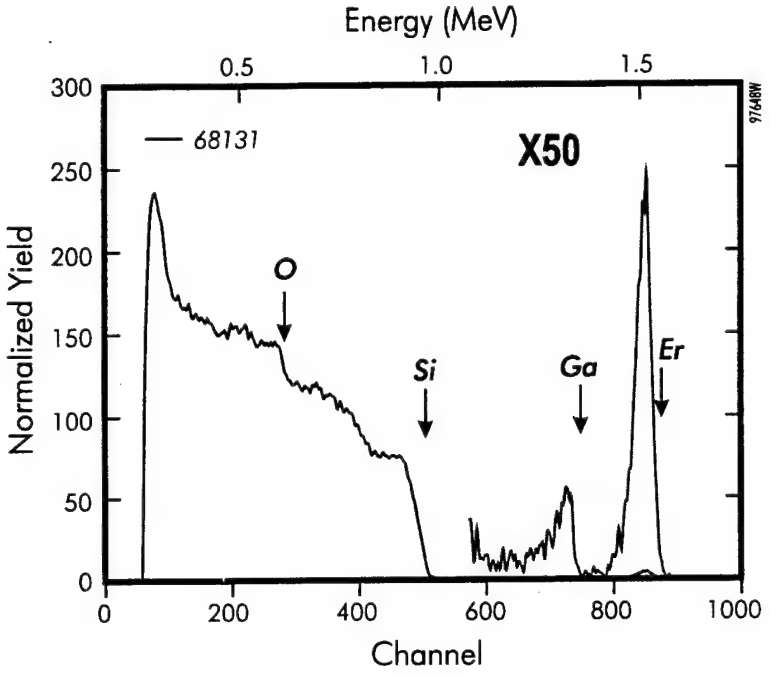

Figure 41 *Near normal incidence RBS spectrum of Er^{3+}:porous Si sample 608131. This sample was etched at 500 mA for 45 minutes. Erbium was implanted into this sample at 380 keV with a fluence of 10^{15} cm^{-2}.*

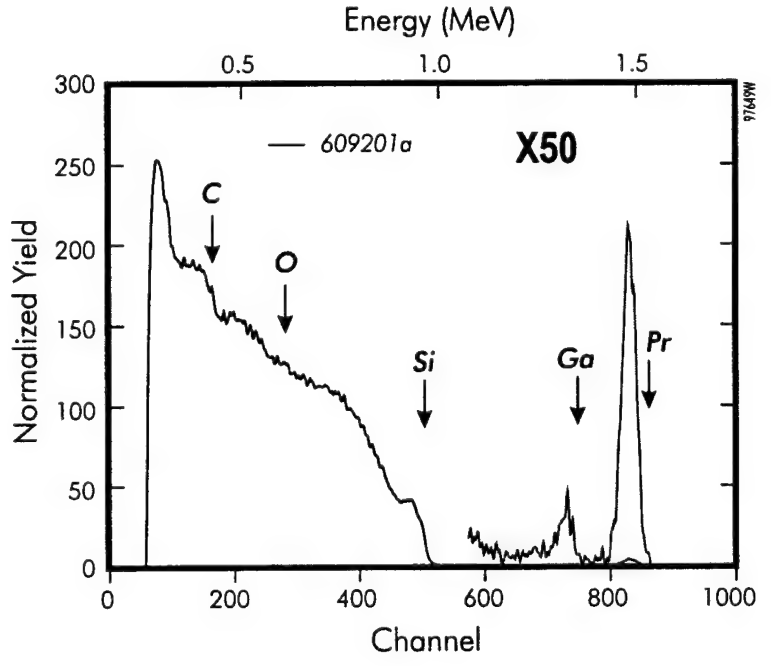

Figure 42 *Near normal incidence RBS spectrum of Pr^{3+}:porous Si sample 609201. This sample was etched at 100 mA for 60 minutes. Praseodymium was implanted into this sample at 190 keV with fluences of 4 x 10^{15} and 6 x 10^{15} cm^{-2}.*

Figure 43 shows the RBS spectrum of sample ErSi-2A. Note that Cl and Mo are clearly seen as impurities in this sample. In fact, considering the scattering cross-section of Er and Mo, the strength of the Mo peak is comparable to that of Er. Note that the scattering peak from erbium appears larger because a scattering cross-section of erbium during RBS measurement is proportional to the mass; *i.e.*, the larger the target atom, the larger the signal. It is clear from this result that molybdenum chloride is a major source of contamination in our implantation system. In order to verify the contamination of molybdenum, we increased the fluence to 1.4×10^{16} cm^{-2} and implanted a silicon sample (ErSiA) with erbium at 190 keV. Figure 44 shows the RBS spectrum (solid line) of sample ErSiA. The dashed line represents the simulated spectrum. Note that the Er signal has increased considerably relative to the Mo and Cl peaks. This observation further suggests that our ion implantation system is contaminated with Mo and Cl. These impurities might be responsible for the absence of Er^{3+} luminescence from our erbium and praseodymium implanted porous and bulk Si samples. From simulation, Er, Mo, C, and Cl atoms are found in the top 1000Å layer of the sample with a composition of Si:Er:C:Mo:Cl = 21.5:35.5:21.5:15.0:6.5. The peak concentration of Er in this layer is approximately 1.8×10^{22} cm^{-3}.

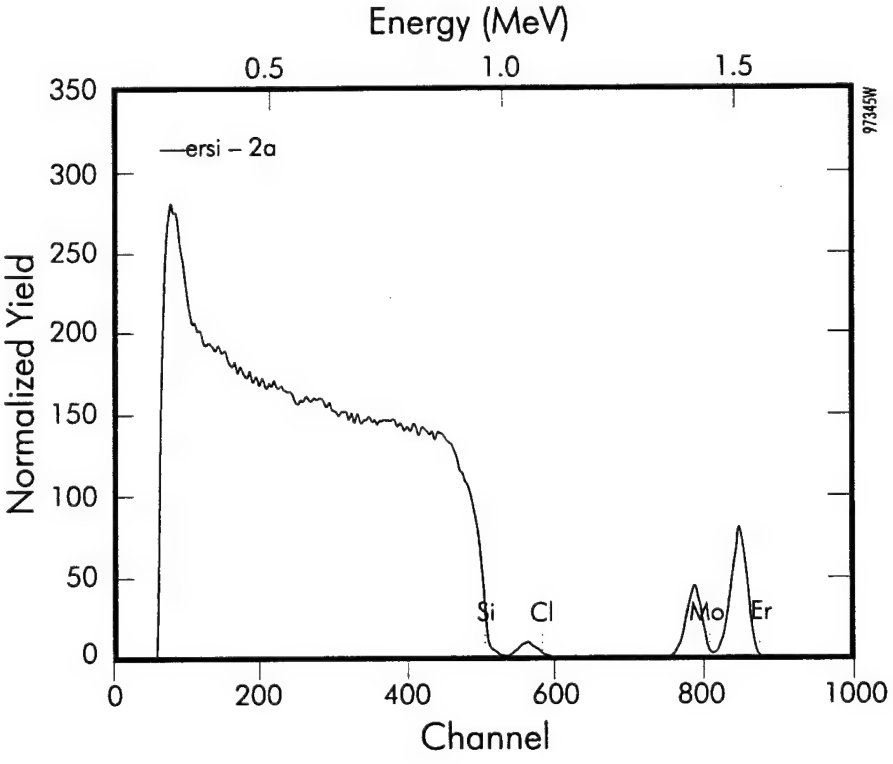

Figure 43 *Near normal incidence RBS spectrum of Er^{3+}:Si sample ErSi-2A. Erbium was implanted into this sample at 190 keV with a fluence of 1.2×10^{15} cm^{-2}.*

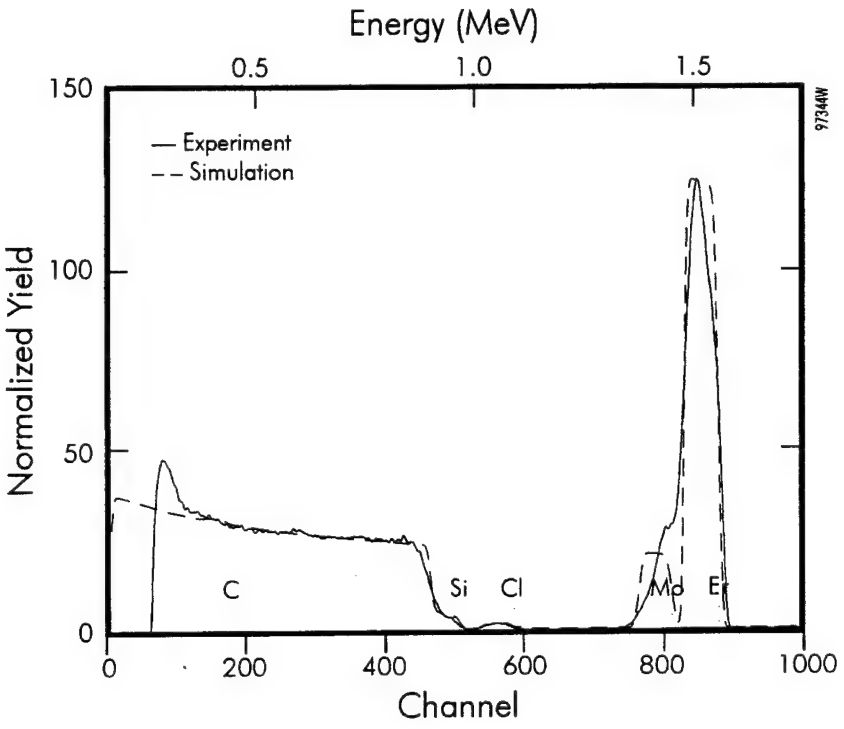

Figure 44 *Near normal incidence RBS spectrum of Er^{3+}:Si sample ErSi-A. Erbium was implanted into this sample at 190 keV with a fluence of 1.4 x 10^{16} cm^{-2}.*

As we have mentioned in the past, most arc chambers for ion implantation are fabricated from molybdenum. Chlorine, which is used to make the erbium beam, reacts with molybdenum to form molybdenum chloride, which has the same mass as erbium. Therefore, we decided that it may be possible to eliminate the source of Mo contamination by replacing the arc chamber. After considerable effort and time, we have designed, fabricated, and installed a new graphite arc chamber. Unfortunately, this new arc chamber did not operate as well as we expected, although the Mo contamination was eliminated. Indeed, the new arc chamber was not very good since graphite absorbs many contaminants and out-gassing the during implantation process. Typical RBS results for the samples implanted using the graphite arc chamber are shown in Figure 45. Figure 45 shows an RBS spectrum of a sample implanted with Er at 380 keV with a fluence of 4.9 x 10^{15} cm^{-2}. We identified the presence of Ti and Cl.

The ion implanter at Spire used for implantation of erbium is a research machine. Most of the problems we have experienced would not occur in a production facility where the implanter is dedicated only to implantation of erbium. In that particular case, the problems would be further simplified by using a sputtering technique to produce erbium ions. Sputtering the erbium would eliminate the need for use of chlorine, thus averting all associated problems. As far as our results are concerned, most of the problems are inherent in implantation of erbium using chlorine. Successful implantation of erbium using this technique requires an extremely experienced and knowledgeable technical person. During the last year, it is unfortunate that Spire has lost two of its most experienced technicians who have been involved in erbium implantation.

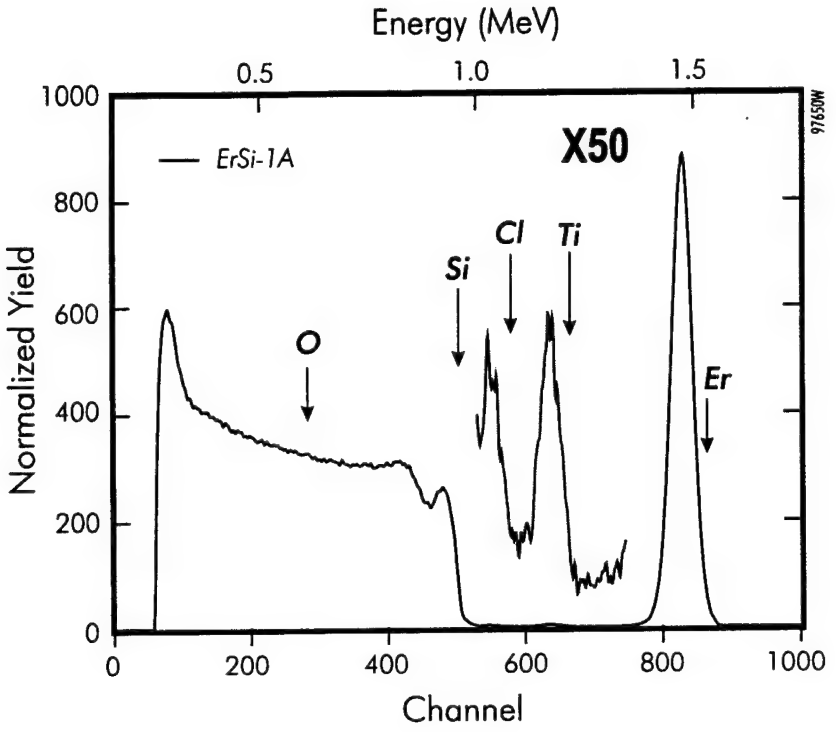

Figure 45 *Near normal incidence RBS spectrum of Er^{3+}:Si sample Er-Si-1A. Erbium was implanted into this sample at 380 keV with a fluence of $4.9x10^{15}cm^{-2}$.*

4.4.2.3 Summary

In summary, extensive effort has been carried out to fabricate batches of Er-implanted porous Si wafers for device fabrication. Wafers implanted with Er and Pr ions have shown very weak IR emission from their respective rare-earth ions. The problem has been studied and its source has been identified as the presence of contaminants such as Mo, Ti, Cl, and C. This contamination is due to the masked $MoCl_2$ and TiCl which goes undetected during the mass separation during implantation. Therefore, it is inherently difficult to eliminate these contaminants in any chlorine-based system. Contaminant elimination can only be achieved indirectly through the implanter operator. An alternative approach would be the use of a sputter source, which adds additional cost and reduces the beam, making the process not commercially viable.

4.4.3 Processes for Deliverable Devices

As a final task of this program, we have fabricated two types of electroluminescence (EL) devices (those operating based on injection-induced luminescence (LEDs) and those operating based on impact-excited luminescence) for delivery in compliance with our contract. As mentioned before, reproducing Er-implanted porous Si wafers remains difficult. It should be noted, as we reported before, that we have not been able to produce Pr beam. Thus, we could not implant Pr successfully into porous Si. We have prepared Si substrates for fabrication of porous Si and subsequently for fabrication of two types of (Er-implanted) light-emitting devices (impact excited and injection-induced) as shown in Table 6.

4.4.3.1 Ion Implantation of Si Wafers for Ohmic Contacts and/or P-N Junctions

Substrates for Impact-excited Devices - Boron and aluminum were implanted into the back of the p-type Si wafers in order to provide a good condition for ohmic back-contacts. The front side of these wafers were later anodically etched to produce p-type porous Si substrates for Er-implanted impact-excited devices.

Substrates for Injection-induced Devices - P-N junctions were fabricated using n- and p-type Si wafers by ion implantation and annealing. All the implanted wafers were later annealed at 900°C in N_2 for 30 minutes in order to recrystallize the implanted regions. Phosphorus was implanted into the back of the n-type wafers in order to make n^+ layers necessary for deposition of good ohmic back-contacts. Boron was implanted into the front side of the n-type wafers in order to form p-n junctions. Similarly, boron was implanted into the back of the p-type Si wafers in order to make p^+ layers necessary for the ohmic back-contacts and phosphorus was implanted into the front side of the wafers in order to form p-n junctions. The front sides of these p-n structures were subsequently anodically etched to produce Er-implanted p-on-n and n-on-p porous Si injection-induced luminescent devices.

The p-type layer is easy to etch and does not require UV-light illumination. On the other hand, UV-light illumination is necessary to generate carriers (holes in particular) to anodically etch n-type layers. When the UV-illumination was used for the entire duration of etch (60 minutes), the n-type porous layers began to peel off. Thus, we carried out runs with shorter periods of UV illumination (about 5 minutes) for the rest of the n-type Si wafers. However, the total etching time was 60 minutes for the n- and p-type wafers.

4.4.3.2 Etching of Porous Si Wafers with and without N-P Structure

Wafers were anodically etched in a 1:1 HF:ethanol solution using conditions to achieve red-emitting porous Si. In order to make sure that the anodic etching apparatus was working properly and to optimize the etching process, we etched some Si dummy samples before etching the device samples. Table 7 shows the sample information and etching conditions for the samples. The sample SW38-7 was intentionally left unetched. We etched this sample after implanting with Er and annealing, and compared the results from this sample with other Er-implanted porous Si samples. A typical room-temperature visible PL spectrum of a p-type porous Si sample (see Tables 6 and 7) is shown in Figure 46.

4.4.4 Implantation of Erbium into Porous Si Wafers with and without N-P Structures

Table 8 summarizes the Er implantation conditions of the wafers selected for the deliverable devices. After Er implantation and annealing, wafers were then masked and patterned using conventional photolithographic techniques. Multilayers of Ti, Pd and Au were deposited onto the back of the wafers for ohmic contacts by electron-beam evaporation. Because of the poor lateral conduction of current due to the physical properties of porous silicon, a gridded contact mask (see Figure 47) was used to deposit ohmic contacts on the front surface in order to increase the current collection efficiency. Multilayers of Ti, Pd and Au were deposited onto the front of the wafers for ohmic contacts by electron-beam evaporation. Finally, the excess metal was removed using a lift-off process. A solid contact tab is provided at one edge for probing or wire bonding.

Table 6 *Wafer information and ion implantation conditions used to fabricate device substrates. The wafers were subsequently annealed at 900°C in N_2 for 30 minutes.*

Sample Name	Back Implantation					Front Implantation				
	Ion	Energy (keV)	Fluence (10^{15}/cm^2)	Beam Current (μA)	Angle (°)	Ion	Energy (keV)	Fluence (10^{15}/cm^2)	Beam Current (μA)	Angle (°)
SW39-1 n <100> 0.15 Ω-cm 3" diameter	P^+	50	20	110-170	15	B^+	130 50	10 10	40 20	0 0
SW39-2 n <100> 0.15 Ω-cm 3" diameter	P^+	50	20	110	15	B^+	130 30 50 50	10 2 8 10	16-46 27 32 20	0 0 0 0
SW38-1 p <100> 0.3 Ω-cm 4" diameter	Al^+ Al^+ BF_2 BF_2	100 30 100 50	20 10 15 15	240 40 120 120	7 7 15 15					
SW38-2 p <100> 0.3 Ω-cm 4" diameter	Al^+ Al^+ BF_2 BF_2	100 30 100 50	20 10 15 15	380 45 130 100	7 7 7 7					
SW38-3 p <100> 0.3 Ω-cm 4" diameter	B^+	30	0.1	1.5	0	P^+	190 50	0.5 0.1	20-55 20-55	0 0
SW38-4 p <100> 0.3 Ω-cm 4" diameter	B^+	30	0.1	1.5	0	P^+	190 50	0.5 0.1	20-55 20-55	0 0
SW38-5 p <100> 0.3 Ω-cm 4" diameter	B^+	30	0.1	1.5	0	P^+	190 50	0.5 0.1	20-55 20-55	0 0
SW38-6 p <100> 0.3 Ω-cm 4" diameter	B^+	30	0.1	1.5	0	P^+	190 50	0.5 0.1	20-55 20-55	0 0
SW38-7 p <100> 0.3 Ω-cm 4" diameter	B^+	30	0.1	1.5	0	P^+	190 50	0.5 0.1	20-55 20-55	0 0

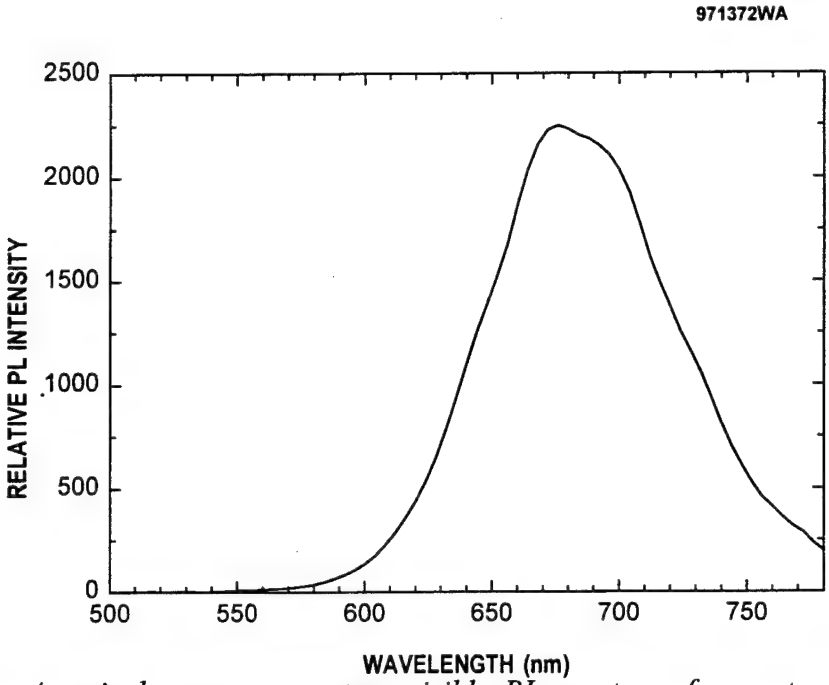

Figure 46 *A typical room-temperature visible PL spectrum from p-type porous Si device wafers (see Tables 6 and 7).*

Table 7 *Etching conditions used to fabricate porous Si on device wafers.*

Sample ID	Device Type	Current (mA)	Time (min.)	Comments
SW38-A (1.5-3 Ω-cm)	p	100	60	Dummy sample
SW38-B (1.5-3 Ω-cm)	p	100	75	Dummy sample
SW39-A (0.15 Ω-cm)	n	100	60	Dummy sample UV lamp ON
SW39-B (0.15 Ω-cm)	n	100	60	Dummy sample UV lamp ON
SW39-1	p on n	100	60	UV lamp ON
SW39-2	p on n	100	60	Not etched
SW38-1	p	100	60	UV lamp OFF
SW38-2	p	100	60	UV lamp OFF
SW38-3	n on p	100	60	1st 3.5 min. UV lamp ON No back contact wafer
SW38-4	n on p	100 200	5 135	UV lamp ON UV lamp OFF With back contact wafer
SW38-5	n on p	100 100	60 15	UV lamp OFF 1st 5 min. UV lamp ON
SW38-6	n on p	100	60	1st 5 min. UV lamp ON
SW38-7	n on p	-	-	Not etched

Table 8 *Summary of Er-implantation and annealing conditions of wafers used in the fabrication of deliverable devices.*

Sample Name	Device Type	Energy (keV)	Fluence ($x10^{15}$ cm^{-2})	Beam Current (μA)	Angle (°)	Annealing condition
SW38-1	Impact Excitation	195	2	2.5-11	0	650°C, 1/2 hr, N_2
SW38-2	Injection (n-on-p)	195	2	2.5-11	0	650°C, 1/2 hr, N_2
SW38-3	Injection (n-on-p)	195	2	2.5-11	0	650°C, 1/2 hr, N_2
SW38-4	Injection (n-on-p)	195	2	2.5-11	0	650°C, 1/2 hr, N_2
SW38-5	Injection (n-on-p)	195	2	2.5-11	0	650°C, 1/2 hr, N_2
SW38-6	Injection (n-on-p)	195	2	2.5-11	0	650°C, 1/2 hr, N_2

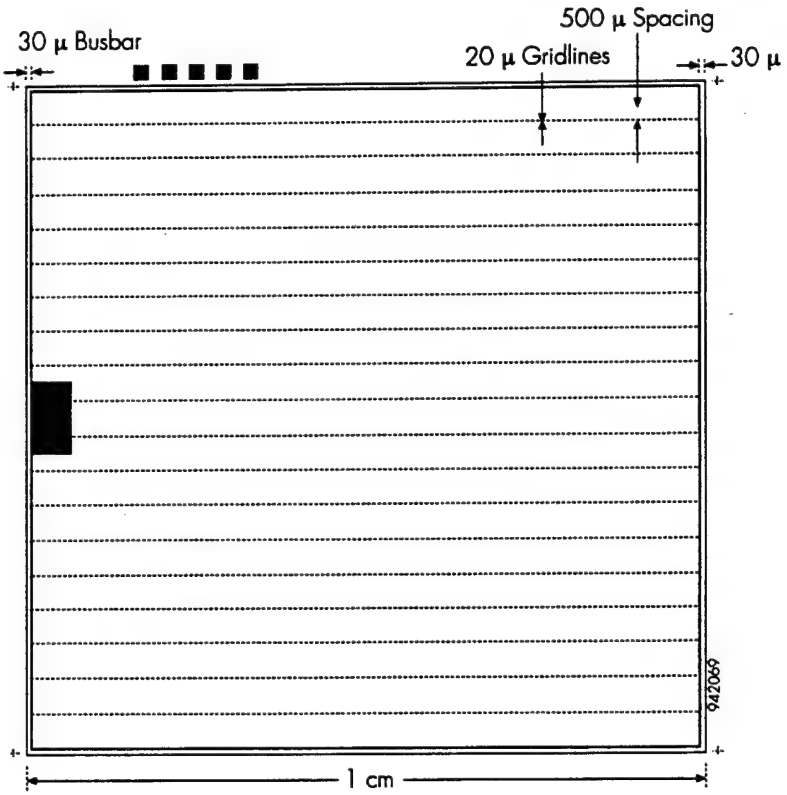

Figure 47 *Dimensions and details of the gridded contact used for the deliverable devices.*

Figure 48 shows a photograph of an actual device. Limitation of time and funding did not permit us to characterize the deliverable devices. We will characterize both types of devices through a collaboration with Prof. Uwe Hömmerich at Hampton University, Virginia.

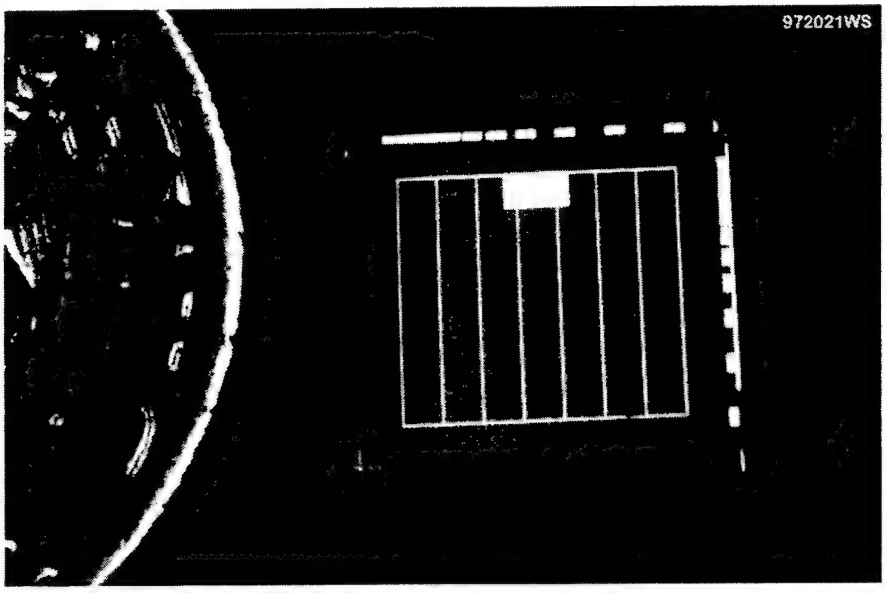

Figure 48 *A close up photograph of typical Er:porous Si devices.*

5 SUMMARY AND CONCLUSIONS

We have demonstrated a strong, room-temperature (RT), 1.54 μm emission from erbium-implanted red-emitting porous silicon. Erbium was implanted into porous Si, bulk Si, and quartz with a dose of $10^{15}/cm^2$ at 190 keV and annealed for 30 minutes in N_2 at temperatures ranging from 500°C to 900°C under identical conditions. No RT infrared (IR) emission was observed from Er implanted quartz and silicon (implanted under similar conditions as Er:porous Si) after annealing at 650°C (although after annealing at 900°C very weak emission was observed from quartz at 9K). The highest RT emission intensity at 1.54 μm was from Er:porous Si with a peak Er concentration of $1.5 \times 10^{20}/cm^3$ and annealed at 650°C. Even the luminescence intensity from Er:porous Si annealed at 500°C was 26 times higher than that observed from Er-implanted quartz at 400 keV and annealed at 900°C. Comparison of results for Er-emission in quartz and Si suggests that Er is not in SiO_2 or Si with bulk properties.

The strong Er^{3+} emission at 1.54μm in Er-implanted porous silicon could be attributed to quantum and physical confinement of Er^{3+} ions in porous Si nanocrystallites. Erbium doped wider bandgap host materials have been shown to have strong 1.54 μm Er^{3+} emission and very weak temperature dependency. The red emitting porous Si has a band gap of approximately 2 eV. Therefore our observation of strong Er-emission and weak thermal quenching is consistent with that reported in the literature. We believe that even non-quantum mechanical confinement (nanocrystallites with dimensions > 50Å) can greatly contribute to enhance the Er^{3+} emission for the following reasons. The excess carriers in bulk Si created by the excitation laser light diffuse away rapidly and have little chance to interact with the implanted erbium because of the large carrier diffusion coefficient. In contrast, in porous silicon, incident photons (specifically at shorter wavelengths) are also absorbed near the surface by creation of electron-hole pairs. However, the physical confinement of Er^{3+} ions in the nanocrystallites of porous Si prevents the excess carriers from diffusing away from the surface. They are confined by the discrete nature of the film to stay where they are created, in the vicinity of the implanted Er, until they recombine and possibly transfer energy to excite the Er^{3+} ion. Therefore, it is not surprising that 1.54 μm PL emission in Er-doped porous Si is stronger than Er-implanted bulk Si.

We have measured the near infrared and visible PL peak intensities as a function of excitation wavelengths. These photoluminescence excitation (PLE) studies on the near infrared and visible PL peaks show nearly identical PLE spectra. These results provide the first direct experimental evidence that the near IR PL emission in Er:porous Si and the visible PL emission have the same origin of excitation. In other words, the 1.54 μm PL emission originates from Er^{3+} ions in spatially confined Si nanocrystallites of porous Si. It can be concluded that the strong IR emission is excited via photogenerated carriers in Er:porous Si. It is again confirming our conclusion that Er is confined in the nanocrystallites of porous Si.

In another set of experiments, we have shown strong 1.54 μm PL emission even at temperatures up to 475K from Er-implanted porous silicon. The full width at half maximum of the 1.54 μm PL peak is 34 cm^{-1} at 15K. The observed large broadening of the 1.54 μm PL emission in Er:porous Si, compared with that reported for crystalline Si, 8 cm^{-1}, indicates that the Er^{3+} ions occupy a range of sites in porous Si, and that the emission spectrum is

inhomogeneously broadened. Indeed, this is consistent with the possible differences in the local environment (crystal field) of Er^{3+} ions due to different grain sizes in the porous layer.

We have also carried out studies to establish correlation between the visible PL emission from porous Si and the IR emission from Er in porous Si. Porous Si samples that exhibited a visible PL spectrum with peak near 750 nm before Er implantation resulted in the strongest 1.54 μm emission. After implantation and annealing, porous Si samples which still emit visible light with peak at 750 nm showed four times stronger Er-emission than those with visible PL peak near 650 nm regardless of the emission characteristics of porous Si before implantation. The Er emission in porous Si samples that showed visible PL peak near 650 nm show weaker thermal quenching (about 60% of the 10K integrated PL intensity at 300K) than those with visible peak near 750 nm, although the absolute PL intensity of the latter is weaker than the former.

One explanation for the observed thermal quenching behavior is that Er^{3+} centers associated with deep and shallow defect levels in the bandgaps are present in porous Si with visible PL peaks near 650 and 750 nm, respectively. Erbium centers associated with deep defect levels are responsible for the weak thermal quenching of 1.54 μm PL, since the energy back transfer from Er^{3+} to the host will be very low up to very high temperatures. On the other hand, erbium centers associated with shallow defect levels are responsible for the strong thermal quenching of 1.54 μm PL since the energy back-transfer from Er^{3+} to the host will be very high at high temperatures. It is possible that in wider bandgap porous Si (PL peak near 650 nm) there are more deep levels than the shallow levels as compared to the narrower bandgap porous Si (PL peak near 750 nm).

Our PL study as a function of excitation laser power density shows a square root relationship. Similar results have been reported for other Er-doped materials and are explained by a two-channel nonradiative recombination scheme. According to this scheme, the Er center can bind excitons (electron-hole pairs) which can recombine through Auger recombination or by transferring energy to the 4f-shell of Er^{3+}. For high pump power intensities Auger recombination dominates and the Er^{3+} excitation is limited leading to a sublinear (square root) power dependence. In addition, the analysis of temperature-dependent PL intensity and lifetime measurements allows us to identify recombination of bound excitons as the most likely excitation mechanism. The observed thermal quenching is explained by both energy back-transfer and thermalization of bound electrons.

We have performed temperature-dependent PL as well as PL decay measurements on Er-implanted porous Si samples up to about 375K. A non-exponential PL decay is observed at all measured temperatures (15 to 375K) as a result of superposition of a fast and a slow decay with lifetimes 145μs and 1.37 ms, respectively at 10 K. The slow component of the lifetime decreases to 930 μs at 375K. The temperature dependence of the 1.54 μm PL intensity and lifetime of the slow decay component are identical below 150K. However, above 150K, PL intensity decreases faster than the lifetime of the slow decay component. PL intensity at 375K is reduced to 45% of that observed at 15K, while the slow lifetime is only decreased to 65% of its value at 15K. The identical temperature quenching behavior between the integrated PL intensity and the slow lifetime component in the temperature range from 15 to 150K suggests that PL quenching arises

from nonradiative processes such as energy back-transfer and multiphonon nonradiative relaxation. We assume that the main process responsible for PL quenching, in this temperature range, is back-transfer. The deviation in the temperature dependence of Er^{3+} PL intensity and lifetime above 150K indicates that an intermediate level such as an Er-related donor level is involved in the Er^{3+} excitation process. From the analysis of temperature-dependent PL intensity and lifetime data, we propose an Er-related energy level which is 104 MeV below the conduction band and the thermal ionization of this level is proposed to be responsible for the thermal quenching of 1.54 μm emission above 150K. A nonradiative process with a thermal activation energy of 15.5 MeV is responsible for the slight thermal quenching below 150K. The thermal quenching of the 1.54 μm emission from Er:porous Si is comparable to the result reported for Er:3C SiC in the literature.

Based on PL (intensity and weak temperature dependence) studies, Er-implanted porous Si appears to be a suitable substrate for 1.54 μm emitting device application. However, our extensive effort to fabricate working Er:porous Si device structures was not successful, mainly due to lack of reproducibility and uniformity of porous Si substrates. The lack of reproducibility and nonuniformity of porous Si originates from the randomness of the porous Si etching process. During the course of this program, we have electrochemically etched a large quantity of 3" and 4" Si wafers under well-defined process conditions. We could hardly reproduce two porous Si wafers with identical physical appearance one after the other in the same etching solution. If porous Si should be used as a substrate for devices, one must first develop a process to fabricate porous Si reproducibly and uniformly. Very often, in our Er-implanted 3" and 4" porous Si wafers, only a small region showed intense Er luminescence. Although Er^{3+} in porous Si nanocrystallites shows a weak temperature dependence and strong PL emission intensity, the electroluminescence is limited by the difficulty to have good electrical contacts to the nano-crystallites as well as poor electrical conductivity of materials. Indeed, the existence of physical and quantum confinement nature of porous Si which provided ideal substrate for strong PL emission from Er has an adverse effect on fabricating EL devices. The question is not only how to make uniform and reproducible porous Si but also how to make a good electrical contact to discrete nanocrystallites.

6 REFERENCES

1. L.T. Canham, *Appl. Phys. Lett.* **57**, 1046 (1990).
2. F. Namavar, H.P. Maruska, and N.M. Kalkhoran, *Appl. Phys. Lett.* **60**, 2514 (1992).
3. A. Richter, W. Lang, P. Steiner, F. Lozlowski, and H. Sandmeier, *Mat. Res. Soc. Symp. Proc.* **246**, 209 (1991).
4. N. Koshida and M. Katsuno, *Appl. Phys. Lett.* **60**, 347 (1992).
5. F. Namavar, R.F. Pinizzotto, H. Yang, N. Kalkhoran, P. Maruska, *Mat. Res. Soc. Symp. Proc.* **298**, 343 (1993).
6. F. Namavar, N.M. Kalkhoran, and H.P. Maruska, U.S. Patent No. 5,272,355 (Dec. 21, 1993).
7. A. Halimaoui, C. Oules, G. Bomchil, A. Bsiesy, F. Gaspard, R. Herino, M. Ligeon, and F. Muller, *Appl. Phys. Lett.* **59** (3), 304 (1991).
8. S.M. Bedair, B.T. McDermott, Y. Ide, M.A. Tishler, N.M. Karam, M. Timmons, and N.A. El-Masry, *Proc. 4th Int'l. Conf. on MOVPE* (May 1988).
9. H. Ennen, J. Schneider, G. Pomrenke, and A. Axmann, *Appl. Phys. Lett.* **43**, 943 (1983).

10. H. Ennen, G. Pomrenke, A. Axmann, K. Eisele, W. Haydl, and J. Schneider, *Appl. Phys. Lett.* **46**, 381 (1985).
11. G.S. Pomrenke, H. Ennen, and W. Haydl, *J. Appl. Phys.* **59**, 601 (1986).
12. A. Polman, D.C. Jacobson, D.J. Eaglesham, R.C. Kistler, and J.M. Poate, *J. Appl. Phys.* **70**, 3778 (1991).
13. B. Zheng, J. Michel, F.Y.G. Ren, L.C. Kimerling, D.C. Jacobson, and J.M. Poate, *Appl. Phys. Lett.* **64**, 2842 (1994).
14. D.J. Eaglesham, J. Michel, E.A. Fitzgerald, D.C. Jacobson, J.M. Poate, J.L. Benton, A. Polman, Y.-H. Xie, and L.C. Kimerling, *Appl. Phys. Lett.* **58**, 2797 (1991).
15. R. Gupta, S. Ahn, J. Michel, J. Palm, F.Y.G. Ren, L.C. Kimerling, MRS Fall Meeting, A15.4 (1994).
16. Y.-H. Xie, E.A. Fitzgerald, and Y.J. Mii, *J. Appl. Phys.* **70**, 3223 (1991).
17. P.N. Favennec, H. L'Haridon, D. Moutonnet, M. Salvi, and M. Gauneau, *Mat. Res. Soc. Symp. Proc.* **301**, 181 (1993).
18. J. Michel, L.C. Kimerling, J.L. Benton, D.J. Eaglesham, E.A. Fitzgerald, D.C. Jacobson, J.M. Poate, and R.F. Ferrante, *Mat. Sci. Forum* **83-87**, 653-658 (1992).
19. D.L. Adler, D.C. Jacobson, D.J. Eaglesham, M.A. Marcus, J.L. Benton, J.M. Poate, and P.H. Citrin, *Appl. Phys. Lett.* **61**, 2181 (1992).
20. J. Michel, J.L. Benton, R.F. Ferrante, D.C. Jacobson, D.J. Eaglesham, E.A. Fitzgerald, Y.-H. Xie, J.M. Poate, and L.C. Kimerling, *J. Appl. Phys.* **70**, 2672 (1991).
21. H.P. Maruska, F. Namavar, and N.M. Kalkhoran, *Mat. Res. Soc. Symp. Proc.* **283**, 383 (1993).
22. H.P. Maruska, F. Namavar, and N.M. Kalkhoran, *Appl. Phys. Lett.* **61**, 1338 (1992).
23. J.I. Pankove, R.J. Feuerstein, *Mat. Res. Soc. Symp. Proc.* **301**, 287 (1993).
24. J. Yu, Y. Shen, X. Xu, B. Luo, G. Zhong, in Electroluminescence, eds. S. Shionoya and H. Kobayashi, *Springer Verlag Proceedings in Physics* **38**, 24 (1989).
25. G. Franzò, F. Priolo, S. Coffa, A. Polman, A. Carnera, *Appl. Phys. Lett.* **64**, 2235 (1994).
26. P.B. Klein, *Solid State Commun.* **65**, 1097 (1988).
27. T. Kimura, A. Yokoi, Y. Nishida, R. Saito, S. Yugo and T. Ikoma, *Appl. Phys. Lett.* **67** (18), 2687 (1995).
28. M. Yoganathan,* Ph.D. thesis, Department of Physics and Astronomy, University of Pittsburgh, PA (1996).
29. T. Benyattou, D. Seghier, G. Guillot, R. Moncorge, P. Galtier and M. Charasse, *Mat. Res. Soc. Symp. Proc.* **163**, 69 (1990).
30. S. Coffa, F. Priolo, G. Franzò, V. Bellani, A. Carnera, and C. Spinella, *Phys. Rev. B* **48**, 11782 (1993).
31. S. Coffa, G. Franzò, F. Priolo, A. Pohlman, and R. Serna, *Phys. Rev. B* **49**, 16313 (1994).
32. A. Polman, G.N. van den Hoven, J.S. Custer, J.H. Shin, R. Serna, and P.F.A. Alkemade, *J. Appl. Phys.* **77**, 1256 (1995).
33. S.M. Sze, *Physics of Semiconductor Devices*, p. 645 (John Wiley & Sons, New York, 1969).
34. *Ibid.*, p. 664.
35. R.O. Bell and G.M. Freedman, *Proc. 13th IEEE Photovoltaic Spec. Conf.*, 89-94 (Washington, DC, 5-8 June 1978).

36. S. Coffa, G. Franzò, F. Priolo, A. Polman, and R. Serna, *Phys. Rev.B* **49**, 16313 (1994).
37. F. Priolo, G. Franzò, S. Coffa, A. Polman, S. Libertino, R. Barklie and D. Carey, *J. Appl. Phys.* **78** (6), 3874 (1995).
38. G.N. van den Hoven, J.H. Shin, A. Polman, S. Lombardo and S.U. Campisano, *J. Appl. Phys.* **78** (4), 2642 (1995).
39. J.H. Shin, G.N. van den Hoven, and A. Polman, *Appl. Phys. Lett.* **67** (3), 377 (1995).
40. S. Coffa, F. Priolo, G. Franzò, V. Bellani, A. Carnera, and C. Spinella, *Phys. Rev. B* **48**, 11782 (1993).
41. J.L. Benton, J. Michel, L.C. Kimerling, D.C. Jacobson,Y.-H. Xie, D.J. Eaglesham, E.A. Fitzgerald, and J.M. Poate, *J. Appl. Phys.* **70** (5), 2667 (1991).
42. M. Needles, M. Schluter, and M. Lannoo, *Phys. Rev. B* **47**, 15533 (1993).
43. C.H. Perry, F. Lu, F. Namavar, N.M. Kalkhoran, and R.A. Soref, *Mat. Res. Soc. Symp. Proc.* **256**, 153 (1992).
44. J. Hartung, L.A. Hansson, and J. Weber, in *The Physics of Semiconductors*, Vol. 3. (eds. E.M. Anastassakis and J.D. Joannopoulos, World Scientific, 1990), pp. 1875-79, and references therein.

APPENDIX A
PL RESULTS OF IMPACT-EXCITED AND INJECTION-LUMINESCENCE Er:POROUS Si DEVICES

PL measurements on the Er:porous Si devices were performed with collaboration from Professor Uwe Hömmerich (Hampton University, VA). An impact excited device and an injection luminescence device and a reference sample (6554-G) were measured. Figure 49 shows room temperature 1.54 μm PL spectra of (a) Er:porous Si impact excited and injection luminescence devices and (b) Er:porous Si sample 6554-G. Note that the room-temperature 1.54 μm PL intensity of the impact excited devices is about 20 times weaker than that of sample 6554-G.

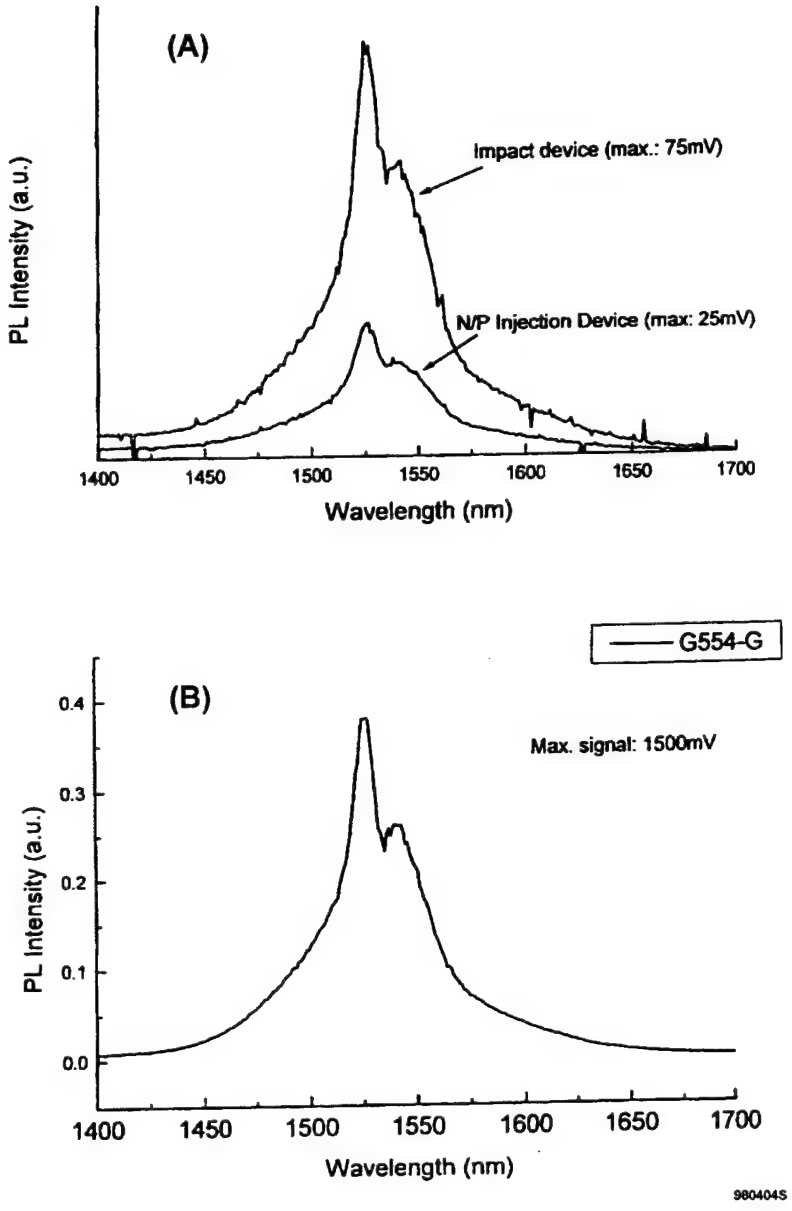

Figure 49 *Room temperature 1.54 μm PL spectra of (a) Er:porous Si impact excited device and injection luminescence device and (b) Er:porous Si sample 6554-G.*

APPENDIX B
PUBLICATIONS

Er-IMPLANTED POROUS SILICON: A NOVEL MATERIAL FOR Si-BASED INFRARED LEDs

FEREYDOON NAMAVAR*, F. LU*** and C.H. Perry** A. Cremins*, N.M. Kalkhoran*, and J.T. Daly* and R.A. Soref***
* Spire Corporation, One Patriots Park, Bedford, MA 01730-2396
** Northeastern University, Boston, MA
*** Hanscom AFB, Bedford, MA 01730

ABSTRACT

We have demonstrated a strong, room-temperature, 1.54 μm emission from erbium-implanted at 190 keV into red-emitting porous silicon. Luminescence data showed that the intensity of infrared (IR) emission from Er implanted porous Si annealed at ≤ 650°C, was a few orders of magnitude stronger than Er implanted quartz produced under identical conditions, and was almost comparable to IR emission from $In_{0.53}Ga_{0.47}As$ material which is used for commercial IR light-emitting diodes (LEDs).

The strong IR emission (much higher than Er in quartz) and the weak temperature dependency of Er in porous Si, which is similar to Er^{3+} in wide-bandgap semiconductors, suggests that Er is not in SiO_2 or Si with bulk properties but, may be confined in Si light-emitting nanostructures. Porous Si is a good substrate for rare earth elements because: 1) a high concentration of optically active Er^{3+} can be obtained by implanting at about 200 keV, 2) porous Si and bulk Si are transparent to 1.54 μm emission therefore, device fabrication is simplified, and 3) although the external quantum efficiency of visible light from porous Si is compromised because of self-absorption, it can be used to pump Er^{3+}.

INTRODUCTION

During the past three years electroluminescence (EL) from anodically-etched porous Si[1] devices has been shown by a number of groups.[2,3,4] There are positive indications[5] that EL from light emitting devices should be possible with the same impressive efficiency levels as the photoluminescence (PL) observed from porous Si, or the emission from liquid junction porous Si[6]. The efficiency of these devices may be increased by improving the quality of the contact or by applying a technique to achieve a contact with conformal coverage to porous Si. Although the external quantum efficiency of visible light emission from porous Si devices may be reduced if a narrow-bandgap semiconductor or metal is used, however, a significant amount of visible light could be lost due to the self-absorption of the spongy porous Si. This problem can be resolved if porous Si is used as a medium or as a light source in the IR range. In that case restrictions on thickness and optical properties of the contact material[7] would be reduced, because IR can exit from the back of the wafer.

Over the last decade, research has focused on the introduction of rare earth elements into semiconductors.[8-10] Erbium has attracted the most interest because it exhibits sharp luminescence at 1.54 μm and because the absorption loss at 1.54 μm is minimum for glass fibers used in optical communications.

Mat. Res. Soc. Symp. Proc. Vol. 358 © 1995 Materials Research Society

Strong room-temperature infrared emission from Er-implanted porous Si

Fereydoon Namavar
Spire Corporation, Bedford, Massachusetts 01730

Feng Lu and Clive H. Perry
Northeastern University, Boston, Massachusetts 02115

Annmarie Cremins and Nader M. Kalkhoran
Spire Corporation, Bedford, Massachusetts 01730

Richard A. Soref
Rome Laboratory, Hanscom Air Force Base, Massachusetts 01731

(Received 21 February 1994; accepted for publication 21 January 1995)

This communication demonstrates a strong, room-temperature (RT), infrared (IR) (1.54 μm) emission from Er-implanted red-emitting (peaked at 1.9 eV) porous silicon (Er:PSi). Erbium was implanted into porous Si, bulk Si, and quartz with a dose of $10^{15}/cm^2$ at 190 keV and annealed for 30 minutes in N_2 at temperatures ranging from 500 °C to 900 °C under identical conditions. No RT IR emission was observed from Er implanted quartz and silicon after annealing at 650 °C (although after annealing at 900 °C very weak emission was observed from quartz at 9 K). The highest RT emission intensity at 1.54 μm was from Er:PSi with a peak concentration of $1.5\times10^{20}/cm^3$ and annealed at 650 °C. Even the luminescence intensity from Er:PSi annealed at 500 °C was 26 times higher than that observed from Er-implanted quartz at 400 keV and annealed at 900 °C. A reduction in photoluminescence (PL) intensity of about a factor of two from Er:PSi over the 9 to 300 K temperature range was observed which is consistent with Er in wide band gap materials. © *1995 American Institute of Physics.*

During the past few years, optically excited visible-light emission[1] from electrochemically etched anodized silicon[2] has provided researchers with the possibility of fabricating a visible light-emitting diode (LED) based on porous silicon.[3–7] In addition, there are indications that the monolithic integration of porous Si into a Si wafer is possible.[8] Porous Si LEDs would be very useful as a component in display panels or in communications in free space; however, their use in optical communication is limited by fiber attenuation in the visible region. On the other hand, minimum loss occurs in the 1.5 μm range, and emission from erbium makes it an excellent candidate for optical communication via glass fibers. The luminescence peak from Er is narrow and possesses rather good temperature stability because of its atomic level transitions.

This communication proposes and demonstrates that porous Si is an excellent host for luminescent rare earth elements. Er implanted into porous Si (Er:PSi) below 200 keV is a low-cost alternative to MeV implantation into bulk Si.[9] Recently there has been a growing interest in Er in bulk Si.[9,10] Several papers[11–13] indicate that, after introducing oxygen or other impurities, the light emission of Er-implanted Si (Er:Si) is enhanced. Extended x-ray absorption fine-structure (EXAFS) show that an optically active species is formed in Czochralski-grown Si. The species involves six-fold bonding of Er to oxygen impurity atoms. However, when Er is implanted in float-zone Si, which contains little oxygen, a twelve-fold bonding of Er to Si results, forming an optically inactive species.[14] Co-implantation of oxygen with Er also results in optical activity.

We assumed porous Si can be an excellent host because the recovery of damage from implantation into Si nanostructures should occur at much lower annealing temperatures than in bulk Si. Defects such as vacancies or interstitials created by Er implantation need only travel a relatively small distance to reach the free surface (sink) as compared to MeV implantation into bulk Si where defects must travel rather long distances (several hundred/thousand angstroms) to reach the sink. Annealing at 900 °C or higher is used to recrystallize the bulk Si; however, this high temperature could result in formation of silicides rather than Er with oxygen coordination. In addition, Er in silicon nanostructures can easily acquire oxygen because

(1) the surface area of the nanostructures is enormous, and
(2) the average distance between the Er and surface oxygen is on the order of only a few nanometers.

In contrast to Er in bulk Si, Er in porous Si does not precipitate because porous Si consists of free-standing, quantum-confined structures with distinct physical boundaries. Porous Si also has a higher band gap (1.8 to 2.0 eV) than bulk Si (1.1 eV); thus a stronger IR emission and weaker temperature dependence are expected.[11]

We have designed experiments to show that strong RT IR emission is not from Er in SiO_2 or Si with bulk properties. Erbium was implanted at 50, 190, and 400 keV with a dose of $10^{15}/cm^2$ into anodically etched porous Si, bulk Si, and quartz. Annealing was performed in a conventional furnace in N_2 for 30 minutes at temperatures ranging from 500 to 900 °C. Er profiling was determined by Rutherford backscattering spectroscopy (RBS) measurements using He^+ at 1.9 MeV.

The IR PL was excited with a Coherent Innova 70 Ar^+ laser at 514 nm, and measurements were carried out for laser

 0021-8979/95/77(9)/4813/3/$6.00

Journal of Electronic Materials, Vol. 25, No. 1, 1996

Visible and Infrared (1.54 μm) Emission From Er-Implanted Porous Si For Photonic Applications

FEREYDOON NAMAVAR

Spire Corporation, Bedford, MA 01730

FENG LU and CLIVE H. PERRY

Northeastern University, Boston, MA 02115

ANNMARIE CREMINS and NADER KALKHORAN

Spire Corporation, Bedford, MA 01730

RICHARD A. SOREF

Rome Laboratory, Hanscom AFB, MA 01731

This paper explores the challenges faced in developing efficient room temperature porous Si-based light emitting diodes. We experimentally demonstrate that porous Si is an excellent host material for erbium ions to emit strong, room temperature, sharp-line luminescence at 1.54 μm. A comparison of photoluminescence data for erbium implanted samples of bulk Si, porous Si, and quartz indicate that quantum confinement likely enhances the erbium IR luminescence efficiency. Due to the 650 to 850°C annealing, it is unlikely that the environment of erbium in our samples is amorphous Si.

Key words: 1.54 μm emission, erbium, porous silicon, room temperature luminescence, Si-based light emitting device

INTRODUCTION

In recent years, attention has focused on the development of new materials which would improve the speed and efficiency of optical information transfer in computer and communication systems. Through the rapid progress of integrated circuit technology, Si is widely recognized as a leading semiconductor material. Unfortunately, its indirect bandgap has prevented its use for photonics. Extensive efforts are in progress to incorporate compound semiconductor light-emitting diodes (LEDs) and laser diode technologies into silicon very large scale integrated (VLSI) processes by heteroepitaxial growth. However, the most promising III-V light-emitting compounds, are not easily processed on silicon substrates due to lattice and thermal expansion mismatches. Incompatibility problems generally degrade the performance of III-V compound LEDs grown on silicon. An alternate approach involves mounting III-V based devices onto silicon wafers, but this is costly, time-consuming, and labor intensive. If a process could be developed to allow efficient light emission directly from Si, Si-based optoelectronic devices could be used as an essential component in optical interconnects for the next generation of high speed computers and low-cost information transfer/display systems.

(Received March 31, 1995)

Porous Si Visible LEDs

During the past four years, strong room temperature visible light emission from anodically etched porous Si has been demonstrated.[1] Electroluminescence (EL) from porous Si devices based on pn junction or Schottky contacts has also been shown by a number of groups.[2-4]

Correlation between visible and infrared (1.54 μm) luminescence from Er-implanted porous silicon

X. Wu and U. Hömmerich[a)]
Hampton University, Research Center for Optical Physics, Department of Physics, Hampton, Virginia 23668

F. Namavar and A. M. Cremins-Costa
Spire Corporation, One Patriots Park, Bedford, Massachusetts 01730

(Received 3 June 1996; accepted for publication 12 July 1996)

A photoluminescence excitation (PLE) study was performed of Er-implanted porous Si with two different porosities. Erbium was implanted at a dose of 1×10^{15} cm^{-2} at 380 keV and the samples were annealed for 30 min at temperatures from 650 to 850 °C. We observed that PLE spectra from Er^{3+} at 1.54 μm are nearly identical to those from the visible-emitting porous Si layers. Our results provide the first direct experimental evidence that infrared photoluminescence at 1.54 μm arises from Er^{3+} ions in porous Si and that ions are excited through the recombination of excess carriers spatially confined in Si nanograms. © *1996 American Institute of Physics.*
[S0003-6951(96)03139-7]

Er-doped porous silicon (Er:PSi) has recently been attracting attention due to its novel optical properties and potential applications in Si-based optoelectronics. To improve the luminescence efficiency of Er-doped bulk Si, erbium has been introduced into porous silicon either through ion implantation, electrolysis, or spin-on techniques.[1–3] Due to the large surface area of porous silicon and the short distance between Er and surface oxygen,[1] a high concentration of optically active Er^{3+} ions has been obtained in this system through easy acquisition of oxygen, leading to a strong 1.54 μm emission even at room temperature.[1–3] However, the major advantage of PSi as a host for Er ions is the weak temperature dependence of Er^{3+} emission in this system. The two-dimensional quantum confinement of carriers in Si nanograins appreciably widens the Si band gap from 1.09 eV to 1.8–2.0 eV[4,5] which significantly reduces the thermal quenching of Er^{3+} luminescence in the infrared.[6] The Er^{3+} emission at 1.54 μm is quenched only by a factor of less than 2 between 15 K and room temperature,[1,7,8] which is superior to other Si-based systems such as polycrystalline and amorphous Si(SIPOS), and Er, O coimplanted crystalline Si, where the Er^{3+} emission was found to decrease by factors of 3.3 and 20, respectively.[9,10] Furthermore, because of the absence of intermediate states between the $^4I_{13/2}$ and $^4I_{15/2}$ manifolds, the lifetime of the upper level is as long as 1–1.5 ms,[11] which makes population inversion possible. Therefore, Er implanted/doped porous Si is very promising for a wide range of devices such as light emitting diodes (LEDs), optical amplifiers, and lasers.

Despite the amount of research, there are many unanswered, questions concerning the location and excitation mechanisms of erbium ions in porous silicon.[1–3,7,8,12] It has been proposed that efficient Er^{3+} excitation results from the recombination of spatially confined photocarriers in silicon nanograins near the incorporated Er.[1,2] Previously we reported that the temperature quenching of Er^{3+} photoluminescence (PL) depends on the porosity of the porous silicon, which strongly suggests a correlation between Er^{3+} PL and size of the porous Si nanostructures.[8]

To date, however, no direct experimental evidence has shown that the implanted Er ions are located in silicon nanograins or that the Er^{3+} ions are excited through a carrier-mediated process. In this letter, we present a study of photoluminescence excitation (PLE) of both visible and infrared PL in Er:PSi. Our results clearly show that the infrared PL at 1.54 μm arises from Er^{3+} ions in the porous Si layer and that these ions are excited through the recombination of photocarriers confined in the Si nanograins.

The erbium-implanted porous silicon samples were prepared at Spire Corporation. The porous silicon layers of two samples (A and B) were obtained by anodically etching 3-in. p-type Si ⟨100⟩ wafers (0.1–1.2 Ω cm) in a HF:ethanol (1:1) solution under constant current conditions (10–100 mA/cm^2) for 1 h. Sample B was etched under a reduced current density making it less porous than sample A. Erbium was implanted at a dose of 1×10^{15} cm^{-2} at 380 keV and annealed in N_2 at temperatures from 650 to 850 °C for 30 min. Since the Er-implanted porous Si samples used in this study were annealed above 600 °C, we believe that epitaxial regrowth of the implanted layer was completed.[1,13] Therefore, it is not likely for an amorphous phase to exist in our porous Si samples ruling out the possibility of Er ions occurring in an amorphous phase.

For photoluminescence excitation measurements, an optical parametric oscillator (Surelite OPO, Continuum) pumped by a Q-switched Nd:YAG laser (Surelite II, Continuum) was used as the excitation source. The PL was dispersed with a 1-m monochromator and detected with either a photomultipler or a liquid-nitrogen cooled Ge detector. The PLE signal was recorded as the ratio between PL intensity and excitation power, and included the system response. The signal was processed by a boxcar average (SR250 Stanford Research Systems). The sample was cooled on the cold finger of a two-stage closed-cycle refrigerator capable of reaching a temperature of 12 K.

Figure 1 shows the low-temperature (15 K) visible and

a)Electronic mail: hommeric@gprc.hamptonu.edu

 0003-6951/96/69(13)/1903/3/$10.00

A spectroscopic study on the luminescence of Er in porous silicon

Uwe Hömmerich[a)]
Research Center for Optical Physics, Department of Physics, Hampton University, Hampton, Virginia 23668

Fereydoon Namavar and Annmarie Cremins
Spire Corporation, Bedford, Massachusetts 01730

Kevin L. Bray
Department of Chemical Engineering, University of Wisconsin-Madison, 1415 Johnson Drive, Madison, Wisconsin 53706

(Received 14 September 1995; accepted for publication 31 January 1996)

We report a spectroscopic study on the photoluminescence (PL) of erbium implanted into porous silicon (Er:PSi). Two different porous Si samples were implanted with a dose of 1×10^{15} Er/cm^2 at 380 keV and annealed at 650 °C for 30 min under identical conditions. Both samples exhibited Er^{3+} luminescence at 1.54 μm, which was quenched by less than a factor of two between 15 K and room temperature. Visible PL studies of Er implanted and annealed porous Si samples showed broad spectra which peaked at ~700 nm for sample A and peaked at ~660 nm for sample B. Sample A showed a four times stronger Er^{3+} luminescence than that observed from sample B. In contrast, temperature quenching of the Er^{3+} luminescence was found to be similar or slightly weaker from sample B than from sample A. The spectroscopic data will be discussed in terms of the excitation mechanisms of Er^{3+} in porous Si nanostructures. © *1996 American Institute of Physics.* [S0003-6951(96)01914-9]

In recent years, the optical properties of Er-doped Si have received a great deal of attention because of the possibility to integrate electronic and optical devices using the mature Si technology.[1] Erbium emission at 1.54 μm, arising from an internal 4*f* transition ($^4I_{13/2}\rightarrow{}^4I_{15/2}$) of Er^{3+} ions, is or particular interest because it overlaps the minimum loss region of optical fibers employed in optical communication. However, for the development of opto-electronic devices based on Er-doped Si, a high concentration of optically active Er ions with strong luminescence at room temperature is necessary. Previous studies have shown that an enhancement in luminescence can be achieved by co-implantation of oxygen and erbium into Si substrates.[1–4]

Recently, 1.54 μm photoluminescence (PL) from Er-implanted[5–7] and doped[8,9] porous silicon (Er:PSi) has been observed. The strong Er luminescence suggested a high concentration of optically active Er^{3+} ions in the inherently oxygen-rich porous silicon host. It has been proposed that Er is incorporated into the nanostructures of porous Si[6,10] and that the weak temperature quenching of the Er luminescence is due to the large band gap of porous Si (~1.8–2.0 eV), similar to Er in wide band-gap III-V semiconductors.[11]

In this letter we report photoluminescence spectroscopy results and properties of two Er: PSi samples with different porosities and different visible PL energies. Er was implanted in both samples under identical conditions. Results of temperature and power dependence of the Er luminescence will be presented. A correlation between visible PL from porous Si and Er^{3+} PL was observed. The data will be discussed in terms of incorporation and excitation of Er in porous Si.

Porous Si was prepared using three-inch *p*-type Si ⟨100⟩ wafers (0.1–1.2 Ω/cm^2). These wafers were anodically etched in a HF: ethanol (1:1) solution under constant current conditions (10–100 mA/cm^2) for 1 h. Sample A (looked purple) was less porous than sample B (looked green-yellow) and was prepared by half the current density. Er was implanted into both samples with a dose of 1×10^{15} Er/cm^2 at 380 keV and annealed at 650 °C for 30 min. Photoluminescence measurements were carried out with an argon ion laser, a 1 m monochromator, and a photomultiplier tube (visible PL) or a liquid-nitrogen cooled Ge detector (infrared PL) for light detection. The PL signal was processed by photon counting or lock-in amplifier technique. In all experiments cooling was achieved by mounting the sample on the cold finger of a closed cycle helium refrigerator. Visible PL was excited at 488 nm and a laser power of 30 mW. The monochromator was set to a spectral resolution of 0.4 nm. A 515 nm long-pass dielectric filter was placed in front of the entrance slit to minimize stray laser light. Infrared PL was excited at 514.5 nm and a laser power of 100 mW. In the power-temperature study the sample was irradiated with a focused excitation beam having a spot size of 1 mm. Power was varied between 20 and 30 mW. A 850 nm long-pass filter was placed in front of the entrance slit to avoid higher order grating scattering. The spectral resolution in the infrared PL measurements was 1.6 nm.

Low-temperature (15 K) infrared PL spectra of sample A and B (after annealing at 650 °C) are shown in Fig. 1. Both exhibited Er^{3+} luminescence at 1.54 μm and a weak broadband luminescence between 1.0 and 1.4 μm, which was probably due to porous Si.[12] The peak at 1.13 μm corresponded to intrinsic band-to-band recombination found in

a)hommeric@gprc.hamptonu.edu

 0003-6951/96/68(14)/1951/3/$10.00

Characterization of visible and infrared (1.54 μm) luminescence from Er-doped porous Si

R. White*, X. Wu*, U. Hömmerich*,+, F. Namavar**, and A. M. Cremins-Costa**
*Hampton University, Research Center for Optical Physics, Department of Physics
Hampton, VA 23668
** Spire Corporation, One Patriots Park, Bedford, MA 01876

+ e-mail: hommeric@gprc.hamptonu.edu

ABSTRACT

Results of a photoluminescence excitation (PLE) study of Er-implanted porous Si (Er: PSi) are presented. Erbium was implanted at a dose of 1×10^{15} Er/cm^2 at 380 keV and annealed for 30 minutes at 650°C. We observed a nearly identical PLE intensity behavior from 1.54 μm and visible-emitting Er: PSi. This observation indicates that both visible and infrared photoluminescence (PL) arise from carrier mediated processes, and that the 1.54 μm Er^{3+} PL is related to the porous Si nanostructures. Measurements of the temperature dependence (15-375K) of Er^{3+} PL intensity and lifetime are also reported.

INTRODUCTION

Er-doped porous silicon has recently attracted significant attention because of its possible applications in Si-based opto-electronics. Porous silicon emits brightly in the visible wavelength range due to the quantum confinement of carriers in silicon nanograins [1,2]. Erbium can be introduced into porous silicon either through ion implantation, electrolysis, or spin-on. In each case, an intensive 1.54 μm Er^{3+} photoluminescence (PL) is observed at room temperature [3-6]. These results suggests a high concentration of optically active Er^{3+} ions and a weak Er^{3+} PL quenching in Er-doped porous Si (Er: PSi). The weak temperature quenching of the Er^{3+} PL has been explained by the large bandgap of porous Si (~1.8-2.0 eV) [3-7].

The exact excitation mechanism of Er^{3+} in porous silicon and its relation to porous silicon nanostructures remain unclear. It was proposed that efficient Er^{3+} excitation resulted from the recombination of spatially-confined photocarriers in silicon nanograins near the incorporated Er [3-5]. We previously reported that the temperature quenching of Er^{3+} PL depends on the porosity of porous silicon, which implies a correlation between Er^{3+} PL and porous Si nanostructures [8]. In this paper, we present a comparison of the photoluminescence excitation (PLE) behavior of visible and infrared PL in Er: PSi. Our results strongly support that Er^{3+} photoluminescence (PL) arises from Er^{3+} ions located in the nanostructures of porous Si. Additional results of the temperature dependence of Er^{3+} PL intensity and lifetime are also discussed.

SAMPLE AND MEASUREMENT

The erbium implanted porous silicon sample was prepared at Spire Corporation. The porous silicon was obtained by anodically etching three-inch p-type Si <100> wafers (0.1-1.2 Ω cm) in a HF:ethanol (1:1) solution under constant current conditions (10-100 mA/cm^2) for one hour. Erbium was implanted at a dose of 1×10^{15} Er/cm^2 at 380 keV and annealed in N_2 at 650°C for 30 minutes.

Mat. Res. Soc. Symp. Proc. Vol. 422 © 1996 Materials Research Society

ELSEVIER

Journal of Luminescence 71 (1997) 13–20

JOURNAL OF LUMINESCENCE

Time-resolved photoluminescence spectroscopy of Er-implanted porous silicon

X. Wu[a], R. White[a], U. Hömmerich[a,*], F. Namavar[b], A.M. Cremins-Costa[b]

[a]*Research Center for Optical Physics, Department of Physics, Hampton University, Hampton, VA 23668, USA*
[b]*Spire Corporation, One Patriots Park, Bedford, MA 01876, USA*

Received 22 April 1996; revised and accepted 12 July 1996

Abstract

We have investigated the time evolution of the 1.54 μm Er^{3+} photoluminescence (PL) intensity of Er-implanted porous silicon in the temperature range from 15 to 375 K. Er was implanted into porous silicon with a dose of 1×10^{15} Er/cm^2 at 380 keV and annealed at 605°C for 30 min. Upon optical excitation at 488 nm, erbium ions are excited by photogenerated carriers and an intense 1.54 μm PL is observed at room temperature. We have compared the time evolution of the $^4I_{13/2} \rightarrow {}^4I_{15/2}$ transition of Er^{3+} to a double-exponential decay. The analysis suggests the existence of two classes of Er sites in porous silicon. This is supported by a study of the Er^{3+} PL decay time as a function of excitation pulse width. The characteristic Er^{3+} lifetimes in the two sites are 145 μs and 1.37 ms, respectively. In the temperature range from 15 to 150 K, the back transfer of energy from the excited erbium level $^4I_{13/2}$ to the host plays the dominant role in the thermal quenching of the Er^{3+} luminescence. At temperatures above 150 K, the reduction in Er^{3+} PL can mainly be ascribed to thermalization of bound electrons to the conduction band. We have compared the observed Er^{3+} PL intensity with the result from a theoretical model and a good agreement is obtained.

Keywords: Photoluminescence; Erbium; Porous silicon

1. Introduction

Erbium-doped porous silicon has recently attracted a great interest in view of its potential applications in opto-electronic devices. The erbium ions in porous silicon give rise to a strong photoluminescence (PL) at 1.54 μm which is quenched by less than a factor of two between 15 K and room temperature [1–3]. The small thermal quenching of the Er^{3+} PL intensity is attributed to the large band-gap of porous silicon (1.8–2.0 eV) [4, 5], which is believed to be due to the quantum confinement effect on the Si band structure [6–8]. The wavelength of the Er^{3+} emission, which arises from an intra 4f shell transition between the $^4I_{13/2}$ and the $^4I_{15/2}$ levels, coincides with the window of maximum transmission for silica-based optical fibers. The Er^{3+} PL lifetime is in the order of milliseconds because of the absence of intermediate levels between the $^4I_{13/2}$ and the $^4I_{15/2}$ manifolds. Therefore, porous silicon doped with optically active Er^{3+} is promising for devices such as amplifiers and lasers. Moreover, this potential silicon-based light source would make it possible to incorporate light emitting diodes and laser diode technologies into silicon very large scale integrated (VLSI) processes.

* Corresponding author.

PII S0022-2313(96)00099-4

Electroluminescence from erbium and oxygen coimplanted GaN

J. T. Torvik,[a] R. J. Feuerstein, and J. I. Pankove[b]
Department of Electrical and Computer Engineering, University of Colorado, Boulder, Colorado 80309-0425

C. H. Qiu
Astralux, Incorporated, 2500 Central Avenue, Boulder, Colorado 80301

F. Namavar
Spire Corporation, 1 Patriots Park, Bedford, Massachusetts 01730-2396

(Received 13 June 1996; accepted for publication 23 July 1996)

Room temperature operation of erbium and oxygen coimplanted GaN *m-i-n* (metal–insulator–*n*-type) diodes is demonstrated. Erbium related electroluminescence at $\lambda = 1.54$ μm was detected under reverse bias after a postimplant anneal at 800°C for 45 min in flowing NH_3. The integrated light emission intensity showed a linear dependence on applied reverse drive current. © *1996 American Institute of Physics.* [S0003-6951(96)04440-3]

Er-doped semiconductors are of great interest for potential electrically pumped, compact, temperature insensitive, broadband, continuous wave sources of 1.5 μm radiation.[1] Room temperature (RT) Er^{3+}-related intra-4*f* shell electroluminescence (EL) at 1.54 μm from semiconductor hosts such as Si,[2,3] GaAs,[4] GaP,[5] and SiC[6] has been demonstrated. However, the efficiencies reported to date have been too low for any practical applications. Historically, the Er^{3+}-related photoluminescence (PL) intensity from low band gap semiconductor hosts, such as Si, ($E_{gap} = 1.11$ eV at RT) and GaAs ($E_{gap} = 1.43$ eV at RT), has been plagued with severe temperature quenching, often several orders of magnitude when going from 77 K to RT.[7] This effect is much less pronounced in the wider bandgap semiconductor hosts such as CdS ($E_{gap} = 2.42$ eV at RT),[8] GaP ($E_{gap} = 2.26$ eV at RT),[5] and GaN ($E_{gap} = 3.4$ eV at RT).[9,10] However, a reverse biased Si:Er,O *p-i-n* light emitting diode (LED), grown by molecular beam epitaxy, was recently demonstrated with constant Er^{3+}-related EL emission intensity from 4 to 300 K.[3] The external quantum efficiency for this device was $\eta_{ext} \sim 10^{-5}$, which is still too low for practical applications.

In this letter, we report promising EL results in GaN:Er,O. Room temperature Er^{3+}-related EL at 1.54 μm from reverse biased GaN *m-i-n* diodes is presented. A layer of *n*-GaN was grown on an *R*-plane sapphire (Al_2O_3) substrate using chemical vapor deposition. A several-μm-thick Zn-doped insulating GaN layer was then grown on the *n* layer. Detailed information on the growth was given by Pankove.[11] The insulating GaN layer was ion implanted with 10^{15} Er^{2+}/cm^2 at 350 keV, and coimplanted with 10^{16} O^+/cm^2 at 80 keV. Codoping with O led to a 20 times increase in the Er^{3+}-related PL, which is consistent with the results presented by Michel *et al.*[12] for Si:Er. A postimplant anneal in a metalorganic chemical vapor deposition (MOCVD) quartz reactor at 800 °C for 45 min in flowing NH_3 was performed to repair the implantation-induced crystal damage. These implantation and annealing conditions have been shown to produce optically active GaN:Er,O films.[13] Indium contacts were soldered to the Er- and O-implanted *i* layer and to the *n* layer completing the *m-i-n* diode structure. A side view schematic of the GaN:Er,O *m-i-n* diode structure is shown in Fig. 1.

The LEDs were dc reverse biased. The emitted light was collected by a lens (numerical aperture = 0.5) through a 0.32 m single-pass grating monochromator (Instruments SA, Inc.), with the grating blazed at 1.5 μm, and detected by a thermoelectrically cooled InGaAs photodiode. A bandpass filter (1515–1600 nm) was used for PL only. The signal was measured with a lock-in amplifier and recorded using a computer.

The Er concentration profile was measured using Rutherford backscattering spectroscopy (not shown). A buried Gaussian Er profile with full width at half-maximum (FWHM) of ~0.1 μm, and a peak depth of about 1.5 μm were found. Most of the Er was found to be located within 0.25 μm of the sample surface.

A typical *I–V* curve for the GaN:Er,O *m-i-n* diodes is shown in Fig. 2. The current in reverse bias is believed to be due to Fowler–Nordheim tunneling through a potential barrier created by pinning of the Fermi level at the *m–i* interface and/or a Schottky barrier and avalanche

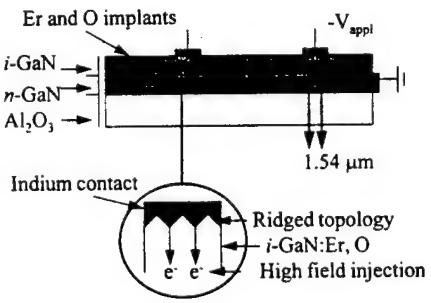

FIG. 1. A side view schematic of a GaN:Er,O implanted *m-i-n* LED. The substrate is *R*-plane sapphire, and the *i* and *n*-GaN layers were grown by CVD. The *i*-GaN layer was ion implanted with 10^{15} Er^{2+}/cm^2 at 350 keV, and coimplanted with 10^{16} O^+/cm^2 at 80 keV. A postimplant anneal in a MOCVD quartz reactor at 800°C for 45 min in flowing NH_3 was performed. The metal contacts are indium.

[a]Electronic mail: torvik@spot.colorado.edu
[b]Also with Astralux, Inc., 2500 Central Ave., Boulder, CO 80301.

 0003-6951/96/69(14)/2098/3/$10.00

hoto-, cathodo-, and electroluminescence from erbium and oxygen o-implanted GaN

J. T. Torvik[a)]
Department of Electrical and Computer Engineering, University of Colorado, Boulder, Colorado 80309-0425

C. H. Qiu
Astralux, Inc., 2500 Central Avenue, Boulder, Colorado 80301

R. J. Feuerstein and J. I. Pankove[b)]
Department of Electrical and Computer Engineering, University of Colorado, Boulder, Colorado 80309-0425

F. Namavar
Spire Corporation, 1 Patriots Park, Bedford, Massachusetts 01730-2396

(Received 15 October 1996; accepted for publication 6 January 1997)

Efficient Er-related photo-, cathodo-, and electroluminescence at 1539 nm was detected from Er and O co-implanted *n*-type GaN on sapphire substrates. Several combinations of Er and O implants and postimplant annealing conditions were studied. The Er doses were in the range $(0.01-5)\times10^{15}$ ions/cm^2 and O doses $(0.1-1)\times10^{16}$ ions/cm^2. GaN films implanted with 2×10^{15} Er^{2+}/cm^2 at 350 keV and co-implanted with 10^{16} O^+/cm^2 at 80 keV yielded the strongest photoluminescence intensity at 1539 nm. The annealing condition yielding the strongest Er-related photoluminescence intensity was a single anneal at 800 °C (45 min) or at 900 °C (30 min) in flowing NH_3. The optimum O:Er ratio was found to be between 5:1 and 10:1. Co-implanting the GaN:Er films with F was also found to optically activate the Er, with slightly (20%) less photoluminescence intensity at 1539 nm compared to equivalent GaN:Er,O films. The Er-related luminescence lifetime at 1539 nm was found to depend on the excitation mechanism. Luminescence lifetimes as long as 2.95±0.15 ms were measured at 77 K under direct excitation with an InGaAs laser diode at 983 nm. At room temperature the luminescence lifetimes were 2.35±0.12, 2.15±0.11, and 1.74±0.08 ms using below-band-gap excitation, above-band-gap excitation, and impact excitation (reverse biased light emitting diode), respectively. The cross sections for Er in GaN were estimated to be 4.8×10^{-21} cm^2 for direct optical excitation at 983 nm and 4.8×10^{-16} cm^2 for impact excitation. The cross-section values are believed to be within a factor of 2–4. © *1997 American Institute of Physics.* [S0021-8979(97)00408-8]

INTRODUCTION

The rare-earth-doped semiconductor is a material system ith potential optoelectronic applications. An electrically umped, temperature insensitive, broadband, and compact ptical amplifier around 1540 nm would be of great interest or optical fiber communications. This important wavelength orresponds to a window of minimum attenuation in silica ased optical fibers. One of the most promising rare earths is rbium (Er), which can emit or amplify light at ~1540 nm hen incorporated into a semiconductor host in its trivalent tate. This Er^{3+}-related photon emission corresponds to an ıtra-4*f* shell transition originating from the first excited tate ($^4I_{13/2}$) and terminating at the ground state ($^4I_{15/2}$).

The first Er^{3+}-related photoluminescence (PL) at 1540 m from a semiconductor host was observed in 1982 from aAs:Er,[1] while the first demonstration of electroluminesence (EL) from Si:Er light emitting diodes (LEDs) followed n 1985.[2] Since then, several groups have produced Er-doped EDs emitting at 1540 nm using semiconductor hosts such as Si,[3,4] GaAs,[5,6] GaP,[7] SiC,[8] and GaN.[9] Particularly promising hosts are the wide band-gap semiconductors GaP (E_{GAP}=2.26 eV), (6H)–SiC (E_{GAP}=3.02 eV), and GaN (E_{GAP}=3.4 eV) which have shown minimal thermal quenching of the Er^{3+}-related luminescence at room temperature.[10] However, rapid advancement of Er-doped semiconductors has unfortunately been hampered by low solubility of Er,[11] and the difficulty in making the incorporated Er optically active in semiconductor hosts.[12] As a consequence, the quantum efficiencies in the devices made to date have been too low for any practical application.[3–9]

As pointed out by other authors,[13,14] it is necessary for future device purposes to demonstrate high Er solubility (probably above 10^{19} Er/cm^3), high pumping efficiency, and high radiative luminescence efficiency (i.e., the PL/EL lifetimes must be long).

In this article, we demonstrate high concentrations of Er in *n*-type GaN, and efficient luminescence from the Er- and O-implanted GaN films. Strong Er^{3+}-related PL, EL, and cathodoluminescence (CL) at 1539 nm was observed from the GaN:Er,O films after thermal anneals. The PL increased linearly with increasing Er concentration until saturation at

Electronic mail: torvik@spot.colorado.edu
[b)]Also with Astralux, Inc., 2500 Central Ave., Boulder, CO 80301.

 0021-8979/97/81(9)/6343/8/$10.00

Photoluminescence excitation measurements on erbium implanted GaN

J. T. Torvik[a] and R. J. Feuerstein
Department of E&CE, University of Colorado, Boulder, Colorado 80309-0425

C. H. Qiu
Astralux, Inc., 2500 Central Avenue, Boulder, Colorado 80301-2845

J. I. Pankove[b]
Department of E&CE, University of Colorado, Boulder, Colorado 80309-0425

F. Namavar
Spire Corporation, 1 Patriots Park, Bedford, Massachusetts 01730-2396

(Received 14 April 1997; accepted for publication 5 May 1997)

The temperature dependence of the optical excitation cross section of Er implanted n-type GaN was studied using photoluminescence excitation spectroscopy. Due to the large 3.4 eV band gap of GaN, it was possible to probe two Er absorption lines using a tunable Ti:sapphire laser in the 770–1010 nm range. Photoluminescence excitation spectra exhibiting several Stark splittings revealed a complex dependence upon temperature. The largest excitation cross section in the third excited state was 1.65×10^{-20} cm^2 at an excitation wavelength of 809.4 nm when measured at 77 K. This value is roughly three times larger than the cross section in the second excited state at 4.8×10^{-21} cm^2 when pumping at 983.0 nm. The Er-related photoluminescence was reduced between 1.5 and 4.8 times when going from 77 K to room temperature, except when pumping around 998 nm. At this excitation wavelength the room temperature photoluminescence was stronger by a factor of 1.26 compared to that at 77 K. © *1997 American Institute of Physics.* [S0021-8979(97)00816-5]

I. INTRODUCTION

Er-doped semiconductors have been extensively studied during the last decade for potential optoelectronic applications. An electrically pumped, temperature insensitive, broadband and compact optical amplifier or source of 1540 nm light is of great interest for optical fiber communications. Unfortunately, rapid advancement of Er-doped semiconductors has been hampered by fundamental problems such as the characteristic thermal quenching of the Er^{3+}-related photoluminescence (PL) intensity.[1] The luminescence is often quenched by several orders of magnitude when going from 77 K to room temperature using semiconductor hosts such as Si and GaAs. The luminescence efficiency at room temperature can be enhanced using impact excitation[2] and codoping with light elements such as O and F.[3] However, the thermal quenching effect is still present, but to a lesser extent.

Wilson *et al.*[4] and our group have previously reported on the temperature dependence of the Er^{3+}-related photo-, and cathodoluminescence in n-type GaN on sapphire substrates.[5,6] Using direct optical excitation (below band gap excitation), indirect optical excitation (above band gap excitation), and impact excitation, the thermal quenching of the Er^{3+}-related luminescence intensity at 1539 nm was found to only be partially explained by a reduction in the luminescence lifetime when going from 77 K to room temperature.

In this article, we report on the optical excitation spectroscopy for Er in GaN at excitation wavelengths ranging from 770 to 1010 nm at room temperature and at 77 K. One advantage with using a wide band gap host such as GaN ($E_{gap}=3.4$ eV), is that the large band gap allows for the investigation of several absorption lines which are not available using smaller band gap hosts such as Si. The temperature dependence of the Er^{3+}-related PL intensity at 1539 nm was found to strongly depend upon the excitation wavelength. At the strongest photoluminescence excitation (PLE) peaks, namely at 809 and 983 nm, the thermal quenching of the PL intensity was as large as a factor of 5 when going from 77 K to room temperature. At other PLE peaks, such as at 822 nm, the PL intensity was reduced much less over the same temperature range. In fact, pumping at 998 nm resulted in a stronger PL intensity at room temperature than at 77 K. However, the PLE peaks are still much weaker when compared to the PLE peaks at 809 and 983 nm.

II. EXPERIMENT

The GaN layers used in this study were grown by the halogen chemical vapor deposition method on R-plane $(1\bar{1}02)$ sapphire substrates, and is described in detail elsewhere.[7] We have previously shown that GaN films grown on C-plane (0001) sapphire substrates by metalorganic chemical vapor deposition (MOCVD) are also suitable hosts for Er.[6] The GaN films were n-type with carrier concentration $\sim10^{18}$ cm^{-3}, and a Hall mobility of ~150 cm^2/V s. The GaN films were implanted with $[Er^{2+}]=2\times10^{15}$ ions/cm^2 at 350 keV, and coimplanted with $[O^+]=10^{16}$ ions/cm^2 at 80 keV. The energy of the coimplanted O was chosen to make the O and Er implantation spatially overlap. The implantation damage caused by the bombardment of Er ($Z=68$) ions, was partially repaired by high temperature anneals performed at 800 °C for 45 min in flowing NH_3. The anneals took place at atmospheric pressure in the quartz reactor of a MOCVD system. The NH_3 was used to prevent the GaN from decomposing at elevated tem-

[a]Electronic mail: torvik@spot.colorado.edu
[b]Also with: Astralux, Inc., 2500 Central Ave., Boulder, CO 80301.

 0021-8979/97/82(4)/1824/4/$10.00

ANNEALING STUDY OF ERBIUM AND OXYGEN IMPLANTED GALLIUM NITRIDE

JOHN T. TORVIK[a], ROBERT J. FEUERSTEIN[a], CHANG H. QIU[b], MOELJANTO W. LEKSONO[b], JACQUES I. PANKOVE[a,b], FEREYDOON NAMAVAR[c].
[a]Department of E&CE, University of Colorado, Boulder, CO 80309-0425.
[b]Astralux, Inc., Boulder, CO 80303.
[c]Spire Corporation, Bedford, MA 01730-2396.

ABSTRACT

A systematic study of photoluminescence (PL) of Er and O ion implanted and annealed n-type GaN grown on R-plane sapphire (Al_2O_3) was performed. The Er implants ranged from 2 x 10^{13} to 1 x 10^{15} Er^{++}/cm^2, and the O co-implants ranged from 10^{14} to 10^{16} O^+/cm^2. The resulting nine different combinations of GaN:Er,O were annealed at 600 °C (4 hrs. in N_2), 700 °C (1.5 hrs. in N_2), 800 °C (0.75 hr. in NH_3), and 900 °C (0.5 hr. in NH_3). Following each annealing step, the Er^{3+}-related PL at 1.54 μm was measured from each sample at 77K, when pumped directly with ~ 135 mW of power at 980 nm. The three samples with the highest dose of Er (1 x 10^{15} Er^{++}/cm^2), regardless of O co-dopant dose, yielded the strongest PL peak intensity at 1.54 μm after all the anneals. The integrated PL from 1.52 to 1.58 μm was reduced by 62 % when going from 77 K to room temperature (RT).

INTRODUCTION

Rare-earth doped semiconductors have been extensively studied as a potential material system for use in optical communications. Possible applications include a low power, temperature insensitive, broad band CW source of IR (1.54 μm or 1.3 μm) radiation, or lossless Y-junction splitters for curbside signal processing.

The rare-earth element erbium (Er) has been shown to luminesce at a particularly important wavelength, approximately λ = 1.54 μm (0.806 eV) corresponding to an intra 4*f*-shell transition between levels $^4I_{13/2}$ and $^4I_{15/2}$ in triply charged Er (Er^{3+}) under the influence of a crystal field from various host semiconductors [1, 2]. At this wavelength there is low loss [3], and no dispersion [4] in some silica based optical fibers. Er has almost exclusively been used as the active element in optically pumped fiber (glass) amplifiers and lasers [5]. However, it was found that the impact excitation cross section for Er in Si is ~ 9 x 10^{-16} cm^2 [6, 7]. This is about 4 - 5 orders of magnitude larger than the optical absorption cross section ~ (4.1 - 7.9) x 10^{-21} cm^2 [8]. Several groups have fabricated RT Er-doped electroluminescent LEDs in Si, GaAs, InP and GaP operating at 1.54 μm [9, 10, 11]. Even so, the quantum efficiencies achieved to date have been too low for any practical application, in part due to the low solubility of Er, which has been found to be < 1 x 10^{18} Er ions/cm^3 in Si [12].

Another practical problem with Si:Er which must be overcome is the observed thermal quenching of the Er^{3+}-related PL and electroluminescence (EL) at 1.54 μm [13]. The PL and EL, from Si and GaAs have been observed to be quenched between 100 - 1000 times, when going from 77 K to RT. This figure has been improved upon by co-doping with lighter elements, such as O and F along with the Er [14,15]. Recently, the EL from a reverse biased (impact excitation) Si:Er:O p^+n^+ LED operating at 1.54 μm, was shown to be reduced by only a factor of 4 when going from 77 K to RT [11].

On the other hand, Favennec et al. suggested the temperature dependent Er^{3+}-related PL intensity at 1.54 μm from semiconductors is correlated to the band gap of the host [13]. In hosts

Mat. Res. Soc. Symp. Proc. Vol. 422 © 1996 Materials Research Society

APPENDIX C
MEDIA REPORTS

Lasers & Optronics
THE INTERNATIONAL APPLICATIONS MAGAZINE
VOLUME 13 • NUMBER 9 • September 1994

Er-Doped Porous Silicon

Spire Corporation, Bedford, Mass., has demonstrated strong, room-temperature 1.54-μm emission from erbium-implanted porous silicon. Luminescence data show emission 100 to 1000 times stronger than that of Er-doped quartz — nearly as high as from InGaAsP material from which commercial infrared LEDs are made, but with a sharper spectral profile. No infrared emission could be observed from Er-doped bulk silicon or germanium-silicon produced under similar implantation and annealing conditions. These results indicate that high luminescence efficiency originates from erbium being confined in silicon nanostructures less than 5 nm in diameter.

III-Vs REVIEW
AN ELSEVIEW PUBLICATION • ISSN 0961-1290

AUGUST 1994

SILICONE UPDATE

Spire Er-doped porous Si for IRLEDs

Spire Corp., Bedford, MA, USA, has announced "the first demonstration of strong, RT 0.154 μm emission from Er-implanted porous silicon.

"Luminescence data shows that the intensity of IR emission from Er-doped porous Si is 100 to 1000 times stronger than that of Er in quartz, and is almost at the level of InGaAsP material which is used for commercial infrared LEDs. No IR emission was observed from Er-doped bulk Si or GeSi produced under similar implantation and annealing conditions." Spire's results indicate that high luminescence efficiency originates from Er being confined in Si nanostructures less than 5 nm in diameter.

Spire has already fabricated visible (red to orange) LEDs based on porous Si which are potentially useful as components in display panels or in free-space communication. However, its use for optical communication is limited by attenuation of visible light in fibre optics, where the minimal loss occurs in the 1.5 μm range. Standard InGaAsP IR LEDs have limited use because of their very broad emission spectra and their spectral dependence on power and temperature. On the other hand, the luminescence peak from Er in porous Si is narrow and possesses excellent temperature stability.

■ *Contact: Fereydoon Namavar, Spire Corp, tel/fax: [1] (617) 275 6000 7470.*

Voice of the Photonics Technology

PHOTONICS®

SPECTRA

TechnologyWorld

Briefs

News & Analysis

Spire Reports New Si-Based Infrared LED

The first demonstration of strong, room-temperature 1.54-μm emission from erbium-implanted porous silicon has been reported by **Spire Corp.** of Bedford, Mass. The firm says that the emission is 100 to 1000 times stronger than that of Er in quartz and almost at the level of InGaAsP, which is used for commercial IR LEDs. Spire said that no IR emission was observed from Er-doped bulk Si or GeSi produced under similar implantation and annealing conditions, and that the results indicate that high luminescence efficiency results from the Er being confined in Si nanostructures less than 5 nm in diameter.

Solid State Technology
Worldwide Semiconductor Production • July 1994 • A PennWell Publication

TECHNOLOGY NEWS

TECH BRIEFS

Spire Corp., Bedford, MA, recently demonstrated a strong room-temperature, 1.54-μm emission from erbium-implanted porous silicon. Luminescence data show that the intensity of IR emission from Er-doped porous Si is 100 to 1000× stronger than that of Er in quartz and is almost at the level of InGaAsP material used for commercial IR LEDs. No IR emission was observed from Er-doped bulk Si or GeSi produced under similar implantation and annealing conditions. Spire's results indicate that high luminescence efficiency originates from Er being confined in Si nanostructures less than 5 nm in diameter. For information, contact F. Namavar, Senior Scientist/Mgr., Advanced Si-Based Technology, 617/275-6000, fax 617/275-7470.

ADVANCED MATERIALS

June 1994

Erbium-Implanted Porous Silicon

Researchers at Spire Corporation have demonstrated strong room temperature 1.54 μm emission from erbium-implanted porous silicon. The intensity of the IR radiation from Er-doped porous silicon is 100 to 1000 times stronger than that of Er in quartz, and is almost at the level of the InGaAsP material used for commercial infrared LEDs. No IR emission was observed from Er-doped bulk silicon or GeSi produced under similar implantation and annealing conditions. The results indicate that the high luminescence efficiency results from the erbium being confined in silicon nanostructures less than 5 nm in diameter. One advantage of devices based on porous silicon would be their easy integration with standard silicon wafer technology.

For more information contact: Fereydoon Namavar, Advanced Si-Based Technology, Spire Corporation, One Patriots Park, Bedford, MA 01730-2396, USA. Fax: (+ 49) 617 275 7470.

Advanced Coatings & Surface Technology

A monthly intelligence service from TECHNICAL INSIGHTS, INC.

ISSN 0896-422X

Volume 7, No. 6 June 1994

IN THIS REPORT.....

"Build it and they will come." The line from the film, Field of Dreams, *has become a staple in the language. An omniscient voice tells the hero to turn his corn field into a baseball field and people will come to watch the game. Researchers have long shared the same paradigm: Invent a better mousetrap and users will beat a path to your door. Only in the past few years have we learned to talk to potential users to ensure we're inventing the mousetrap they want and need. That trap might prove a low-temperature route to harder stainless steel (p. 1) or a degradable coating for bioimplants (p. 2). Or it might be a skillful adaptation of an existing technology, such as the use of plasma to strip solder from circuit boards without CFCs or the use of waterjets to clean asbestos-filled coatings from natural gas pipes. In each case, the developers understand what users want. Today's paradigm calls for what major league teams have done for years: selling tickets before the season begins.*

Alan F. Brown
Editor, *ACST*

POROUS Si EMITS STRONG IR AT ROOM TEMPERATURE

Spire Corp. has developed a technique to boost the intensity of porous silicon room-temperature infrared (IR) emissions to levels nearly as high as conventional InGaAsP IR emitters. Compared with InGaAsP, porous silicon has narrower emission spectra and better temperature stability. Spire has demonstrated strong 1.54-μ emissions, a range which transmits clearest in fiber optics used for telecommunications and computer networks.

Spire achieves high IR emissions by implanting erbium into porous silicon and annealing. (Treatment of bulk Si and GeSi produced no results.) Implantation take place in the economical kiloelectron volt (keV) range, rather than the more expensive megaelectron volt (MeV) range typically used with bulk silicon. The process would fit in easily with those used on a conventional silicon wafer manufacturing line.

IR luminescence ranges for Er/Si ranks 100 to 1000 times stronger than Er/quartz and nearly equal to InGaAsP. But InGaAsP, unlike Er/Si, has a wide IR spectra that varies with both temperature and power. Er/Si's emission efficiencies result from confining Er to Si nanostructures <5-nm dia.

Details: Feredoon Namavar, Manager, Advanced Si-Based Technology, Spire Corp., 1 Patriot Park, Bedford, MA 01730-2396. Phone: 617-275-6000, ext. 286. Fax: 617-275-7470.

III-Vs REVIEW
AN ELSEVIEW PUBLICATION • ISSN 0961-1290

JUNE 1994

NEW PRODUCTS

Spire Si-based LED

Spire Corp has demonstrated srong, room-temperature 1.54 μm emission from Er implanted porous Si. Luminescence data show that the intensity of IR emission from Er-doped porous Si is 100 to 1000 times stronger than that of Er in quartz, and is almost at the level of inGaAsP material which is used for commercial infrared LEDs. No IR emission was observed from Er-doped bulk Si or GeSi produced under similar implantation and annealing conditions. Spire's results indicate that high luminescence efficiency originates from Er being confined in Si nanostructures less than 5 nm in diameter.

SEPTEMBER 1996
A PENNWELL PUBLICATION
ADVANCES IN OPTICS, ELECTRO-OPTICS, AND OPTOELECTRONICS
Laser Focus World

Diode lasers for desktop manufacturing
Back to Basics: Infrared array detectors
Chalcogenide fibers deliver IR power
Product Focus: Photomultiplier tubes

POROUS SILICON

Erbium-doped porous silicon emits at 1.54 μm

Optically pumped porous silicon implanted with trivalent erbium ions (Er^{3+}) generates visible output from the silicon and luminescence at 1540 nm from the Er^{3+} ions. The bandgap properties of the porous-silicon host reduce thermal quenching of the Er^{3+} luminescence to a factor of two for a temperature range from 15 K to room temperature. In contrast, thermal quenching of Er^{3+} emission from other doped-silicon-based hosts such as polycrystalline and amorphous—or crystalline—silicon reduces output by factors of 3.3 and 20, respectively.

With good performance over a broad temperature range and a long upper-level lifetime, the doped porous-silicon material has considerable potential for optoelectronic components such as light-emitting diodes, lasers, and optical amplifiers, but researchers have not clearly understood the excitation mechanism. Now photoluminescence excitation (PLE) studies by Uwe Hömmerich and his group at the Research Center for Optical Physics at Hampton University (Hampton, VA) and collaborators at Spire Corp. (Bedford, MA) have shown that the Er^{3+} excitation is driven by excitation of the silicon host, which offers a method for controlling Er^{3+} emission efficiency.[1]

Photoluminescence excitation studies

Led by F. Namavar, scientists at Spire prepared porous-silicon hosts by etching *p*-type silicon wafers in a solution containing hydrofluoric acid and ethanol under constant-current conditions, using two different current densities to create one high-porosity sample and one low-porosity sample. Both hosts were implanted with Er^{3+} at a concentration of 1×10^{15} cm^{-2}, then annealed in a nitrogen atmosphere at 850°C; by annealing above 600°C, the researchers ensured epitaxial regrowth of the implanted layer, making the existence of an amorphous phase in the samples unlikely.

A Nd:YAG-pumped optical parametric oscillator (Continuum, Santa Clara, CA) excited the samples with pulsed output at wavelengths from 400 to 600 nm. The cold finger of a two-stage, closed-cycle refrigerator cooled the samples to 15 K.

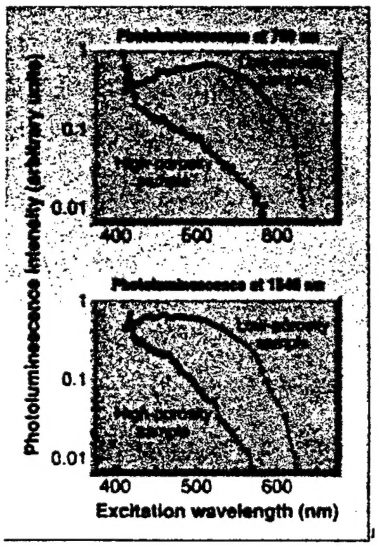

Photoluminescence excitation studies of Er^{3+} implanted porous silicon show strong correlation between the excitation spectrum of visible luminescence from the silicon (top) and infrared luminescence from the Er^{3+} (bottom), indicating that the ions are excited by recombination of excess carriers spatially confined in silicon nanograins.

Spectra from the two samples showed a broad visible luminescence from the silicon and a sharp infrared wavelength luminescence centered at 1540 nm from the Er^{3+} ions. The peak of the visible luminescence shifts from 640 nm in the first sample to 750 nm for the second sample, caused by bandgap-widening in the more porous material. Excitation performed at 400, 450, 500, and 550 nm successively showed that the silicon-based photoluminescence spectra are essentially independent of pump wavelength.

To draw a correlation between porous silicon carrier activity and Er^{3+} output, the researchers examined excitation spectra of the visible luminescence amplitude at 750 nm and Er^{3+} luminescence at 1540 nm. For excitation wavelengths varying continuously from 400 to 650 nm, the plots of the Er^{3+} luminescence are essentially the same as those for the silicon luminescence (see figure on p. 42). The excitation of the implanted Er^{3+} ions follows the generation of photocarriers in the porous silicon.

This experimental evidence led the researchers to conclude that the IR luminescence arises from Er^{3+} ions located in porous-silicon nanograins and that photogenerated electrical carriers confined in the nanograins excite the ions into luminescence. The bandgap of porous silicon can be thus controlled by the porosity, an effect that can be used to control the efficiency of the Er^{3+} emission.

Kristin Lewotsky

REFERENCE
1. X. Wu, U. Hömmerich, F. Namavar, and A. M. Cremins-Costa, *Appl. Phys. Lett.*, Sept. 23, 1996; in press.